SC3-RAV^{TM} Triaxial Seismic Data Interval Velocity Analysis

by:
Baziw Consulting Engineers, Ltd
3943 West 32nd Avenue
Vancouver, BC
Canada V6S 1Z4

July 2020

BCE's mission is to provide our clients around the world with state-of-the-art geotechnical signal processing systems, which allow for better and faster diagnostics of the sub-surface. Please visit our website (www.bcengineers.com) or contact our offices for additional information:

e-mail: info@bcengineers.com

phone: Canada: (604) 733 4995 – USA: (903) 216 5372

Table of Contents

1.0 Introduction

This document is intended to provide a guide for utilizing the *SC3-RAV*^{TM} software to estimate interval velocities from data acquired during Downhole Seismic Testing (DST). The methods of analysis covered range from basic trend line estimation to the recommended advanced technique, which utilizes iterative forward modeling, polarization analysis and signal decay. Depending on the data collected, the basic analysis technique may not result in an acceptable outcome, but it will allow the user to make a first attempt to generate a simple velocity – depth profile (in both table and graph format) from the collected seismic data.

The main focus of the data processing techniques outlined in this document is for data collected with a SH source. However, the outlined techniques are readily applicable to seismic data acquired with a P-wave source.

The effort required to analyze data depends to a large extent on the type and configuration of the wave source. In Appendix 1 of this document the recommended source apparatuses and configurations are outlined for both SH-wave and P-wave investigations.

Appendix 2 outlines the five Seismic Trace Characterization (STC) parameters which quantify the quality of the acquired DST data sets and act as a guide for the processing of those data sets to calculate interval velocities. Appendix 3 outlines a 2018 DFI Conference paper entitled "The use of seismic trace characterization to guide the analysis of DST results to obtain more accurate soil parameters". This paper outlines how the STC parameters can guide the data analysis to derive more accurate interval velocity results. Appendix 4 outlines a 2022 DFI Conference paper entitled "Analytically modelling DST arrival time databases with high order polynomials for optimal high resolution imaging". This paper outlines a new DST analysis technique which "best fits" a high order polynomial to arrival time data sets.

It is recommended that Appendices 2, 3 and 4 are reviewed prior to proceeding with the training manual. It is also recommended to apply the interval velocity estimation methodologies outlined in Sections 4 and 5.

This document is not meant to replace the manual for the *SC3-RAV*^{TM} software, and we strongly recommend users of the software to carefully review this manual before using the software to analyze data.

Finally, BCE staff are always available to provide guidance and assistance with the analysis of seismic data.

Assumption: **It is assumed that tri-axial seismic data have been collected and that the *SC3-RAV*^{TM} program is available to analyze the data.**

2.0 Estimating Interval Velocities utilizing Vertical Seismic Profiles (VSPs), Dominant Responses and Trend Lines

Step 2.1 – Create data folders

Select SC3-RAV™ software option *Utilities→SH file manipulation→without stacking.* In the user interface dialog box navigate to the directory where the seismic data resides (e.g., “C:\JOBS\SCPT\SC3 Systems Training - 2020\SC3-RAV Exercise\SC3-RAV 2020 Test Data”) and select all acquired seismic data files for a specific DST or SCPT profile. Next press the **Open** button. Note that the option *with stacking* will apply stacking to all data sets acquired at the same depth and polarity.

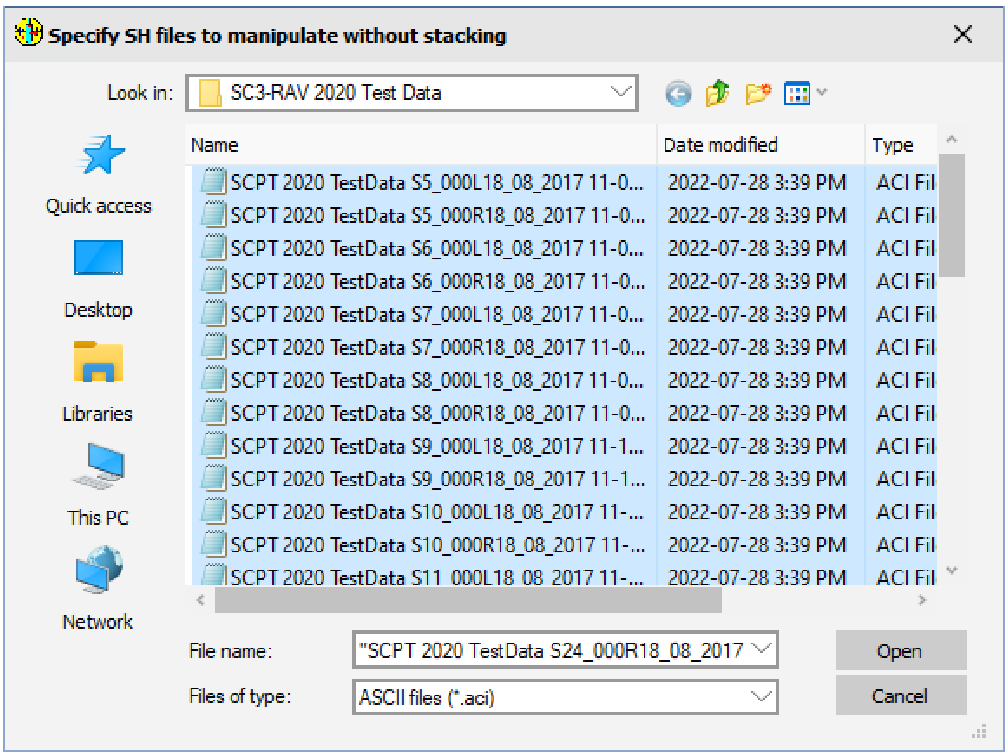

SC3-RAV™ will then create the following subdirectories:

'...\Left Side\';
'...\Right Side\';
'...\Left Side\Full Waveform\' ;
'...\Right Side\Full Waveform\';
'...\Reverse Polarity\';
'...\SCPT Results\';

Based upon SC*-DAC™ automatic file naming convention[1] the acquired raw seismic data files are moved to the appropriate '...\Left Side\' (if 'L' is identified in file name) and '...\Right Side\' (if 'R' is identified in file name) directories.

If multiple "Stacked" files were acquired and saved at each depth interval it is recommended that user retain only the latest (higher stack count) saved trace within the appropriate '...\Left Side\' and '...\Right Side\' directory. This will save significant time in post processing. For example, the two files SCPT408S1_0R3-6-2010 8-28-10 and SCPT408S1_0R3-6-2010 8-29-15 are acquired at depth interval 1.0m on the right side. Since SCPT408S1_0R3-6-2010 8-29-15 has a later time stamp (i.e., 8-29-15 as opposed to 8-28-10) it should be saved, while file SCPT408S1_0R3-6-2010 8-28-10 should be deleted from directory '...\Right Side\'. Alternatively, the user can implement SC3-RAV option *Utilities→SH file manipulation→with stacking*.

Step 2.2 – Selection of the most appropriate component

Perform the following steps:

- Open *SC3-RAV*™.
- Select the following menu options: *View→X-Y-Z-FW Seismic Profile Display*.
- In the explorer window that then appears select a consecutive series of 10 – 15 data files from either Folder Left or Folder Right.
- In the *Seismic Profile Parameter Specification* window select that you want to display the x-axis and the y-axis and select different colors for the traces (see the manual for further details).
- In the same window click on the **Refilter Time Series** button at the top of the window, and in the Cascadable Filters window enable the low pass filter (typically with a 200 Hz the low pass frequency. Also specify Start Time if so desired, after which you hit the **OK** button.
- In the *Seismic profile parameter specification* window hit the **Re-display Depth Profile** button at the top of the window.

This will generate a graph with the x and y component of the seismic data (select option *Normalize locally* as shown below) and you can now select the component that is the

---

[1] A typical SC*-DAC™ automatic file name for a seismic file saved with the Automatic Specification check box enabled is outlined and defined as follows:

SCPTS0_0R05_07_08 10-12-52 PM.aci

SCPT	-	specified by the user in the Site Name edit box
S	-	S-wave (S) or P-wave (P) - dominant source wavelet type
0_0	-	probe depth specification
R	-	right (R), left (L), or no (N) source polarization radio buttons
05_07_08	-	day data acquired (i.e., day_month_year)
10-12-52 PM	-	time data acquired (i.e., hour-minute-second)
.aci	-	user specified data type

most dominant (i.e., “dominant response”). The component defined as the dominant response is that which has predominantly greater source wave amplitudes throughout the depth profile. For example, in the *View→X-Y-Z-FW Seismic Profile Display* plot at the bottom of the page the x axis has predominantly greater amplitudes compared to the y axis for the depth increments shown; therefore, the x axis should be defined as the “dominant response”.

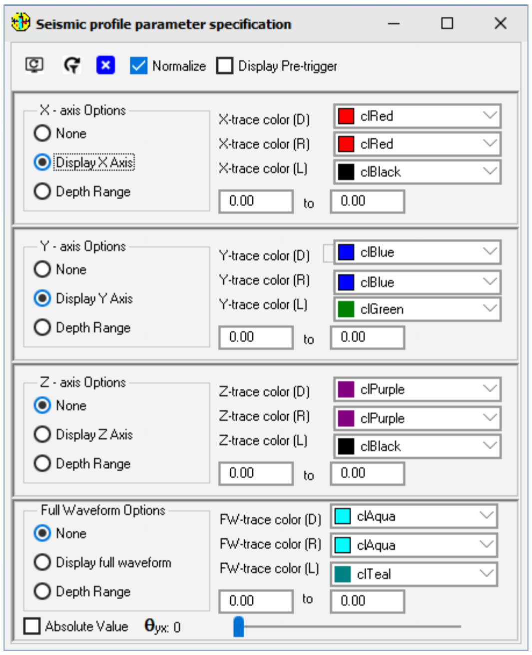

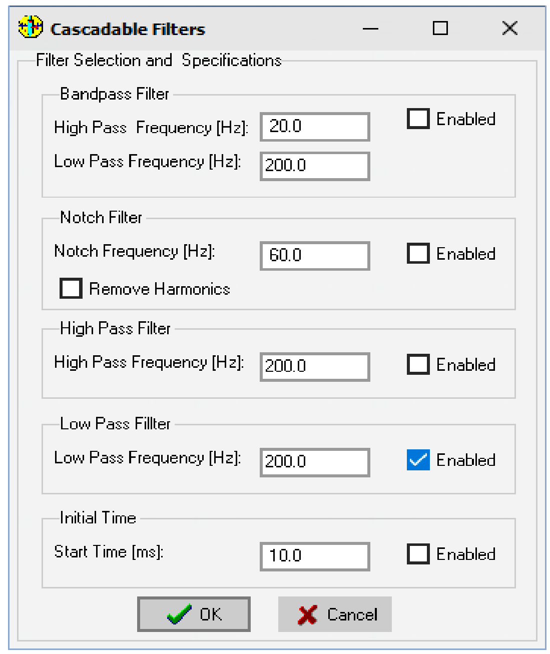

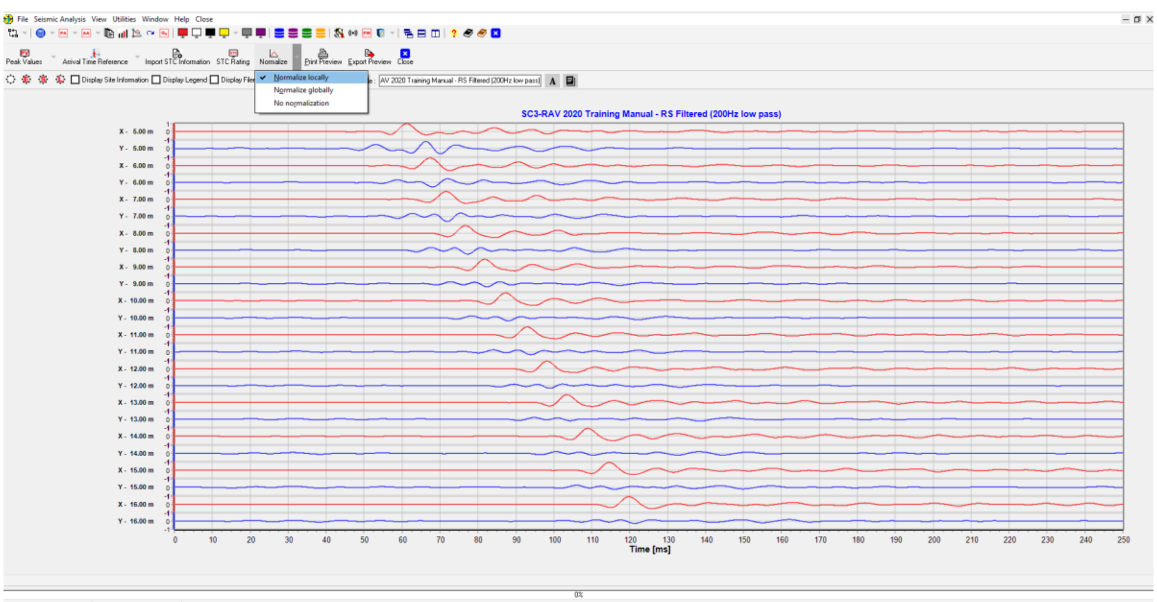

Step 2.3 – Estimate VSP Trend Line Interval Velocities (Right Side)

Perform the following steps:

- Select the following menu options: *View→Seismic Profile Display*.
- In the explorer window that then appears select a consecutive series of 10 – 15 data files from folder Right Side.
- In the *Seismic Profile Parameter Specification* window select that you want to display only the axis associated with the dominant responses as determined in Step 2.2 (see the manual for further details).
- In the same window click on the **Refilter Time Series** button at the top of the window, and in the Cascadable Filters window enable the Low Pass Filter (with typical value of 200 Hz specified). Also specify Start Time if so desired, after which you hit the **OK** button.
- In the *Seismic Profile Parameter Specification* window hit the **Re-display Depth Profile** button at the top of the window. This will generate a graph with seismic data for the dominant component at the various depths. If the chart shows PPs, click the **Display PPs** button at the top of the window to remove them.
- In the graph that is generated beginning at the top signal line, place the cursor on the first or second dominant peak or trough and "middle click" the mouse button. Repeat this operation for the reference peaks or troughs at greater depth, each time "middle clicking" the first or second peak or trough that occurs after the one that was clicked on before.
- The graph labels that will appear give the value for the Right Side Trend Line Estimates at a given depth. This graph can be used to display the simple velocity – depth profile graphically for the right side interval velocity trend lines. It is advised that the data be copied into a table to present the data in tabular form. This will allow for comparisons with trend line interval velocity estimates from the left side of the seismic probe and reverse polarity trend line estimates. Selecting the **Save TLEs** button allows the user to save the trend line estimates to file.

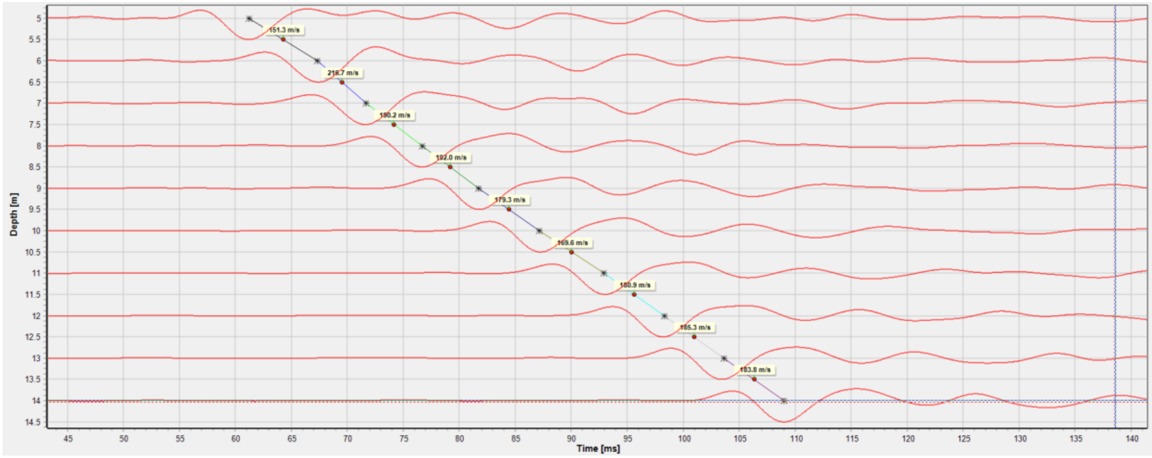

Step 2.4 – Estimate VSP Trend Line Interval Velocities (Left Side)

Perform the following steps:

- Select the following menu options: *View→Seismic Profile Display*.
- In the explorer window that then appears select a consecutive series of 10 – 15 data files from folder Left Side.
- In the *Seismic Profile Parameter Specification* window select that you want to display only the axis associated with the dominant responses as determined in Step 2.2 (see the manual for further details).
- In the same window click on the **Refilter Time Series** button at the top of the window, and in the Cascadable Filters window enable the Low Pass Filter (with typical value of 200 Hz specified). Also specify Start Time if so desired, after which you hit the **OK** button.
- In the *Seismic Profile Parameter Specification* window hit the **Re-display Depth Profile** button at the top of the window. This will generate a graph with seismic data for the dominant component at the various depths. If the chart shows PPs, click the **Display PPs** button at the top of the window to remove them.
- In the graph that is generated beginning at the top signal line, place the cursor on the first or second dominant peak or trough and “middle click” the mouse button. Repeat this operation for the reference peaks or troughs at greater depth, each time “middle clicking” the first or second peak or trough that occurs after the one that was clicked on before.
- The graph labels that will appear give the value for the Left Side Trend Line Estimates at a given depth. This graph can be used to display the simple velocity – depth profile graphically for the left side interval velocity trend lines. It is advised that the data be copied into a table to present the data in tabular form. This will allow for comparisons with trend line interval velocity estimates from the right side of the seismic probe and reverse polarity trend line estimates. Selecting the **Save TLEs** button allows the user to save the trend line estimates to file.

Step 2.5 – Create Reverse Polarized Traces

Perform the following steps:

- Copy the files located in directories '...\Left Side\' and '...\Right Side\' into directory '...\Reverse Polarity\'.
- Select the following menu options: *View→Seismic Profile Display*.
- In the explorer window that then appears select a consecutive series of 10 – 15 data files from Folder '...\Reverse Polarity\'.
- In the *Seismic Profile Parameter Specification* window select that you want to display only the axis associated with the dominant responses as determined in Step 2.2 and select different colors for the traces from the left and those from the right (see the manual for further details).
- In the same window click on the **Refilter Time Series** button at the top of the window, and in the Cascadable Filters window enable the Low Pass Filter (with typical value of 200 Hz specified). Also specify Start Time if so desired, after which you hit the **OK** button.
- In the *Seismic Profile Parameter Specification* window hit the Re-display **Depth Profile button** at the bottom of the window. This will generate a graph with seismic data for the dominant component at the various depths. If the chart shows PPs, click the **Display PPs** button at the top of the window to remove them.

Step 2.6 – Estimate Reversely Polarized Trend Line Interval Velocities

- In the graph generated in Step 2.5 beginning at the top pair of signal lines, place the cursor on the first or second cross-over and “middle click” the mouse. Repeat this operation for the cross-overs at greater depth, each time “middle clicking” the first cross-over that occurs after the one that was clicked on before.
- The graph labels that will appear give the value for the Reversely Polarized Trend Line Estimates at a given depth. This graph can be used to display the simple velocity – depth profile graphically, or the data can be copied into a table to present the data in tabular form. Selecting the **Save TLEs** button allows the user to save the trend line estimates to file.

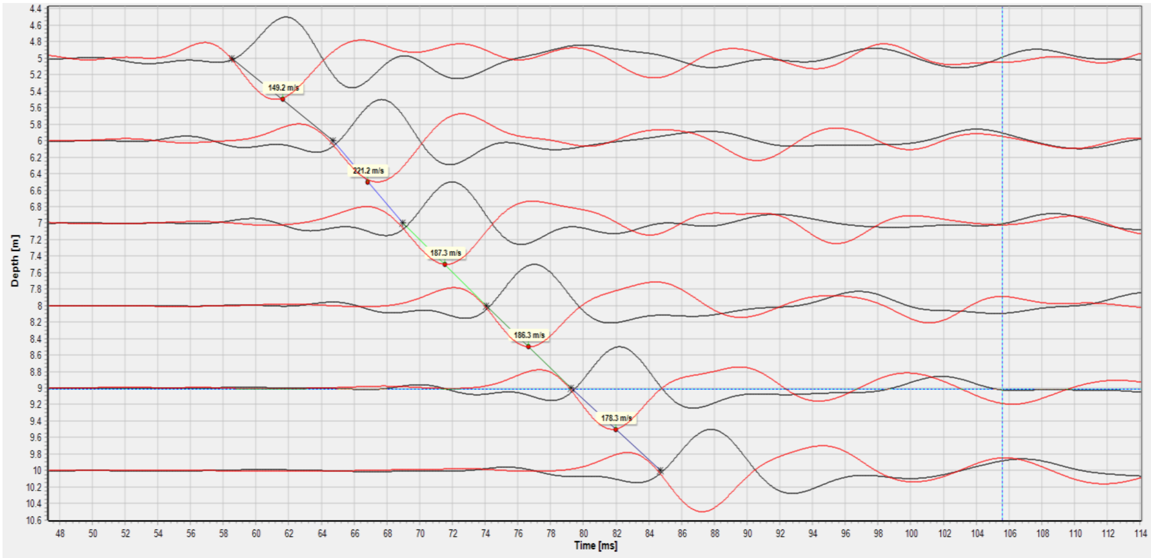

Step 2.7 – Summarize Results

- Present results obtained in Steps 2.3 – 2.6 in tabular form as illustrated below.

Table 1. *SC3-RAV*™ interval velocity estimates utilizing VSPs and trend lines

Interval Depth (m)	Trend Line Velocity Estimate (right side) (m/s)	Trend Line Velocity Estimate (left side) (m/s)	Average Trend Line Velocity Estimate (m/s)	% Difference	Reverse Polarity Velocity Estimate (m/s)
0-5	N/A	N/A	**N/A**	**N/A**	**N/A**
5-6	151.3	154.08	**152.7**	**0.91**	**149.2**
6-7	216.7	206.70	**211.7**	**2.36**	**221.2**
7-8	190.2	193.52	**191.9**	**0.87**	**187.3**
8-9	179.3	184.74	**182.0**	**1.49**	**186.3**
9-10	169.6	173.41	**171.5**	**1.11**	**178.3**
10-11	180.9	180.40	**180.7**	**0.14**	**170.3**
11-12	185.3	174.96	**180.1**	**2.87**	**185.4**
12-13	183.8	188.24	**186.0**	**1.19**	**178.5**
13-14	182.19	182.06	**182.1**	**0.04**	**180.9**
14-15	178.36	185.66	**182.0**	**2.01**	**194.4**
15-16	193.12	189.33	**191.2**	**0.99**	**180.0**
16-17	188.28	182.92	**185.6**	**1.44**	**173.7**
17-18	179.05	176.91	**178.0**	**0.6**	**171.8**
18-19	152.52	165.82	**159.2**	**4.18**	**185.1**
19-20	183.95	197.26	**190.6**	**3.49**	**172.0**
20-21	188.91	187.63	**188.3**	**0.34**	**172.1**
21-22	152.82	156.86	**154.8**	**1.3**	**176.4**
22-23	205.32	178.02	**191.7**	**7.12**	**185.5**
23-24	184.34	178.10	**181.2**	**1.72**	**145.2**

3.0 Estimating Interval Velocities utilizing the Cross-correlation Technique, Batch Job Analysis, and Dominant Responses

Step 3.1 – Data selection

- Perform previously outlined Steps 2.1 and 2.2 to sort files and identify the dominant component responses

Step 3.2 – Estimate Interval Velocities from Right Side

Perform the following steps:

- Select the following menu option: *Seismic Analysis→Interval Velocity Calculation→Cross-correlation Method*.
- In Batch Job Analysis dialog box press button **Begin Processing**.
- In the explorer window that then appears select the desired files to process from the folder Right Side and press button **Open**.

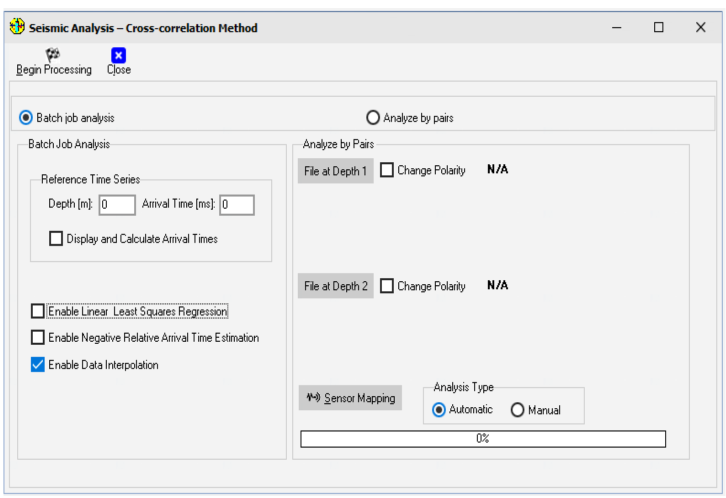

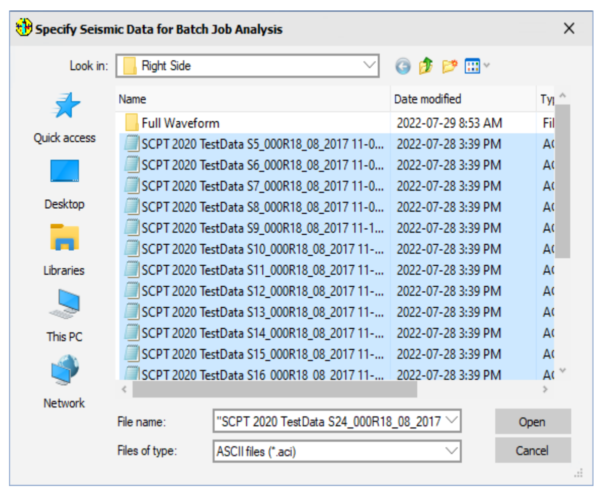

- in the Cascadable Filters window enable the Low Pass Filter (with typical value of 200 Hz specified). Also specify Start Time if so desired, after which you hit the **OK** button.

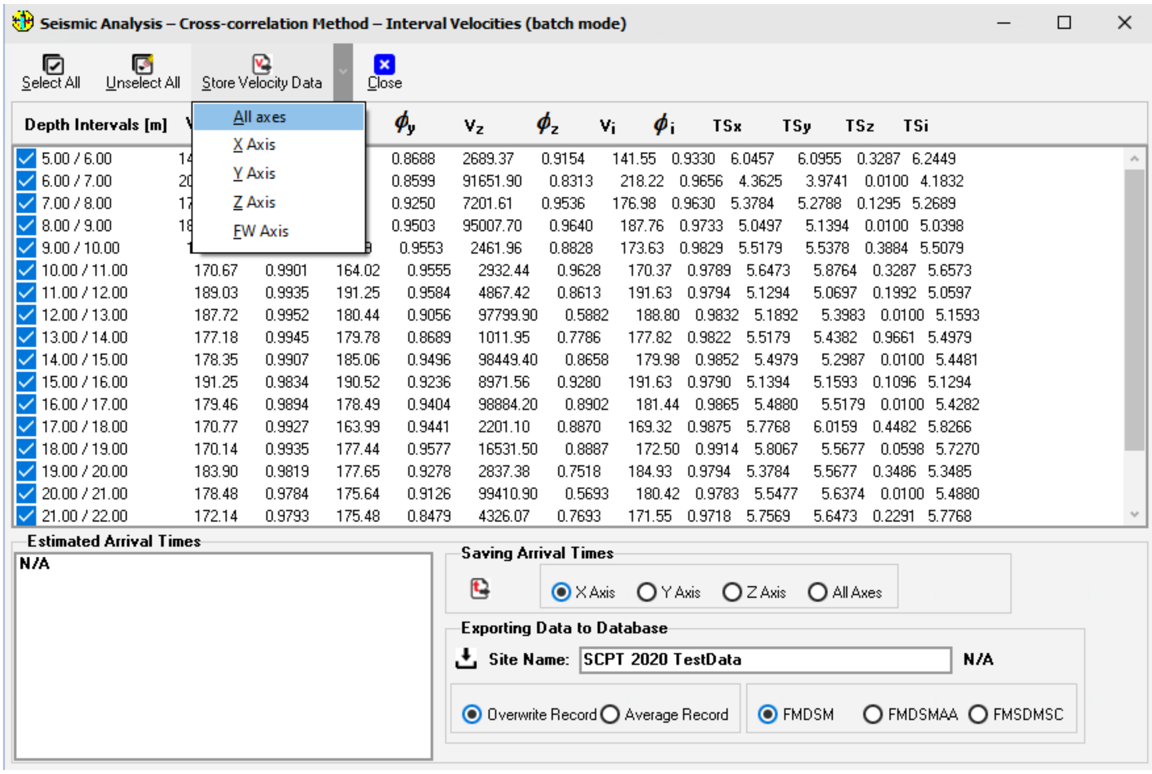

- Store the cross-correlation interval velocity estimates for the component with the dominant responses in a data file and copy into a table to present the data in tabular form as shown in step 3.5 below.

The *Batch Job Analysis* output user interface is thoroughly outlined in the *SC3-RAV™* user's manual. In general terms, *Store Velocity Data* facilitates saving the results to file (eg., for later Interval Velocity profiling (*View->Interval Velocities Display*) or storing in a simplified ASCII format) by putting check marks next to the values to be saved (all the results can be selected automatically be selecting the check button *Select All*) and selecting the *Store Velocity Data* drop down buttton. Selecting option *Store Velocity Data->All axes* outputs the *SC3-RAV™* user interface for storing the estimated interval velocities formatted for displaying with option *View->Interval Velocities Display*.

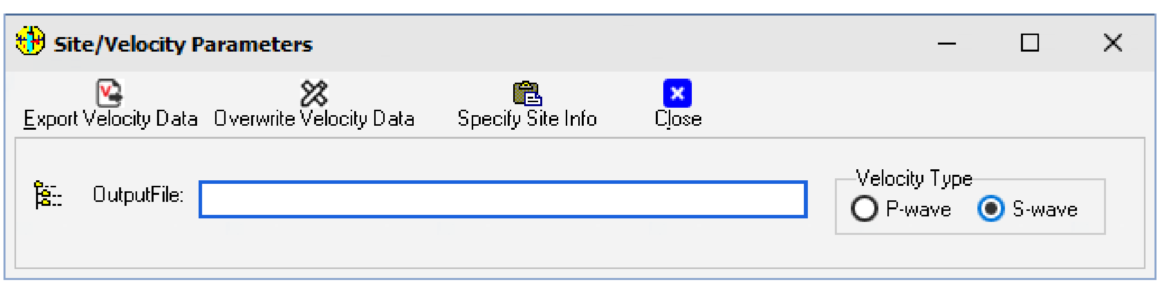

Store Velocity Data dropdown button options X axis, Y axis, Z axis, and FW axis allow for the user to save interval velocity estimates of the All, X, Y, Z, or FW axis in a simplified format. This option is provided so that output can be generated, which can be easily incorporated into a Word® table or Excel® spread sheet. The user simply selects the appropriate axis to store and then user interface is provided for specification of the single axis velocity filename In this interface the *FW axis* refers to the estimated interval velocities, which were calculated based upon the absolute amplitude $\rho(t) = \sqrt{x(t)^2 + y(t)^2 + z(t)^2}$. This is not the same as the full waveform obtained from *Polarization Analysis* and mapped to the X axis.

Step 3.3 – Estimate Interval Velocities from Left Side

- Perform the same action items outlined in Step 3.2, but now with files selected from the folder Left Side.

Step 3.4 – Estimate Interval Velocities Utilizing LLSR

- The *SC3-RAV^{TM}* program also allows the user to perform this analysis while applying at the same time a Linear Least Square Regression (LLSR). Using this option results in smoothing highly variable adjacent interval velocities (please see *SC3-RAV^{TM}* user's manual for more detail).

  To activate this option the user should check the Enable Linear Least Squares Regression within the Batch Job Analysis dialog box and input the reference depth (5 m) and arrival time (54 ms) as outlined in Section 4.4., after which the procedure described in either step 3.2 or 3.3 can be followed.

Step 3.5 – Summarize Results

- Present results obtained in Steps 3.2 – 3.4 in tabular form as illustrated below.

Table 2. *SC3-RAV™* Interval velocity estimates (Cross-correlation Technique LLSR)

Interval Depth (m)	CCT Right Side (m/s)	CCT Left Side (m/s)	Average CCT (m/s)	% Difference	LLSR Right Side (m/s)	LLSR Left Side (m/s)	Average LLSR (m/s)	% Difference
0-5	N/A	N/A	N/A	**N/A**	N/A	N/A	N/A	N/A
5-6	146.450	147.180	**146.8**	**0.25**	171.030	172.430	171.7	**0.41**
6-7	208.770	211.670	**210.2**	**0.69**	171.030	172.430	171.7	**0.41**
7-8	173.050	182.850	**178.0**	**2.75**	180.080	182.960	181.5	**0.79**
8-9	187.760	183.060	**185.4**	**1.27**	180.080	182.960	181.5	**0.79**
9-10	173.310	171.460	**172.4**	**0.54**	172.130	175.080	173.6	**0.85**
10-11	170.970	178.870	**174.9**	**2.26**	172.130	175.080	173.6	**0.85**
11-12	189.030	175.400	**182.2**	**3.74**	188.180	181.140	184.7	**1.91**
12-13	187.360	187.360	**187.4**	**0**	188.180	181.140	184.7	**1.91**
13-14	177.180	178.150	**177.8**	**0.27**	177.760	181.850	179.8	**1.14**
14-15	178.350	185.750	**182.1**	**2.03**	177.760	181.850	179.8	**1.14**
15-16	190.880	192.370	**191.6**	**0.39**	185.110	185.970	185.5	**0.23**
16-17	179.790	180.120	**180.0**	**0.09**	185.110	185.970	185.5	**0.23**
17-18	170.770	174.080	**172.4**	**0.96**	170.450	170.580	170.5	**0.04**
18-19	170.140	167.270	**168.7**	**0.85**	170.450	170.580	170.5	**0.04**
19-20	183.900	197.430	**190.7**	**3.55**	181.130	188.410	184.8	**1.97**
20-21	178.480	180.420	**179.5**	**0.54**	181.130	188.410	184.8	**1.97**
21-22	171.850	166.950	**169.4**	**1.45**	177.680	169.130	173.4	**2.47**
22-23	184.060	171.390	**177.7**	**3.56**	177.680	169.130	173.4	**2.47**
23-24	195.380	171.210	**183.3**	**6.59**	195.380	171.210	183.3	**6.59**

4.0 Estimating Interval Velocities utilizing Batch Polarization Analysis, Batch Signal Decay and Iterative Forward Modeling (Advanced Technique)

To make full use of the recorded triaxial data, the data acquired on the x, y and z axis is rotated onto the full waveform axis utilizing batch Polarization Analysis (PA), which dramatically increases the signal-to-noise ratio. In addition, PA allows the investigator to apply BCE's proprietary Seismic Trace Characterization (STC) technique (see Appendix 2). By applying Source Wave Signature Isolation (SWSI) as well any outliers from the peak source wave responses are removed so that possible reflections and systematic noise is minimized.

The ability to dramatically increase the probability of identifying and quantifying critical layers utilizing SCPT can be achieved by applying larger than normal sensor-source radial offsets and implementing analysis techniques which incorporate Fermat's principle such as the FMSDM provided within *SC3-RAV™*. By doing this the source wave can refract and travel within critical layers for an extended time, dramatically increasing characterization of the layer or depth under analysis. In addition, larger than normal offsets allows for greater SCPT vertical resolution because small depth increments are feasible.

Step 4.1 – Sort Data

- Perform previously outlined Steps 2.1 and 2.2 to sort files and identify the dominant component responses

Step 4.2 – Implement batch Polarization Analysis (PA)

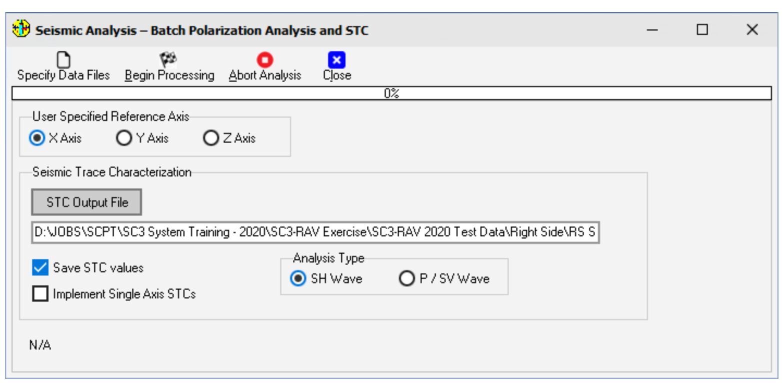

- Implement *SC3-RAV™* software option *Seismic Analysis→ Polarization Analysis and Seismic Trace Classification→Batch Processing* on data moved to directories '...\Right Side\' and '...\Left Side\' . This option allows for the rotation of the SH source wave responses onto the Full Waveform Axis (FWA). Once the software option is selected a dialog box appears, which allows the user to define a specific Reference Axis (dominant source wave responses). Specify a text data file to store the estimated STCs (e.g., 'RS STC.txt') and specify the Analysis Type (i.e., SH Wave or P/SV Wave). The estimated STCs should be presented in Tabular form.

A typical STCs output file is illustrated below:

Depth [m]	LIN [0-1]	SSP [0-1]	CCC [0-1]	PSD [0-1]	SNR [0-1]	STC [A-F]
5	0.6184	0.63	0	0.87	0.93	N/A
6	0.8386	0.691	0.9221	0.93	0.98	D
7	0.8111	0.642	0.9528	0.93	0.98	B
8	0.776	0.612	0.9688	0.83	0.98	B
9	0.8193	0.57	0.9761	0.85	0.98	B
10	0.8512	0.615	0.984	0.81	0.98	B
11	0.8332	0.641	0.9905	0.9	0.98	A
12	0.8542	0.612	0.9946	0.91	0.98	A
13	0.8865	0.61	0.9904	0.85	0.98	A
14	0.8577	0.604	0.9934	0.83	0.98	A
15	0.8578	0.595	0.9895	0.9	0.98	B
16	0.8612	0.65	0.9822	0.92	0.98	A
17	0.8544	0.653	0.986	0.93	0.98	A
18	0.8171	0.672	0.9931	0.93	0.98	A
19	0.8263	0.624	0.9935	0.93	0.98	B
20	0.8522	0.618	0.9826	0.93	0.98	B
21	0.8099	0.557	0.9772	0.93	0.98	D
22	0.8941	0.507	0.9775	0.93	0.98	D
23	0.8248	0.577	0.9787	0.93	0.98	D
24	0.8386	0.488	0.9375	0.93	0.98	D

SSP Values which drop below the 0.57 threshold value will automatically result in STC 'D' values. This is a flag that the traces may require time windowing via option *Seismic Analysis→ Source Wave Signature Isolation*.

Next the user select the **Select Data Files** button, which allows the user to select the files to have full waveform conversion applied. Once the files for full waveform conversion have been selected press button **Begin Processing**. The Cascadable Filters dialog box appears so that the user can specify desired filters. Once the files are converted they are stored in directories '...\Left Side\Full Waveform\' or '...\Right Side\Full Waveform\'. The files are renamed with extension '_FW' appended to the file name. For example, file SCPT408S1_0R3-6-2010 8-29-15.aci is renamed to SCPT408S1_0R3-6-2010 8-29-15_FW.aci.

The SH full waveforms are stored on the X axis on the rotated trace (i.e., only the X axis (FWA) for file SCPT408S1_0R3-6-2010 8-29-15_FW.aci should be analyzed). The results of the file rotation is evident by analyzing the trace utilizing *SC3-RAV™* software option *View→ Display X-Y-Z-Full Waveform VSP* with option *Normalize Locally* enabled. Compared to the “Before” the amplitudes of the Y axis trace will be much smaller in the “After” as the full wave form displayed on the X axis in the “After” is much stronger than the original X axis wave as illustrated below.

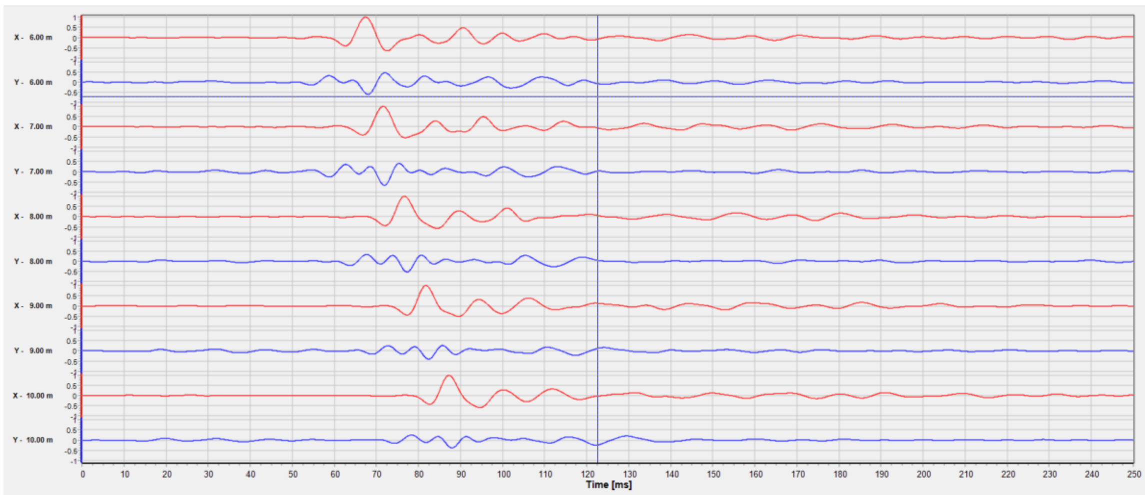

View→ Display X-Y-Z-Full Waveform VSP **with option *Normalize Locally* enabled displaying vertical seismic profile “before” batch polarization**

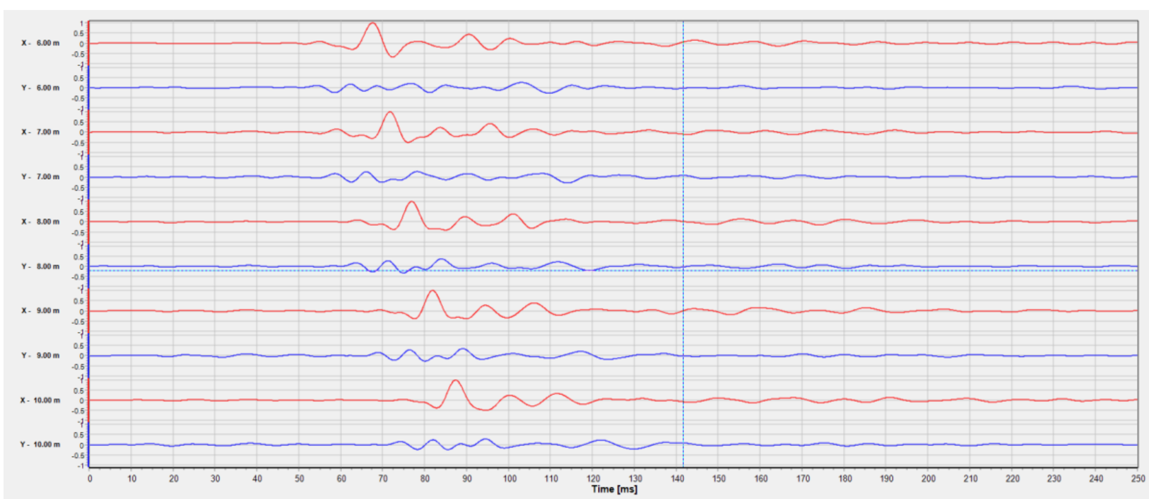

View→ Display X-Y-Z-Full Waveform VSP **with option *Normalize Locally* enabled displaying vertical seismic profile “after” batch polarization**

Only FWA traces should be used if the associated LIN ≥ 0.8. For the RS data set traces recorded at 5m and 8m have LIN values < 0.8. In this case the X Axis responses will be required at these depths when estimating interval velocities. The user should verify that the LIN values are for the seismic source wave responses and not from relatively higher amplitude measurent noise. This is readily done by plotting both the FWA traces and associated X/Y original traces within *View→ Display X-Y-Z-Full Waveform*. This is shown below.

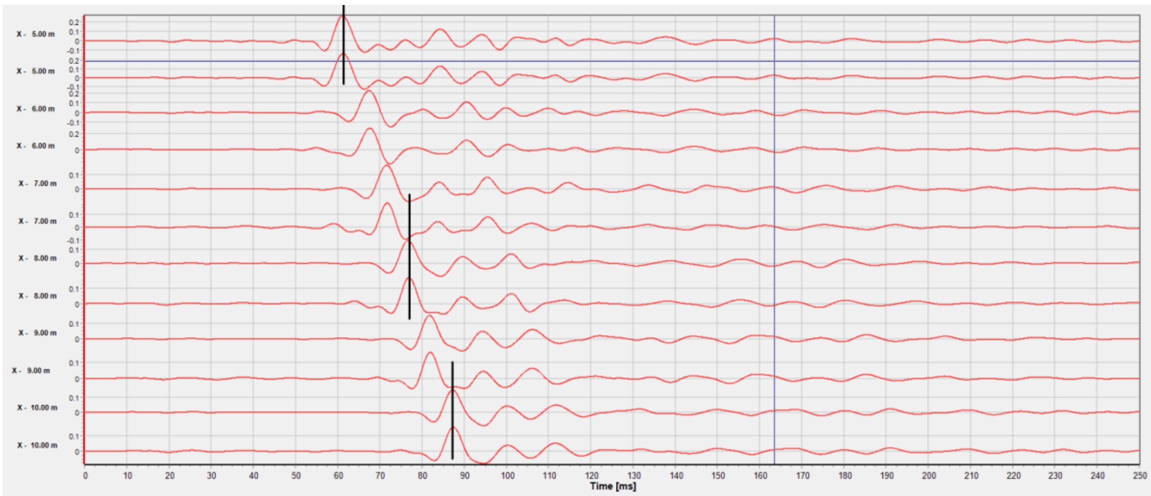

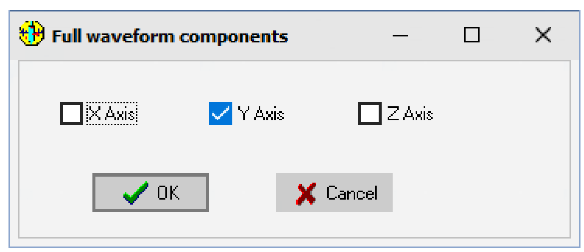

The investigator can readily process mixed FWA (LIN ≥ 0.8) and dominant X axis (LIN < 0.8) responses for a specific profile and RS/LS polarity by simply copyng the relevant files to a working directory (e.g., copy original X axis traces from depths 5m and 8m to directory directories '...\Right Side\Full Waveform\').

When utilizing mixed FWA (LIN ≥ 0.8) and dominant Y axis (LIN < 0.8) traces for a specific profile and RS/LS polarity it is first necessary to map the Y Axis responses onto the FWA. In this process *Utilities→Full waveform* components should be selected and X Axis and Z Axis boxes unchecked. Next implemenet *Seismic Analysis→ Polarization Analysis and Seismic Trace Classification→Batch Processing* where the Y Axis is selected as the reference axis and *Save STC Values* is unchecked. Next Specify Data Files for the Y Axis traces to be rotated onto the FWA and select *Begin Processing*. After rotation of the desired Y Axis responses onto the FWA it is necessary that the user recheck the X Axis and Z Axis check boxes in *Utilities→Full waveform components* interface.

Step 4.3 – Implement Source Wave Signature Isolation

- Implement *SC3-RAV™* software option *Seismic Analysis→Source Wave Feature Isolation (SWFI)* on FWA data located in directories '...\Right Side\Full Waveform\' and '...\Left Side\Full Waveform\'. This option allows for further Signal-to-Noise Ratio (SNR) improvement by removing responses due to possible source wave reflections or "unclean" SH source hammer impacts. In general terms, it allows isolation of trending source wave features (i.e, peak or trough). *SWFI* software option *Batch analysis type* without *Enable user defined feature checked* determines the time index, t*, which is the location of the absolute maximum amplitude of the seismic trace under analysis. An exponential decay is then applied at the second zero crossing from t* for both the front end and back end of the trace. Please see SC3-RAV user's manual and Appendix 3 for further details of the *SWFI* software options.

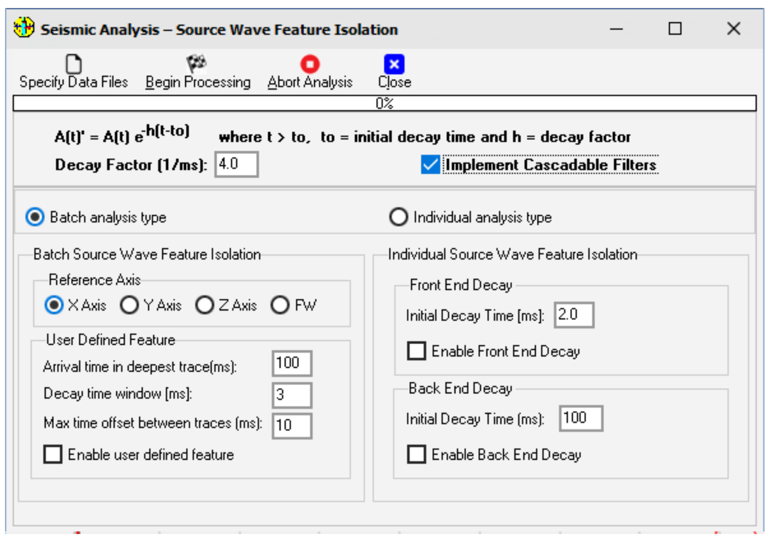

Upon selecting software option *SWFI* the user interface illustrated to the left appears. The *Decay Factor* is defaulted to 4.0. As the *Decay Factor* is increased there is a sharper decay of the time series. User interface *Reference Axis* allows for the specification of the reference axis (X Axis, Y Axis, Z axis, and FW Axis), from which the time index, t*, location of the absolute maximum amplitude of the seismic trace under analysis is determined. In addition, the user specified *Reference Axis* instructs the algorithm which axis SWFI should be applied to.

The user presses button **Select Data Files** and selects the files to have signal decay applied (from directories '...\Left Side\Full Waveform\' and '...\Right Side\FullWaveform\'). The files which have had the *SWFI* standard *Batch analysis type* are stored in directories '...\Left Side\Full Waveform\FIB\' and '...\Right Side\Full Waveform\FIB\'. The files are renamed with extension '_GSD' appended to the file name. For example, file SCPT408S1_0R3-6-2010_8-29-15_FW.aci is renamed to SCPT408S1_0R3-6-2010_8-29-15_FW_GSD.aci. When processing the Full Waveform data a specification of a *Cascadable Filter* is not required because a filter has already been applied during the batch PA process. In addition, the Reference Axis should be specified as the X Axis.

The figure below illustrates the VSP output after applying software option *FW SWFI* standard *Batch analysis type*. As is evident, the seismic SH source wave pulse (trending peak) has been isolated.

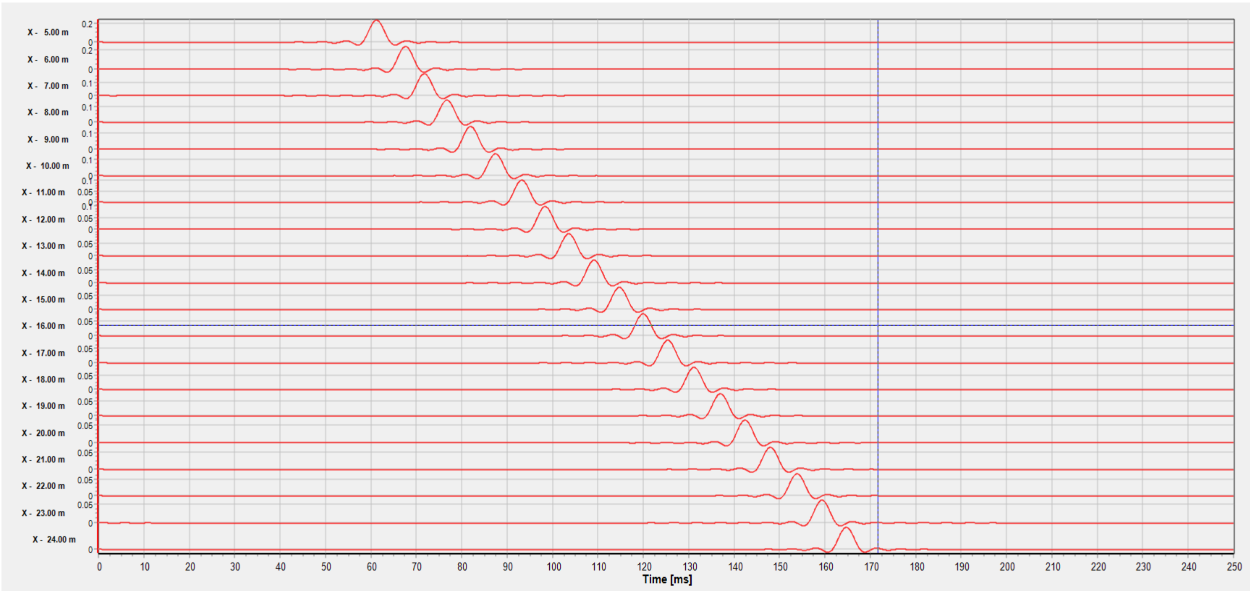

The figures below shows the application of *Start Time* within software option *Seismic Analysis→ Source Wave Signature Isolation→ Standard Batch analysis type*. In the figure on the left a VSP is displayed where there is a strong seismic response (within 20 ms) prior to the arrival of the desired SH wave (starting at approximately 60 ms at depth 12m. The figure on the right shows the VSP after the application of *Start Time = 60 ms*.

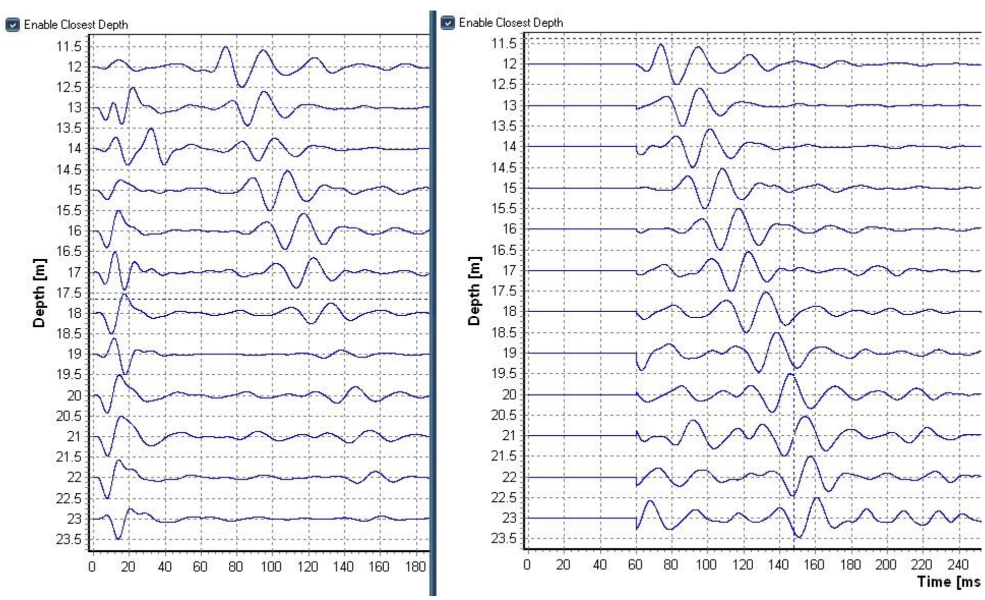

Step 4.4 – Estimate Reference Arrival Time

Perform the following steps:

- Select the following menu options: *View→Seismic Profile Display* or *View→X-Y-Z-FW Seismic Profile Display.*
- In the explorer window that then appears select a consecutive series of the shallowest 1 – 5 data files from folder '...\Reverse Polarity\' where the Right Side and Left Side traces have been copied to. A reference trace is utilized were a “clean” source wave is present. It should be noted that near surface source waves are significantly more susceptible to refraction which contaminates the recorded seismogram; therefore, the first “clean” near surface trace with minimal evidence of refraction is utilized. In the Cascadable Filters window a relatively higher low pass frequency (e.g., 400Hz or greater) is specified so that the signal definition at first break is retained. Select the reference trace at a depth (starting at near surface) where a clear arrival is present.
- In the Seismic Profile Parameter Specification window select that you want to display only the axis associated with the dominant component and select different colors for the traces from the left and those from the right (see the manual for further details).
- In the same window click on the **Refilter Time Series** button at the top of the window, and in the Cascadable Filters window do not enable any of the digital filters. Hit the **OK** button.
- In the Depth Profile Parameter Specification window hit the **Re-display Depth Profile** button at the top of the window. This will generate a graph with seismic data for the dominant component at the various depths. If the chart shows PPs, click the **Display PPs** button at the top of the window to remove them.
- From the unfiltered VSP plot, identify seismic waves from a specific depth, *Arrival Depth*, which have source waves with the highest signal to noise ratio (e.g., seismic waves at depth 5m in VSP plot illustrated below (note that this DST started at a depth of 5 m).

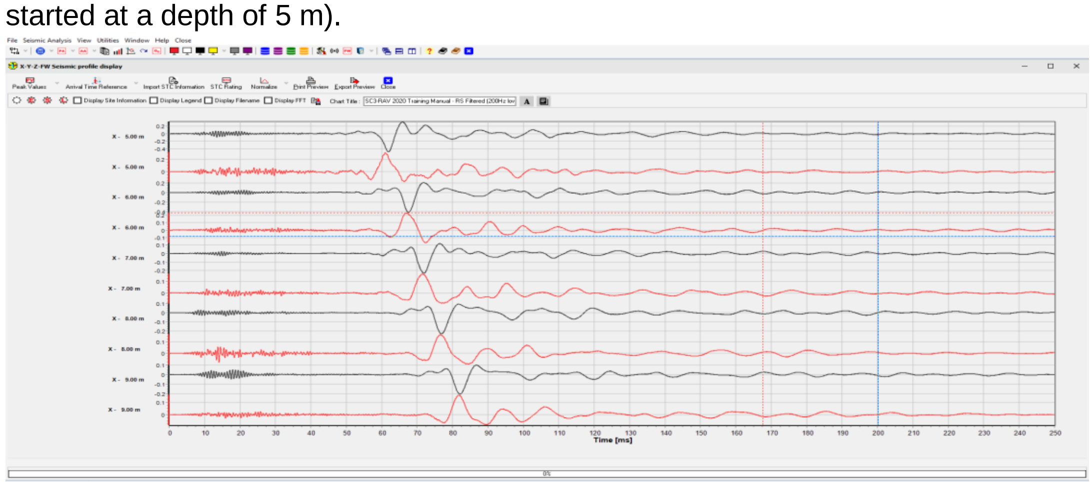

- In the same window click on the **Refilter Time Series** button at the top of the window, and in the Cascadable Filters window enable the Low Pass Filter (typically with a cut-off frequency of 400 to 500 Hz). Also specify Start Time if so desired, after which you hit the **OK** button.
- In the Depth Profile Parameter Specification window hit the **Re-display Depth Profile** button at the top of the window.
- In the filtered VSP plot, zoom-in on the seismic traces at the *Arrival Depth* by clicking the left mouse button while scrolling in with the mouse. Quantify the first break arrival time by placing the cross-hairs at the first break (e.g., 55ms at 5m for VSP plot shown below). Make note of *Arrival Depth* and corresponding *Arrival Time*.

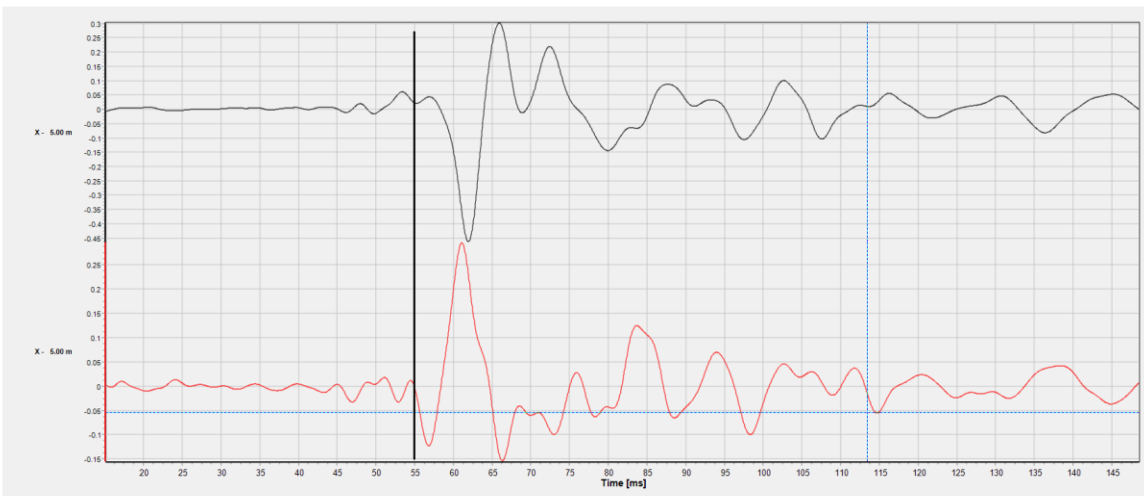

Step 4.5 – Estimate Arrival Times and Enter Data into the Database

- Implement *SC3-RAV™* software option *Seismic Analysis→Interval Velocities→Crosscorrelation Technique* on FWA signal decayed data located in directories '...\Right Side\Full Waveform\GSD\' and '...\Left Side\Full Waveform\GSD\' so that source wave arrival times can be determined. The arrival times are utilized within the FMDSM technique.

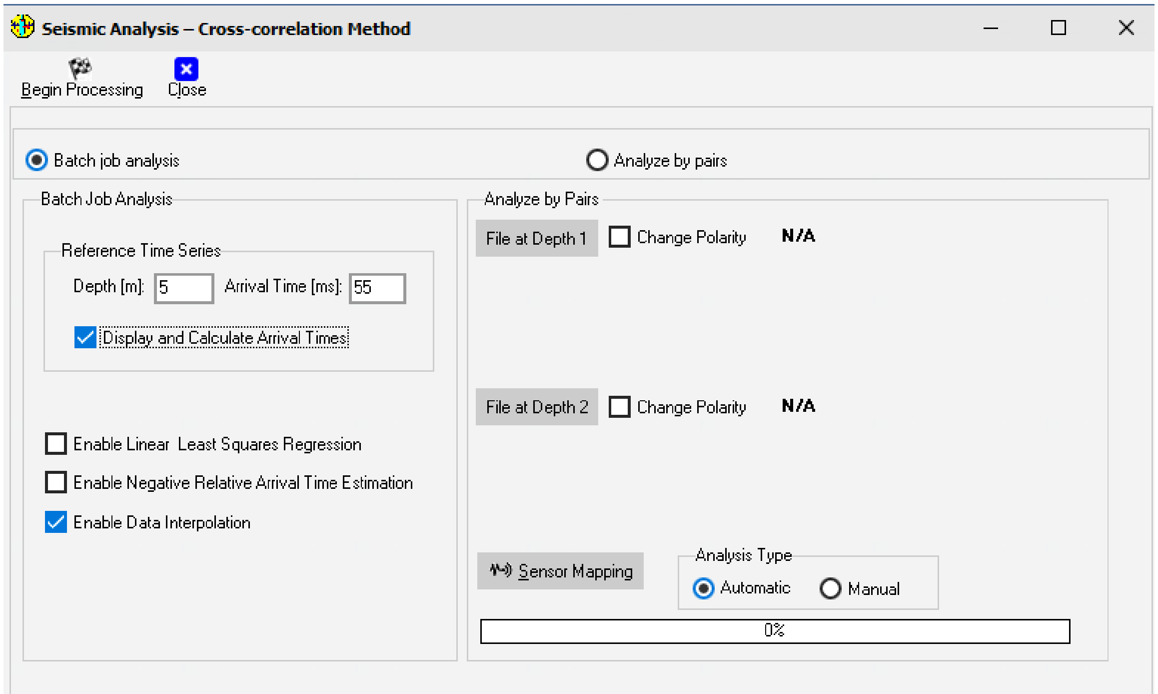

As illustrated above and outlined in the *SC3-RAV*™ user's manual, fundamental inputs for the FMDSM technique are the referenced arrival time and the corresponding depth. The reference depth (5m) and arrival time (55ms) values are inputted in the *Batch Job Analysis* interface. The reference depth and time for both the 'Right Side' and Left Side' should be fairly close in value. Option *Display and Calculate Arrival Times* is also checked.

In the *Batch Job Analysis* panel select button **Begin Processing**. Once the *Begin Processing* button is selected the file input dialog box user interface appears, where the user selects the files to have arrival times calculated from either the '...\Right Side\Full Waveform\GSD\' directory or '...\Left Side\Full Waveform\GSD\' depending upon the reference depth and time.

The *Batch Job Analysis* output is illustrated below for the processed filtered traces residing in directory '...\Right Side\Full Waveform\GSD\'. In the top box the estimated interval velocities are listed (using a BCE patented crosscorrelation technique) whereby a straight ray trajectory is assumed. Again only the FWA X axis results are of interest. The bottom list box displays the estimated arrival times based upon the user specified reference depth and arrival time and crosscorrelation calculated relative arrival times.

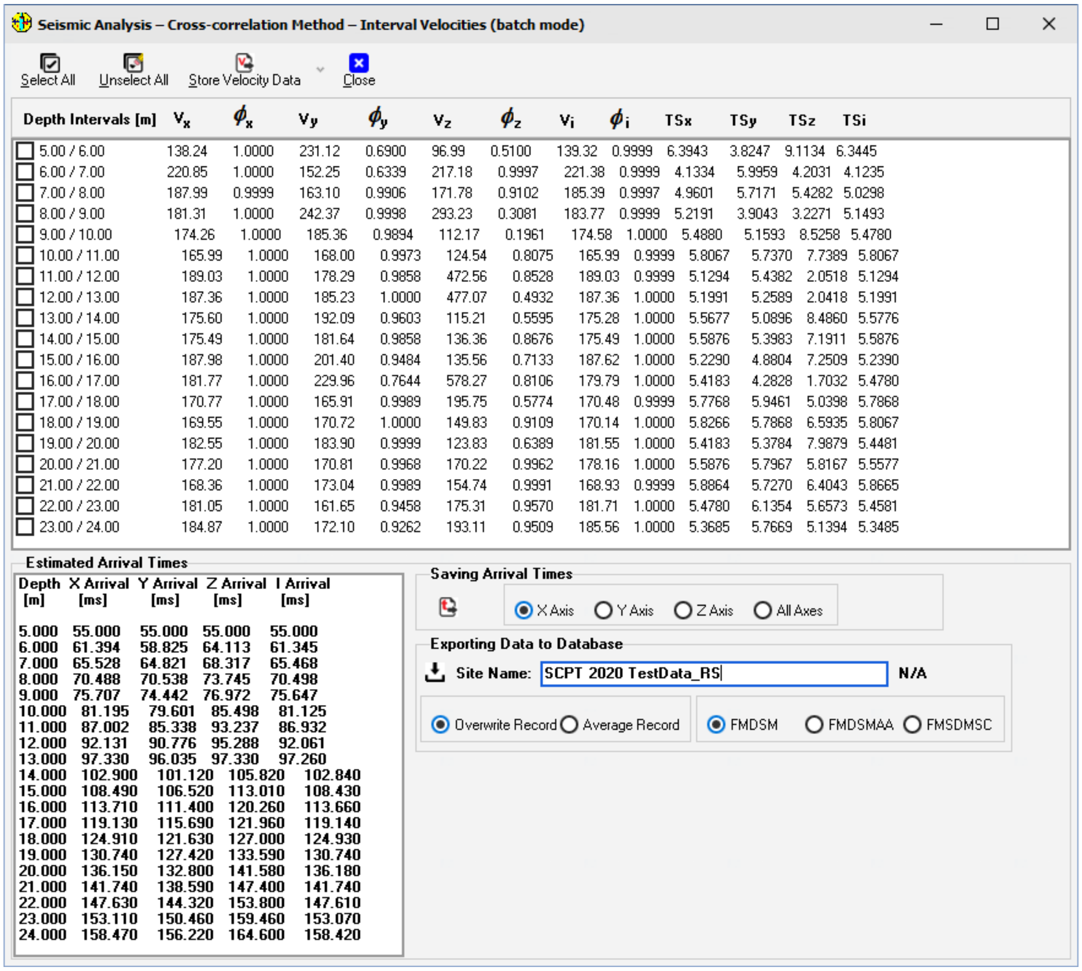

The ability to export the estimated arrival times to the FMDSM database provides significant post processing time saving. The *SC3-RAV*™ software extracts the site name from a *SC*-DAC*™ file based upon the automatic file naming convention as previoulsy outlined. The extracted *Site Name* is placed within text box *Site Name*. The user can readily modify or change the *Site Name*. In the above example, the Site Name has RS appended to the site name to denote the right side estimates. Button facilitates exporting estimated arrival times to the FMDSM database. In the automated SH wave high-spec batch job analysis the user first processes the data set on the '...\Right Side\Full Waveform\GSD\' directory. Option *Overwrite Record* is selected (default setting) and button is pressed (with FWA (X axis) selected for export). The corresponding X axis arrival times are then copied to the FMDSM database with measurement weights set 1. Note that user interface radio button options X Axis, Y Axis, Z Axis and All Axes allow for copying the X Axis, Y Axis, Z Axis and absolute amplitude $\rho(t) = \sqrt{x(t)^2 + y(t)^2 + z(t)^2}$ Axis arrival times, respectively, to the FMSDM database.

Next the estimated X axis arival times from the dataset located under directory '...\Right Side\Full Waveform\GSD\' are exported to the FMDSM database with option *Overwrite Record* selected and RS appended to the site name. This will allow for the right side and left side interval velocities to be compared. An example FMDSM database with the above process implemented is illustrated below.

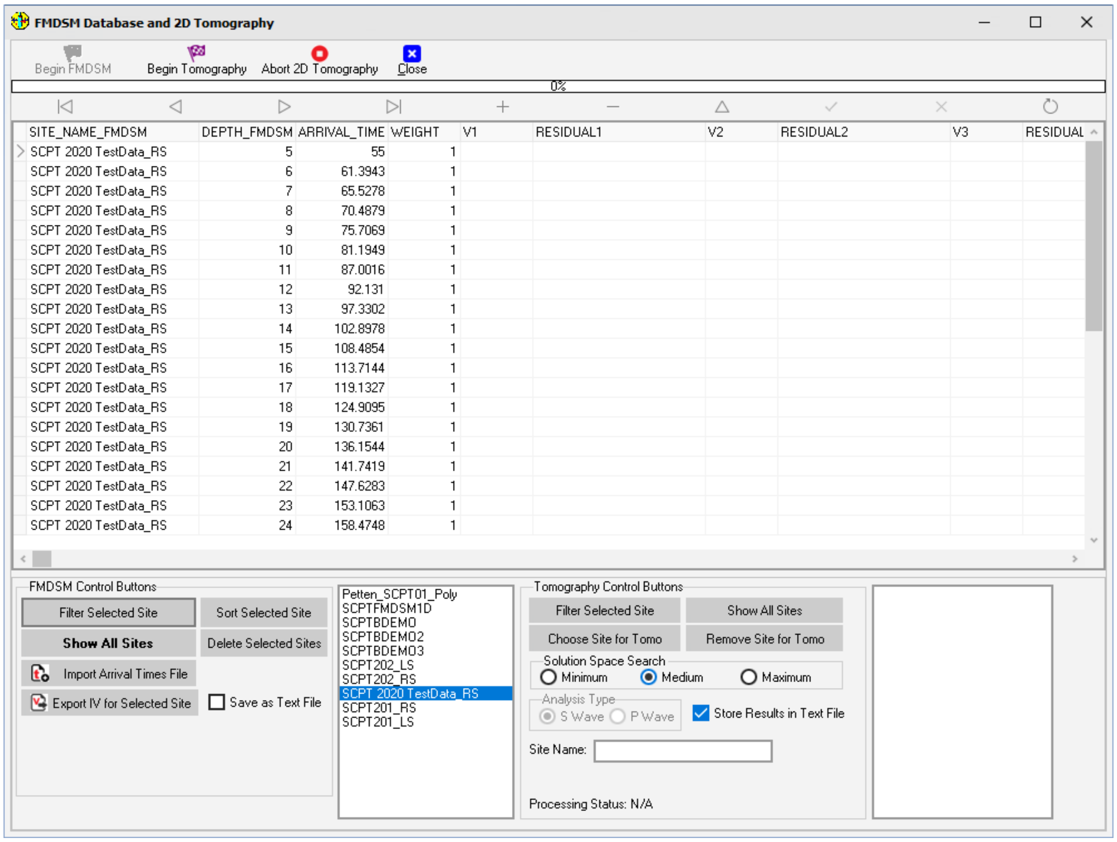

- Implement *SC3-RAV™* software option *Seismic Analysis→Interval Velocities→FMDSM* on the previously saved arrival times from datasets located under directories directories '...\Right Side\Full Waveform\GSD\' and '...\Left Side\Full Waveform\GSD\'. The user specifies the source *Radial* Offset, source *Depth* offset within the FMDSM graphical user interface. Next the user selects the FMDSM **Database** button so that the appropriate database can be selected from the FMDSM database as outlined in the *SC3-RAV™* user's manual. In the above example database SCPT 2020 TestData_RS has been selected. The user then presses button **Begin Processing**. The figure below illustrates the FMDSM output, which graphically shows the estimated interval velocities and corresponding ray tracing of the travel path of the source waves to the downhole seismic sensors.

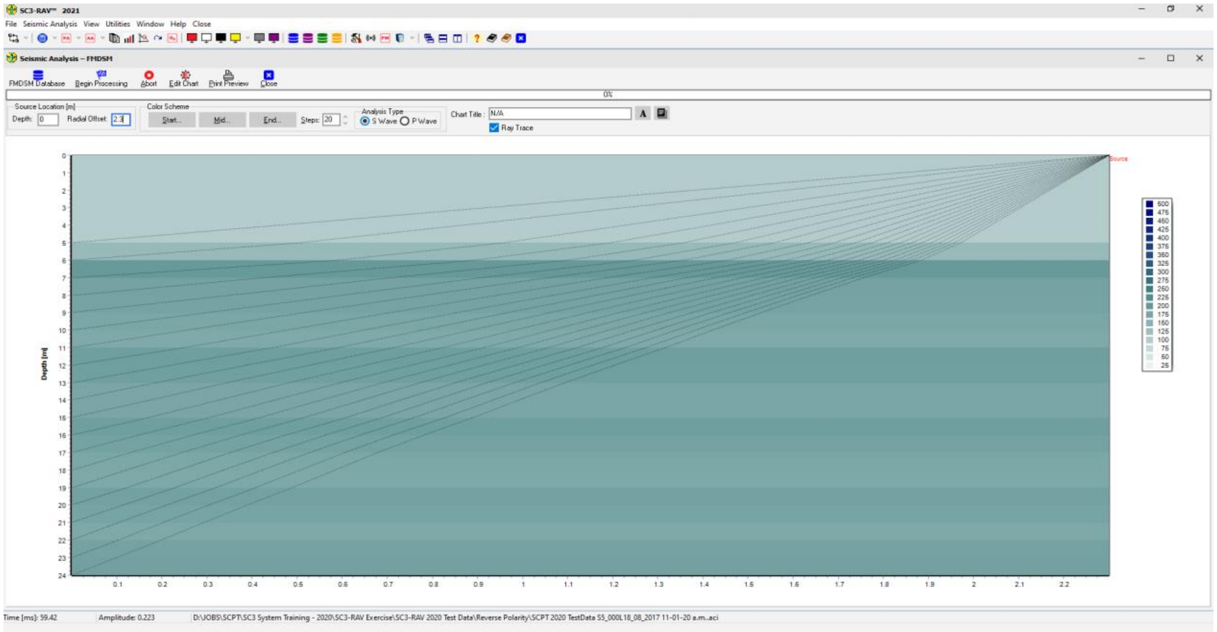

Reselecting the **FMDSM Database** button will result in the reopening of the FMDSM database with the estimated interval velocities displayed as shown below. The results given below are tabulated and submitted to the client along with the right side results.

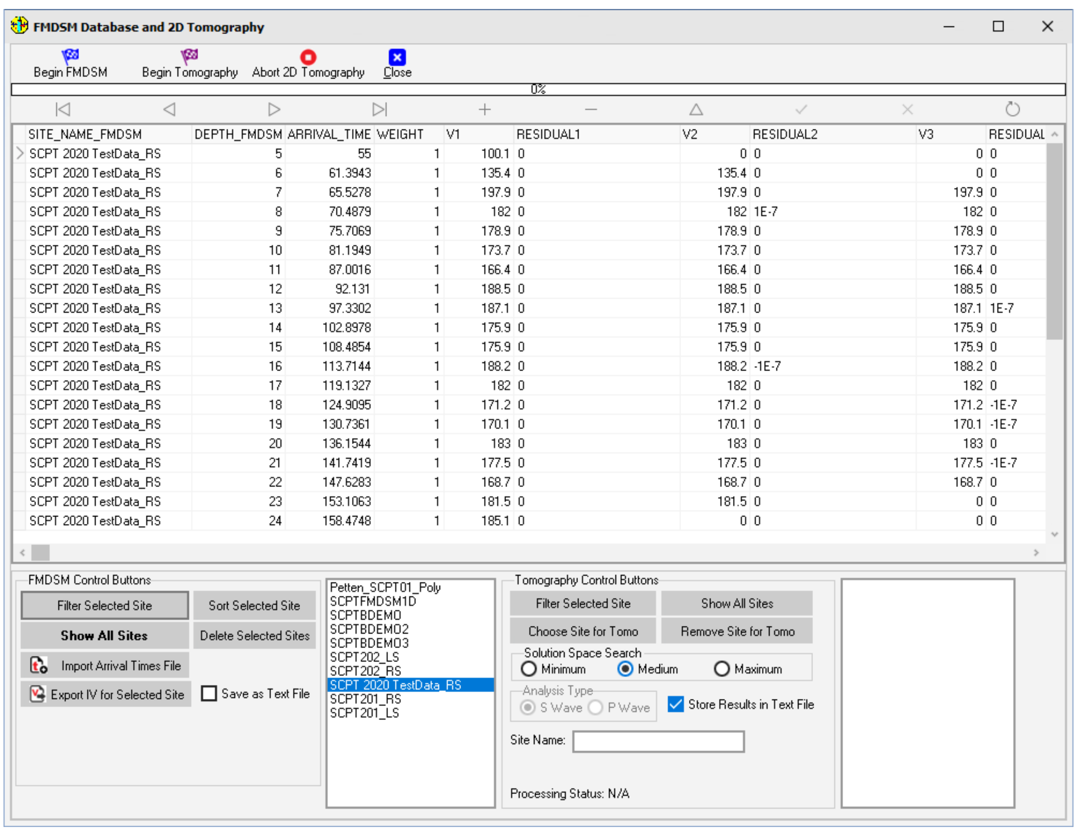

SITE_NAME_FMDSM	DEPTH_FMDSM	ARRIVAL_TIME	WEIGHT	V1	RESIDUAL1	V2	RESIDUAL2	V3	RESIDUAL
SCPT 2020 TestData_RS	5	55	1	100.1	0	0	0	0	0
SCPT 2020 TestData_RS	6	61.3943	1	135.4	0	135.4	0	0	0
SCPT 2020 TestData_RS	7	65.5278	1	197.9	0	197.9	0	197.9	0
SCPT 2020 TestData_RS	8	70.4879	1	182	0	182	1E-7	182	0
SCPT 2020 TestData_RS	9	75.7069	1	178.9	0	178.9	0	178.9	0
SCPT 2020 TestData_RS	10	81.1949	1	173.7	0	173.7	0	173.7	0
SCPT 2020 TestData_RS	11	87.0016	1	166.4	0	166.4	0	166.4	0
SCPT 2020 TestData_RS	12	92.131	1	188.5	0	188.5	0	188.5	0
SCPT 2020 TestData_RS	13	97.3302	1	187.1	0	187.1	0	187.1	1E-7
SCPT 2020 TestData_RS	14	102.8978	1	175.9	0	175.9	0	175.9	0
SCPT 2020 TestData_RS	15	108.4854	1	175.9	0	175.9	0	175.9	0
SCPT 2020 TestData_RS	16	113.7144	1	188.2	0	188.2	-1E-7	188.2	0
SCPT 2020 TestData_RS	17	119.1327	1	182	0	182	0	182	0
SCPT 2020 TestData_RS	18	124.9095	1	171.2	0	171.2	0	171.2	-1E-7
SCPT 2020 TestData_RS	19	130.7361	1	170.1	0	170.1	0	170.1	-1E-7
SCPT 2020 TestData_RS	20	136.1544	1	183	0	183	0	183	0
SCPT 2020 TestData_RS	21	141.7419	1	177.5	0	177.5	0	177.5	-1E-7
SCPT 2020 TestData_RS	22	147.6283	1	168.7	0	168.7	0	168.7	0
SCPT 2020 TestData_RS	23	153.1063	1	181.5	0	181.5	0	0	0
SCPT 2020 TestData_RS	24	158.4748	1	185.1	0	0	0	0	0

The light green background below is a visual indicator that FMDSM estimated RS and LS interval velocities have percent differences < 10% and are highly reliable.

Table 3. ***SC3-RAV***^{TM} **FMDSM interval velocity estimates**

Interval Depth (m)	FMDSM Right Side (m/s)	FMDSM Left Side (m/s)	Average FMDSM (m/s)	% Difference
0-5	100.1	100.1	**100.1**	**2.34**
5-6	135.4	141.9	**138.7**	**1.57**
6-7	197.9	191.8	**194.9**	**1.42**
7-8	182	176.9	**179.5**	**0.33**
8-9	178.9	180.1	**179.5**	**1.02**
9-10	173.7	170.2	**172**	**3.51**
10-11	166.4	178.5	**172.5**	**3.32**
11-12	188.5	176.4	**182.5**	**0.27**
12-13	187.1	186.1	**186.6**	**0.79**
13-14	175.9	178.7	**177.3**	**2.49**
14-15	175.9	184.9	**180.4**	**0.74**
15-16	188.2	191	**189.6**	**0.72**
16-17	182	179.4	**180.7**	**0.61**
17-18	171.2	173.3	**172.3**	**0.68**
18-19	170.1	167.8	**169**	**3.99**
19-20	183	198.2	**190.6**	**0.06**
20-21	177.5	177.7	**177.6**	**0.24**
21-22	168.7	167.9	**168.3**	**2.83**
22-23	181.5	171.5	**176.5**	**2.92**
23-24	185.1	174.6	**179.9**	**2.34**

5.0 Fitting Higher Order Polynomials to DST Arrival Time Data Sets for High Resolution Imaging

The DST arrival times have associated measurements errors and resolution limitations which become more pronounced as the depth interval of analysis is reduced. Transducer based triggers (e.g., geophone) as opposed to "contact" based triggers can also result in increased measurements errors. The errors in arrival time measurements can result in extensive fluctuations in the estimated interval velocities with numerous outliers. BCE has developed a new DST analysis technique, the so-called *DSTPolyKF* algorithm, where analytically modelling of the DST arrival time data sets is accomplished by fitting high order polynomials. The main advantages of this new technique are five-fold. 1) Ability to utilize all arrival time estimates irrespective of measurement errors. 2) Ability to process small depth interval (≤ 0.5m) arrival time data sets. 3) Analytical polynomial "best fit" function allows for user specification of desired depth intervals for data interpolation. 4) Facilitates sophisticated data fusion for significantly more accurate DST interval velocity estimation. 5) Polynomial regression accuracy parameters quantify how well the "best fit" polynomial fits the acquired arrival time data sets.

Appendix 4 of this document outlines the mathematical details of the DST arrival time best fit polynomial algorithm. It has found that this technique has worked exceptionally well when processing DST acquired from offshore investigations. Offshore DST investigations typically have numerous data sets available at each depth increment (right side and left side top and bottom seismic sensors offset by from 0.5m to 1.0m). In addition geophone triggers are utilized.

There are four parameters which are utilized to evaluate the accuracy of the polynomial regression best fit. These four parameters are mean squared error (MSE) of the polynomial estimator, Mean Absolute Percentage Error (MAPE), coefficient of determination (R^2), and adjusted coefficient of determination (R^{*2}). Appendix 4 outlines the four polynomial regression accuracy parameters by their mathematical representations and important characteristics. It is recommended that polynomial regressions of order 2 to 7 are derived for the estimated DST source wave arrival times. The polynomial aggression order which results in the "best" accuracy parameter values as defined in Appendix 4 and lowest polynomial order is utilized. This approach addresses the well-known bias-variance tradeoff of polynomial regression.

Step 5.1 – Identify the DST Arrival Times from Data Set Available

The Figure below illustrates the estimated TSLS (Top Sensor Left Side), TSRS (Top Sensor Right Side), BSLS (Bottom Sensor LS) and BSRS (Bottom Sensor RS) estimated arrival times for the offshore DST data set.

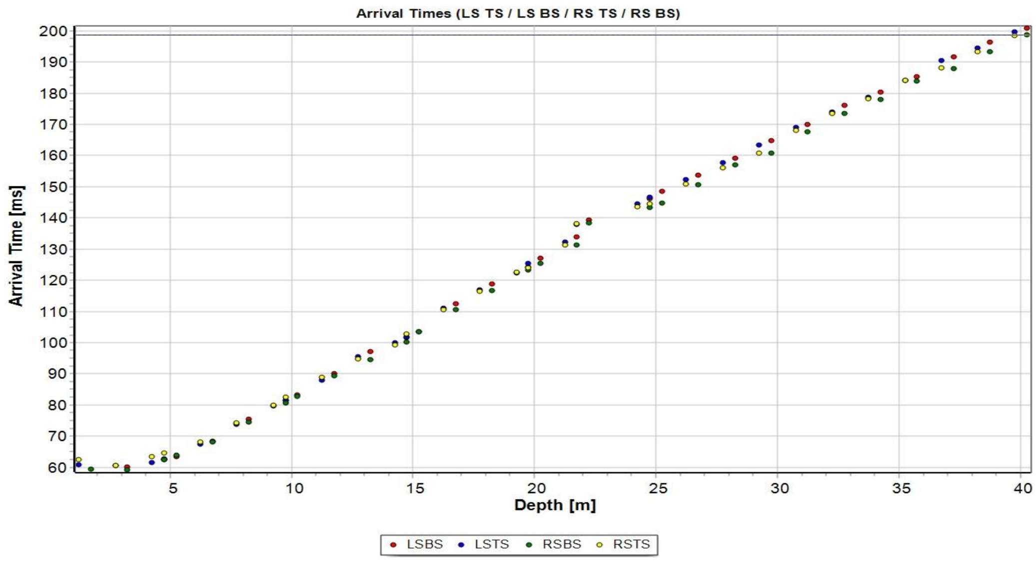

Step 5.2 – Calculate Average Arrival Times, Calculate the Associated Four Polynomial Parameters and Select the Order of the Polynomial and Calculate Polynomial Best fit

Table 4. Estimated polynomial accuracy parameters for averaged arrival times obtain from arrival times illustrated above

Polynomial Order	RMS	MAPE	R^2	R^{*2}
2	4.8413	4.2236	0.998327	0.998264
3	2.4921	1.9924	0.999565	0.99954
4	1.2825	1.0099	0.999887	0.999878
5	1.0571	0.7638	0.999925	0.999917
6	1.0357	0.6924	0.999929	0.999921
7	0.9672	0.6404	0.99994	0.999931

Table 4 outlines the corresponding polynomial regression estimated accuracy parameters for the averaged arrival times (TSLS, TSRS, BSLS, and BSRS) illustrated in the figure above and orders 2 to 7. From the results outlined in Table 4, the 6th and 7th order polynomial aggressions have overall "best" accuracy parameter values as defined in Table 4. Although, the 5th order polynomial regression result are also very close to 6th and the 7th order polynomial results. The figure below illustrates the averaged TSLS, TSRS, BSLS and BSRS arrivals times with the 7th order polynomial regression best fit line. It is recommended that both 6th and 7th order polynomial regression best fit estimates are obtained and resulting interval velocities compared.

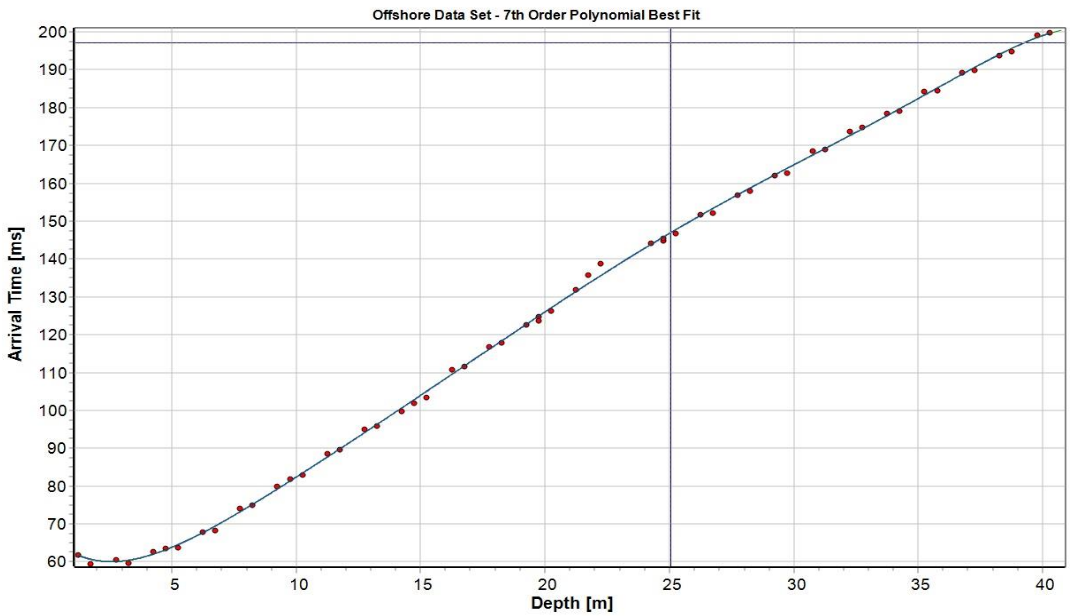

Averaged arrival times (red dots) and 7th order polynomial regression best fit (blue line) for the offshore real DST analysis.

Step 5.3 – Specify the Depth Resolution of Best Fit Polynomial, Generate Associated Arrival Times and Import Best Fit Polynomial Arrival Times into the FMDSM Database

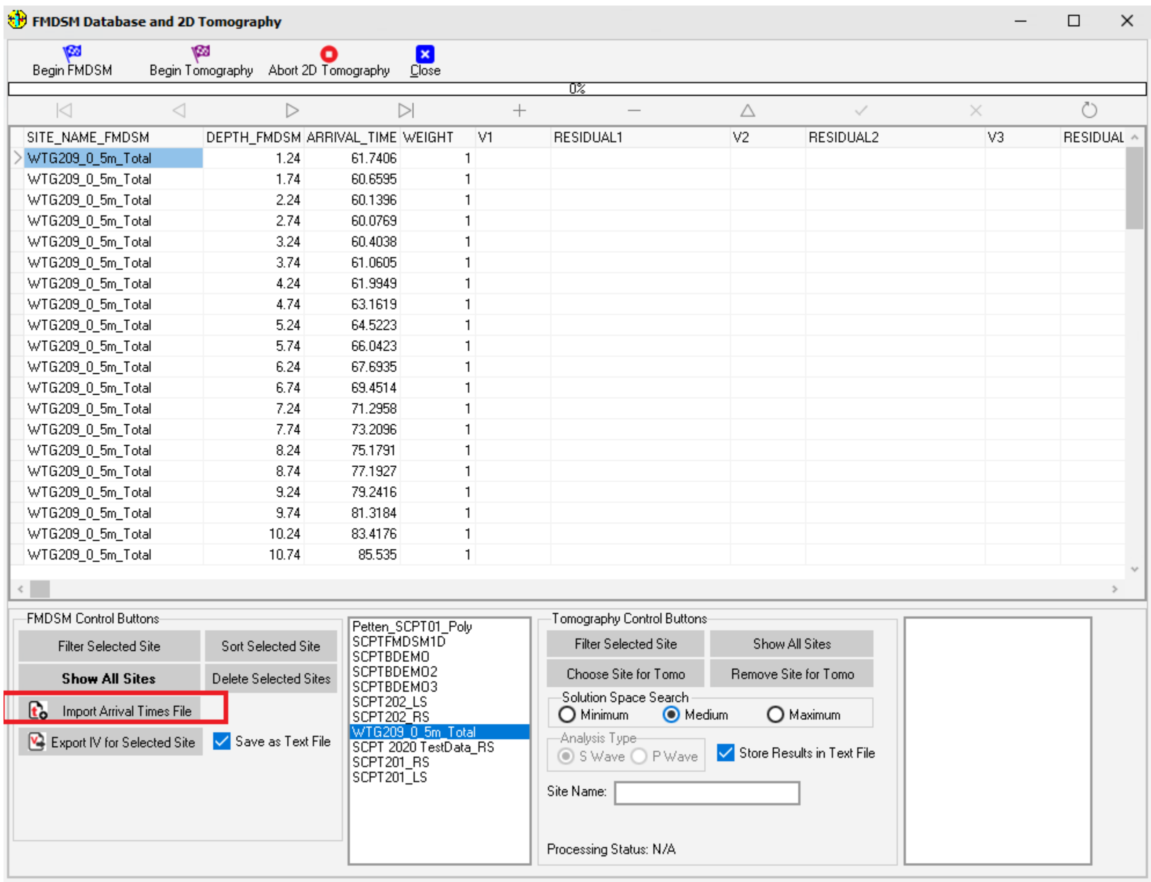

Step 5.4 – Implement FMDSM Algorithm on Imported Best Fit Polynomial Arrival Times and Tabulate and Plot Interval Velocities

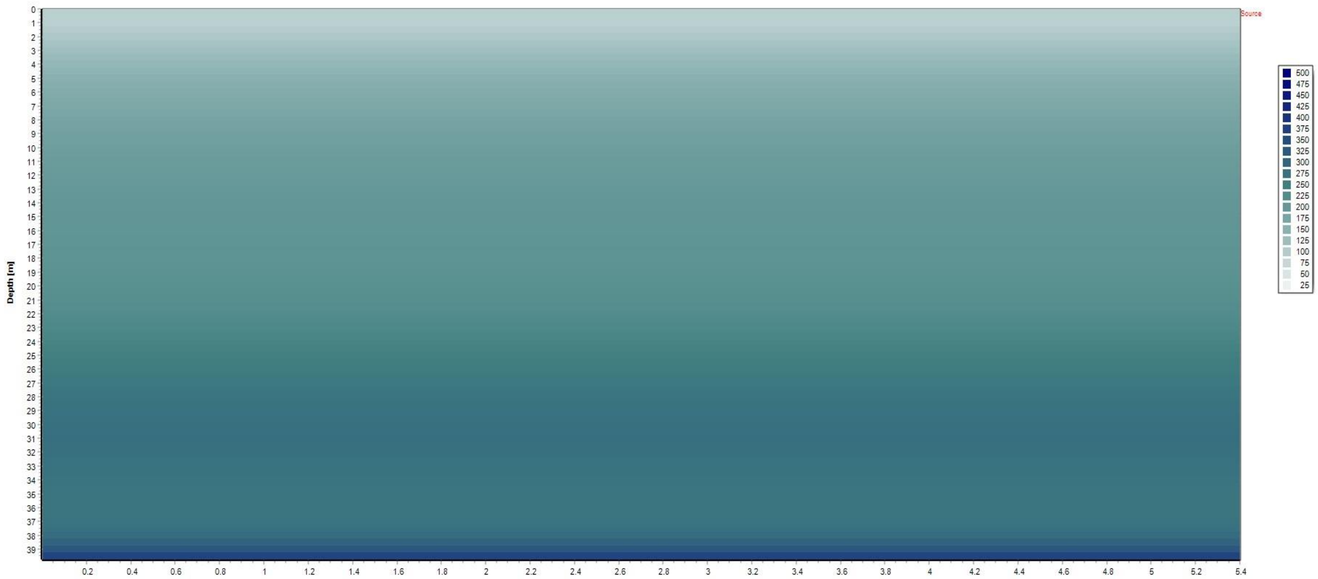

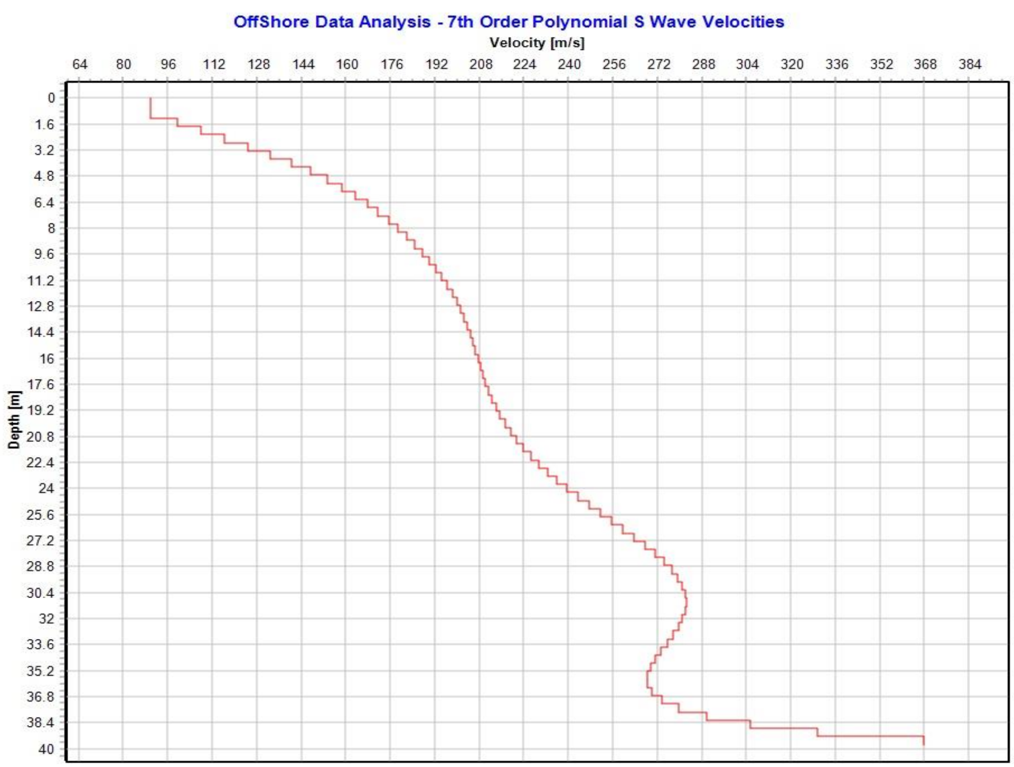

Table 5. Estimated interval velocities and percent differences for polynomial regressions of orders 6 and 7.

Depth [m]	6th Order Interval Velocity [m/s]	7th Order Interval Velocity [m/s]	6th and 7th Order Precent difference
1.24	89.7	89.7	0
1.74	98.3	99.6	0.7
2.24	105.9	108	1
2.74	114.2	116.5	1
3.24	123.1	125	0.8
3.74	132.3	133.1	0.3
4.24	141.2	140.6	0.2
4.74	149.6	147.3	0.8
5.24	157.1	153.3	1.2
5.74	163.7	158.7	1.6
6.24	169.1	163.4	1.7
6.74	173.5	167.8	1.7
7.24	177	171.7	1.5
7.74	179.8	175.4	1.2
8.24	181.9	178.8	0.9
8.74	183.6	181.9	0.5
9.24	185	184.8	0.1
9.74	186.2	187.6	0.4
10.24	187.4	190.1	0.7
10.74	188.5	192.4	1
11.24	189.7	194.6	1.3
11.74	190.9	196.6	1.5
12.24	192.2	198.4	1.6
12.74	193.7	200	1.6
13.24	195.3	201.4	1.5
13.74	196.9	202.7	1.5
14.24	198.7	203.8	1.3
14.74	200.6	204.9	1.1
15.24	202.5	205.8	0.8
15.74	204.6	206.7	0.5
16.24	206.7	207.6	0.2
16.74	208.8	208.4	0.1
17.24	211	209.3	0.4
17.74	213.3	210.3	0.7
18.24	215.5	211.4	1
18.74	217.8	212.6	1.2
19.24	220.1	214	1.4
19.74	222.3	215.5	1.6
20.24	224.6	217.2	1.7
20.74	226.8	219.2	1.7
21.24	229.1	221.4	1.7
21.74	231.3	223.8	1.6
22.24	233.5	226.5	1.5
22.74	235.6	229.4	1.3
23.24	237.8	232.6	1.1
23.74	239.9	236	0.8
24.24	242	239.7	0.5

24.74	244.1	243.5	0.1
25.24	246.2	247.4	0.2
25.74	248.3	251.5	0.6
26.24	250.5	255.7	1
26.74	252.6	259.8	1.4
27.24	254.8	263.8	1.7
27.74	257	267.7	2
28.24	259.2	271.2	2.3
28.74	261.5	274.5	2.4
29.24	263.8	277.2	2.5
29.74	266.1	279.5	2.5
30.24	268.5	281.1	2.3
30.74	270.9	282.1	2
31.24	273.4	282.4	1.6
31.74	275.9	282.1	1.1
32.24	278.3	281.1	0.5
32.74	280.7	279.7	0.2
33.24	283.1	277.8	0.9
33.74	285.4	275.6	1.7
34.24	287.5	273.4	2.5
34.74	289.4	271.3	3.2
35.24	291.1	269.6	3.8
35.74	292.4	268.6	4.2
36.24	293.3	268.6	4.4
36.74	293.8	270.1	4.2
37.24	293.7	273.6	3.5
37.74	292.9	279.8	2.3
38.24	291.3	289.9	0.2
38.74	289	305.5	2.8
39.24	285.7	329.7	7.1
39.74	281.4	368	13.3

Appendix 1 - Recommended source apparatuses and configurations for a SH-wave and P-wave investigations.

It very important in DST that proper SH-source and P-wave sources are utilized. The BCE recommended source design and set-up configuration are outlined below.

SH-Source design and configuration

1. Apply Right and Left polarized “point” SH source plates with specially designed ribs. Point sources should be utilized so that the source location (x, y, and z coordinates) can be quantified accurately for subsequent interval velocity calculation. For example, if a large SH-hammer beam is utilized, it becomes difficult to specify the exact location of the seismic source. Moreover with a point source the concern of proper coupling between the beam and the soil underneath along the entire length of the beam is mitigated.

2. Use an aluminum strike plate for the source plates to reduce the “pinging” noise when they are struck with a heavy sledge hammer.

3. Use a “Contact” trigger with a strike plate which acts an electrical switch trigger (i.e., trigger occurs when hammer makes contact with the strike plate). The set-up offers an excellent “Contact” type trigger as illustrated in the figure below.

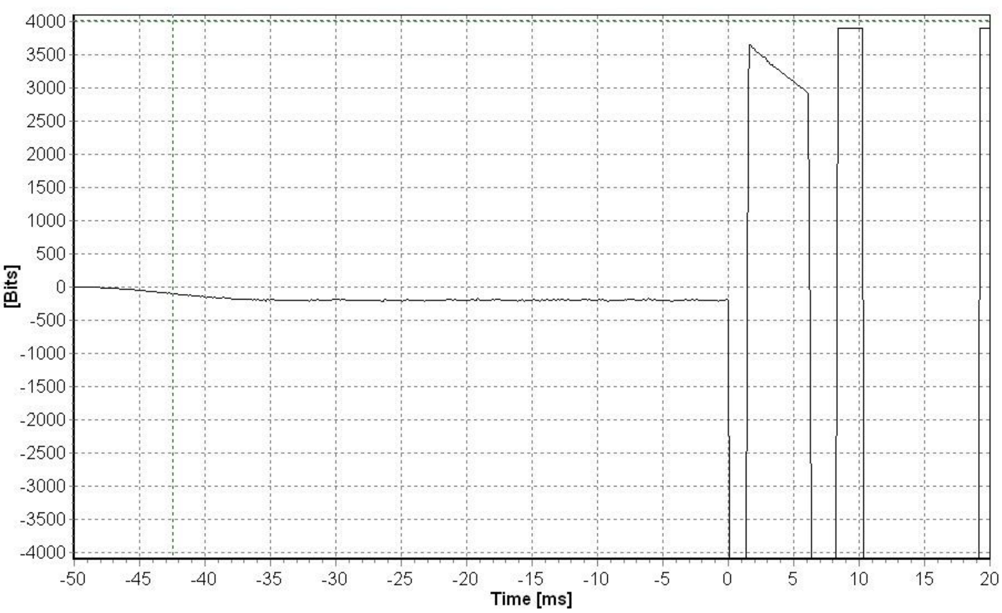

4. Apply relative large sensor-source radial offsets (SSROs) and in case of SCPT, decouple the SH source from the test rig. Large SSROs decrease near field amplitudes considerably, resulting in significantly higher signal-to-noise ratios of the recorded seismic data, which in turn allows for more accurate near surface stratigraphy characterization. In addition, in case of SCPT this approach results in minimal recording of "rod" noise. Finally, large SSROs increase the characterization of the layer or depth under analysis due to the fact that the source wave refracts and travels within stratigraphic layers for a longer period of time

5. Load SH source plates so that slip between plates and the soil underneath does not occur, while at the same time the lateral displacement upon hammer impact is restricted as little as possible. It has been found that a good way to achieve this is to have vehicle air filled rubber wheels loaded upon the SH source plates.

P-Source design and configuration

In general terms, a P-wave source requires symmetric (with respect to volume change) displacement such as an explosive source detonated within the medium near the surface. Some acceptable P-wave source consists of buffalo guns (i.e., 12 gauge shot gun shell fired in the ground), air guns, electrical sparker system and vertical hammer impact which results in a symmetric displacement of a membrane placed within the medium near surface. The previously described P-wave source will typically also generate SV waves, which are subsequently recorded by the downhole seismic sensors. A typical SV wave source configuration consists of lowering a shear type source within a borehole and then clamping the SV wave source against the side of the borehole (using a pneumatic or mechanical clamp). The SV wave type source then facilitates the investigator applying a vertical shearing impact to the side of the borehole so that a predominantly SV source wave is generated. Some investigators apply a vertical impact on the ground surface to generate a P-wave source. The major disadvantages of utilizing this type of mechanism are two-fold:

1. Only one-third of the energy generated by a vertical source on a uniform half-space is transformed into body waves (compression and shear), while the other two-thirds of the energy generated is transformed into surface waves.

2. Body waves at the surface have lower amplitudes than body waves in the half-space.

Contact type triggers should be used with the P-wave source. These types of triggers can readily be incorporated into the P-wave source.

Appendix 2 - Seismic Trace Characterization Parameters

Introduction

BCE has invested considerable resources into the development of techniques and algorithms to characterize acquired Downhole Seismic Testing (DST) data sets for shear wave velocity assessment, and to use that characterization as a guide for the processing of those data sets to calculate interval velocities.

The characterization is based on various independent parameters of the acquired DST data at a particular depth. Currently five parameters are considered:

- Parameter 1: the linearity estimates (LIN) from polarization analysis. The LIN trace metric quantifies the correlation between X, Y and Z axis responses.
- Parameter 2: the Cross Correlation Coefficient (CCC) of the full waveforms at the particular depth and the preceding depth. The CCC trace metric gives an indication of the similarity between the two waves being correlated when deriving relative arrival times.
- Parameter 3: the Signal Shape Parameter (SSP). The SSP trace metric quantifies the deviation of the shape of the frequency spectrum from an ideal bell shape
- Parameter 4: the Peak Symmetry Differential (PSD) trace metric facilitates the identification of traces whose peak source wave responses have been significantly skewed due to measurement noise or source wave reflection interference.
- Parameter 5: Signal to Noise Ratio (SNR). The SNR trace metric is solely provided to quantify what portion of the spectral content of the recorded seismogram resides within the desired source frequency spectrum irrespective of source wave distortions such as near-field effects, reflections, refractions, and “dirty sources”.

For these five parameters the part of the data sets that will be used and filtered is shown in the table below:

Parameter	Part of trace that is reviewed	Applied Signal Filtering
LIN	Largest peak/trough ± 30 ms	200 Hz low pass
CCC	Largest peak/trough -30ms for upper trace Largest peak/trough +30ms for lower trace	200 Hz low pass
SSP	Entire trace	200 Hz low pass
PSD	Largest peak/trough ± 2 crossovers	200 Hz low pass
SNR	Largest peak/trough ± 2 crossovers	None / 200 Hz low pass

This Technical Note introduces the parameters, while Technical Note 21 provides a guide for the recommend post data processing and seismic signal processing based upon these parameters.

It should be noted that the characterization process may be updated as more data set are reviewed.

Parameter 1: LIN

The linearity or rectilinearity values can be obtained from hodograms, i.e. by plotting the X, Y and Z axis amplitudes against one another and fitting least squares best fit lines. Since hodograms with linearity values nearing 1.0 identify seismic recordings that have highly correlated responses on the X, Y and Z axes and strong directionality, the interval velocities calculated from such recordings are likely to be accurate. Hodograms with lower linearity values on the other hand indicate lower signal-to-noise ratios or SNRs (whether due to poor source generation, near-field waves, ambient noise that is not easily filtered out or source wave reflections) and thus the resulting interval velocity values are likely to be less accurate.

To provide for a more accurate quality assessment of the recorded data minimal digital frequency filtering should be applied to the raw data, while more refined and aggressive digital frequency can be applied during the actual data analysis to determine the interval velocities.

The X, Y and Z responses in Figure 1 below from a SH source (after applying a low pass frequency filter of 200 Hz) have clearly high SNRs values: the peaks and troughs on the X and Y axis line up, and there are minimal recordings on the Z axis as would be expected for this kind of source.

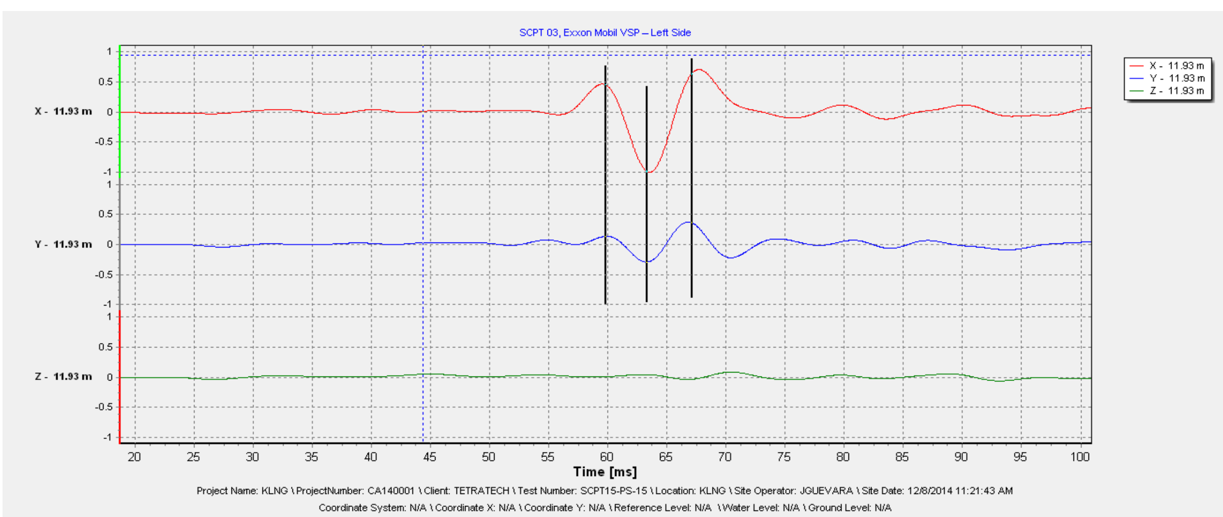

Figure 1: Correlated triaxial responses resulting in high linearity values. The source wave X and Y axis peaks and troughs are aligned

The hodogram plot for this triaxial recording is shown in Figure 2 below. In this hodogram the amplitudes of the X and Y axes recordings (dominant energy for a SH source) are plotted as green circles and the red line is the best fit straight line (with a calculated linearity of 0.92). This clearly reflects a good quality seismic source recording with a high correlation between the X and Y axis and high directionality along an axis with an azimuth of approximately 13º.

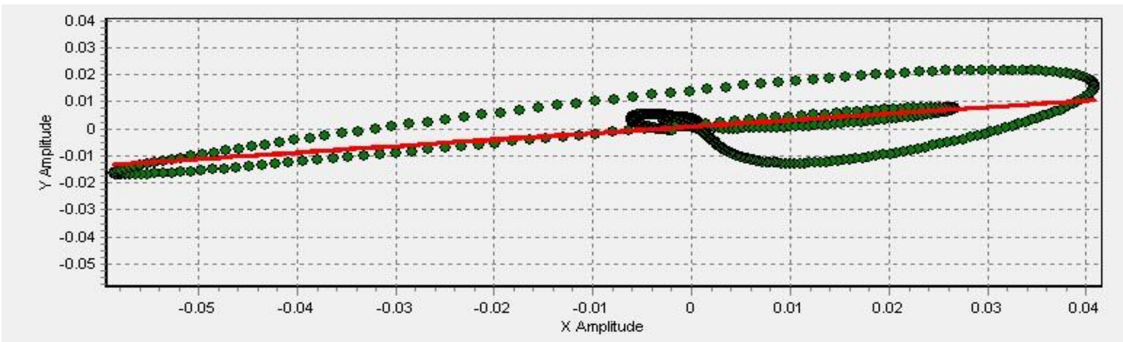

Figure 2: The hodogram plot for the triaxial responses illustrated in Fig. 1. The hodogram clearly reflects a good quality seismic source recording with a high correlation between the X and Y axis and high directionality along an axis with an azimuth of approximately 13º.

In the triaxial seismic trace recording in Figure 3 the peaks and troughs on the X, Y and Z do not line-up and the background noise (whether due to a poor source, vibrations within the testing vehicle upon impact of the SH wave sledge hammer and/or other causes) has frequency components similar to the source wave making the isolation of the source wave with frequency filters a challenging tasks.

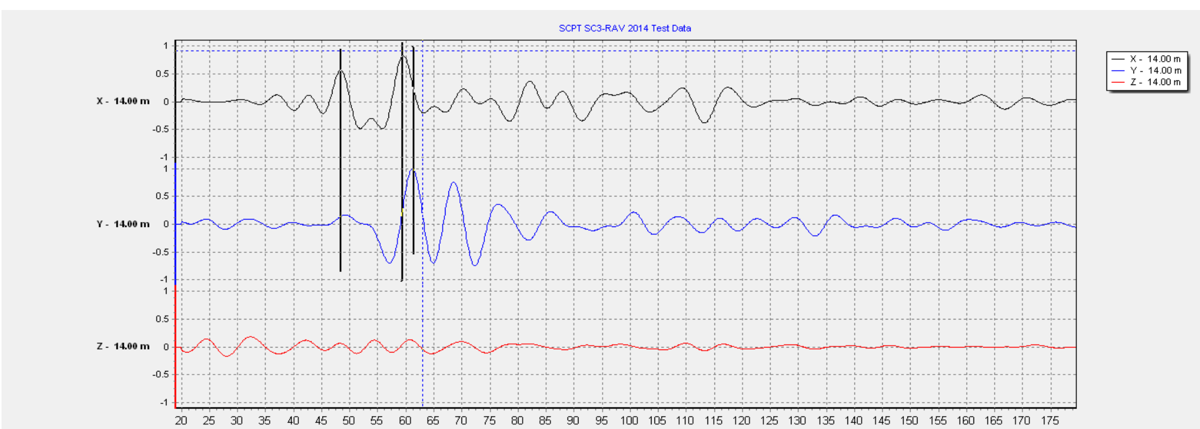

Figure 3: Poorly correlated triaxial responses resulting in low linearity values. The source wave X and Y axis peaks and troughs are not aligned.

The hodogram plot for this recording is shown in Figure 4 below. The amplitudes of the X and Y axes recordings are plotted (green circles) and the red line is again the best fit straight line, but obviously with a much lower calculated linearity than in the first example (0.61 vs. 0.92).

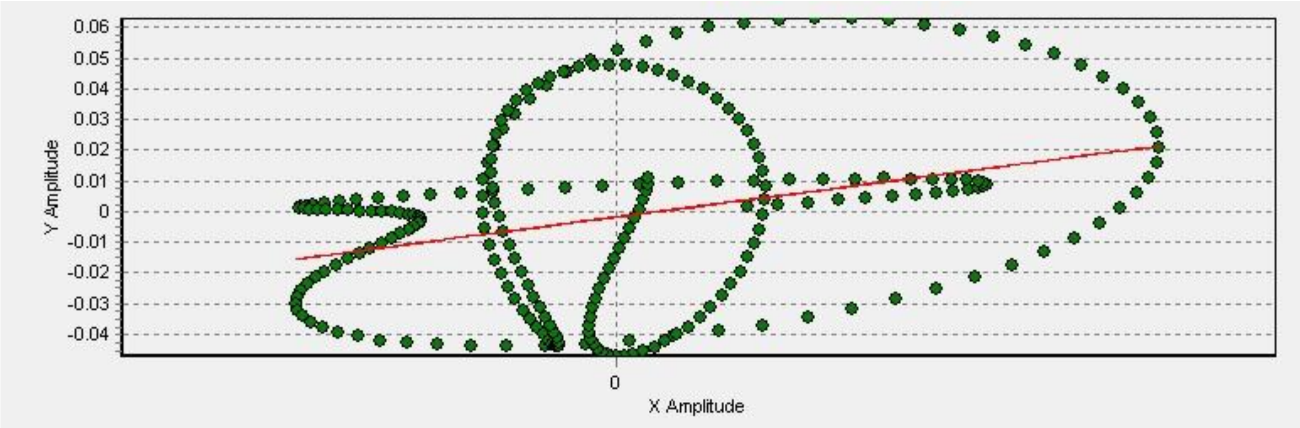

Figure 4: The hodogram plot for the triaxial responses illustrated in Fig. 3. The hodogram clearly reflects a poor quality seismic source recording with a low correlation between the X and Y axis and low directionality.

Parameter 2: CCC

The cross-correlation between two time or distance offset seismograms is given as (Gelb 1974)

$$\varphi_{xy}(\tau) = \sum_k X_k Y_{k+\tau} \tag{1}$$

where $\varphi_{xy}(\tau)$ is the cross-correlation function, Y_k the sampled data at distance 1 and at sample time k, X_k the sampled data at distance 2 at sample time k, and τ the time shift between the two sets of recorded waves (note: distance 2 > distance 1). The value of the time shift at the maximum cross-correlation value is assumed to be the relative travel time difference, Δt, for the source wave to travel the distance increment. This technique has several advantages over selecting time markers within the seismogram (Baziw 1993, 2002), among others the human bias associated with visually selecting a reference point or time marker is minimized.

Normalizing the cross-correlation of the zero mean seismic signals by their standard deviations gives the cross-correlation coefficient:

$$\rho_{xy}(\tau) = \sum_k X_k Y_{k+\tau} \Big/ \sqrt{\sum_k X_k^2} \sqrt{\sum_k Y_K^2} \tag{2}$$

The CCC between the two DST waves is typically used to assess the quality of the interval velocity estimate as this parameter gives an indication of the similarity between the two waves being correlated. While on its own the CCC has proven to be an unreliable indicator of the overall quality of a seismic trace (since it is highly dependent on the digital filter applied to the raw seismic signals), it is still a useful component of seismic trace characterization. As an STC parameter the CCC value is calculated on the full waveforms after applying polarization analysis.

Parameter 3: SSP

The probability density of a normal (or Gaussian) distribution is given as

$$f(x|\mu,\sigma^2) = \frac{1}{\sigma\sqrt{2\pi}} e^{-\frac{(x-\mu)^2}{2\sigma^2}} \qquad (3)$$

where μ denotes the mean or expectation of the distribution and σ denotes the standard deviation with variance σ^2. The area under the normal pdf curve is unity. Figure 5 illustrates example of normal pdfs for varying μ and σ^2 values. All the curves in Fig. 1 have the classical bell-shape.

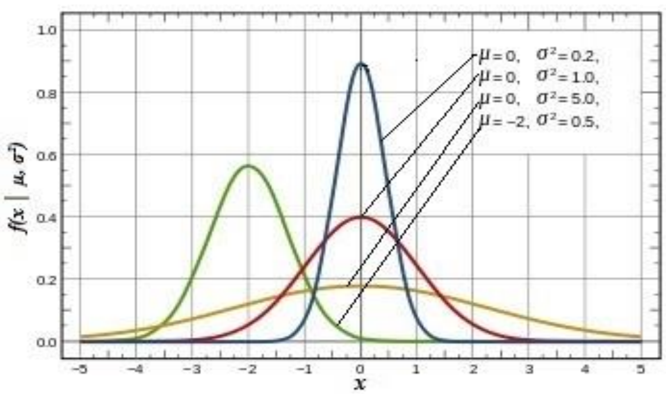

Figure 5: Example of normal pdfs for varying μ and σ^2 values. (after, http://www.dplot.com/probability-scale.htm

Figure 6 illustrates a Berlage source wave (Baziw and Ulrych (2006), Baziw and Verbeek (2014)), which is commonly used within seismic signal processing for simulation purposes. The Berlage source wave is analytically defined as

$$w(t) = AH(t)t^n e^{-ht} \cos(2\pi f t + \emptyset) \qquad (4)$$

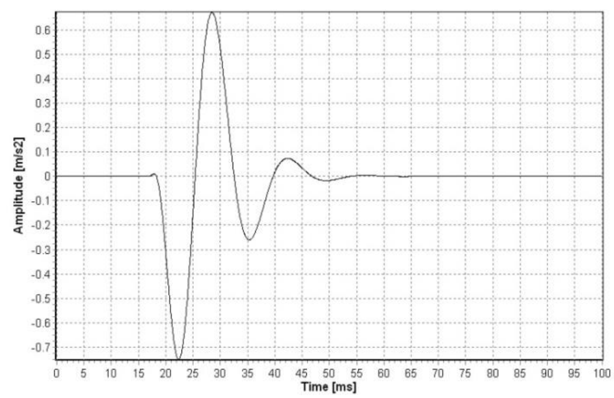

Figure 6: Berlage source wave with of f = 70 Hz, n = 2, h = 270 and ϕ = 40º specified.

where *H(t)* is the Heaviside unit step function [$H(t) = 0$ for $t \leq 0$ and $H(t) = 1$ for $t > 0$]. The amplitude modulation component is controlled by two factors: the exponential decay term *h* and the time exponent *n*. These parameters are considered to be nonnegative real constants. Figure 7 illustrates the frequency spectrum (solid black line) of the Berlage source wave shown in Fig. 6 with the normal pdf approximation shown as a dotted grey line, with μ = 69 Hz and σ = 32.5 . As is evident from Figure 7, the frequency spectrum of the simulated Berlage source wave closely matches that of a bell-shaped curve.

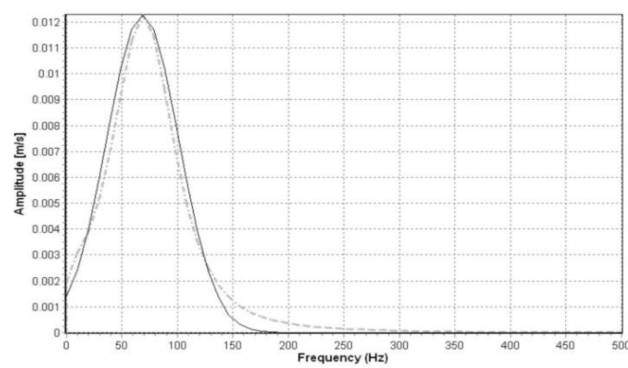

Figure 7: Frequency spectrum (solid black line) of Berlage source wave illustrated in Fig. 2 with the normal pdf approximation shown as a dotted grey line.

To determine the deviation of the source wave frequency spectrum from a desirable bell-shaped curve the following process is proposed:

Apply a digital zero-phase shift frequency filter to the entire seismic trace so that high frequency measurement noise is removed.

1. Calculate frequency spectrums for *X(t)* and *Y(t)* recordings, $S_X(f)$ and $S_Y(f)$, and determine which axis has the dominant frequency response axis (denote as *S(f)*).
2. Force the area under *S(f)* to approach unity by uniformly modifying the amplitudes within *S(f)*. This step is outlined below by eqs. 5(a) and 5(b).

$$Area_{S(f)} = \Delta f \sum_{i+1}^{n} S(f)_i \tag{5a}$$

$$\sum_{i+1}^{n} S(f)_i = S(f)_i / Area_{s(f)} \tag{5b}$$

   In eq. 5(a), Δf denotes the frequency increment resolution.
3. Determine μ (dominant frequency), $p(\mu)$ (maximum spectral amplitude), and $\sigma = 1/(p(\mu)\sqrt{(2\pi)})$ utilizing an iterative forward modelling (IFM) technique such as the Simplex method (Baziw, 2002, 2011). In this IFM case the cost function to minimize is the RMS difference between the normalized area under *S(f)* and the derived area (using eq. (3)) from a normal pdf which utilizes the currently estimated μ and σ values.
4. Calculate *p(f)* via equation (1) utilizing the IFM estimates μ and σ from Step 4.
5. Calculate $\epsilon_1 = \sum_{i+1}^{n} abs(S(f)_i - pdf(f)_i))$
6. Calculate $\epsilon_2 = \sum_{i+1}^{n} abs(S(f)_i)$
7. Calculate parameter R which is defined as $R = \varepsilon_1/\varepsilon_2$
8. Signal Shape Parameter (*SSP*) is then calculated as *SSP = 1-R*.

Parameter 4: PSD

The "Peak Symmetry Differential" (PSD) parameter facilitates the identification of traces whose peak source wave responses have been significantly skewed due to measurement noise or source wave reflection interference. Fig. 8 illustrates this phenomenon. In Fig. 8(A) we have an ideal source wave recording where no interference is present. In this case the time difference between the two zero crossings bounding the peak response (A_1) are identical ($\Delta t_1 = \Delta t_2$). In Fig. 8(B) we have a source wave recording with interference, resulting in skewing or time shifting of the peak source wave response. The "peak symmetry" error assessment is also carried out on the adjacent peaks and/or troughs if the amplitude exceeds 70 % of that for the peak response

The PSD parameter is determined as follows:

1. Apply a frequency filter to the entire seismic trace to eliminate irrelevant zero crossings

2. Identify the largest peak/trough of the seismic trace and determine the time differential from the moment the peak occurs to the zero crossings on either side (Δt_1 and Δt_2 respectively)
3. Calculate $\Delta t = |\Delta t_1 - \Delta t_2|$.
4. If the amplitude of the adjacent trough/peak on either side exceeds 70 % of that for the largest peak/trough response calculate the Δt value for that trough/peak.
5. Determine the maximum Δt value
6. The PSD is then:

for $\Delta t \leq 0.02$	PSD = 1
for $0.02 \leq \Delta t \leq 0.8$	PSD = $1.026 - \Delta t/0.78$
for $\Delta t \geq 0.8$	PSD = 0

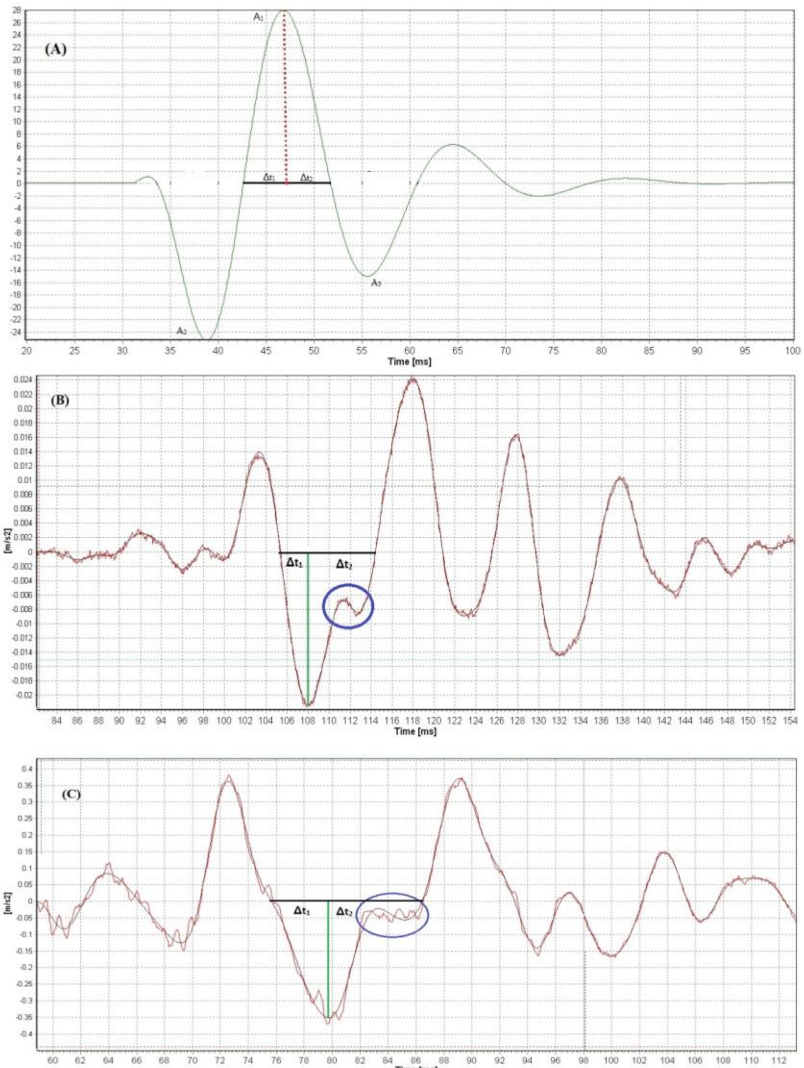

Figure 8: Source wave peak distortions due to measurement noise or source wave reflection interference. (A) Ideal source wave recording where no interference is present. (B) and (C) Source waves with interference resulting in skewing or time shifting of the peak

Parameter 5: SNR

The initial four parameters (LIN, CCC, SSP and PSD) are derived after filtering (albeit to a minimal extent) the seismic traces under analysis. The last parameter uses as input the as-recorded seismic trace and compares it with the filtered trace to assess the extent of background noise. To get a complete assessment it is essential that the recorded trace reflects accurately the signals that exist at the sensor location, in other words that the sensors display with minimal distortion the background noise and seismic source waves (see also BCE Technical Note 10). In the remainder of this Technical Note it is therefore assumed that sensors are used where the sensor output accurately represent the sensor input.

Figure 9 illustrates various seismic traces with varying signal-to-noise ratios. In each figure the filtered black traces (200 Hz low pass filter) are superimposed upon the corresponding virtually unfiltered seismic red traces (a 700 Hz low pass filter was applied to remove electrical noise). In Fig. 9(A) the unfiltered dominant source wave recording closely matches that of the filtered trace, which implies a high signal-to-noise ration. In Figs. 9(B) to (D) the unfiltered traces correlate a lot less with the filtered traces.

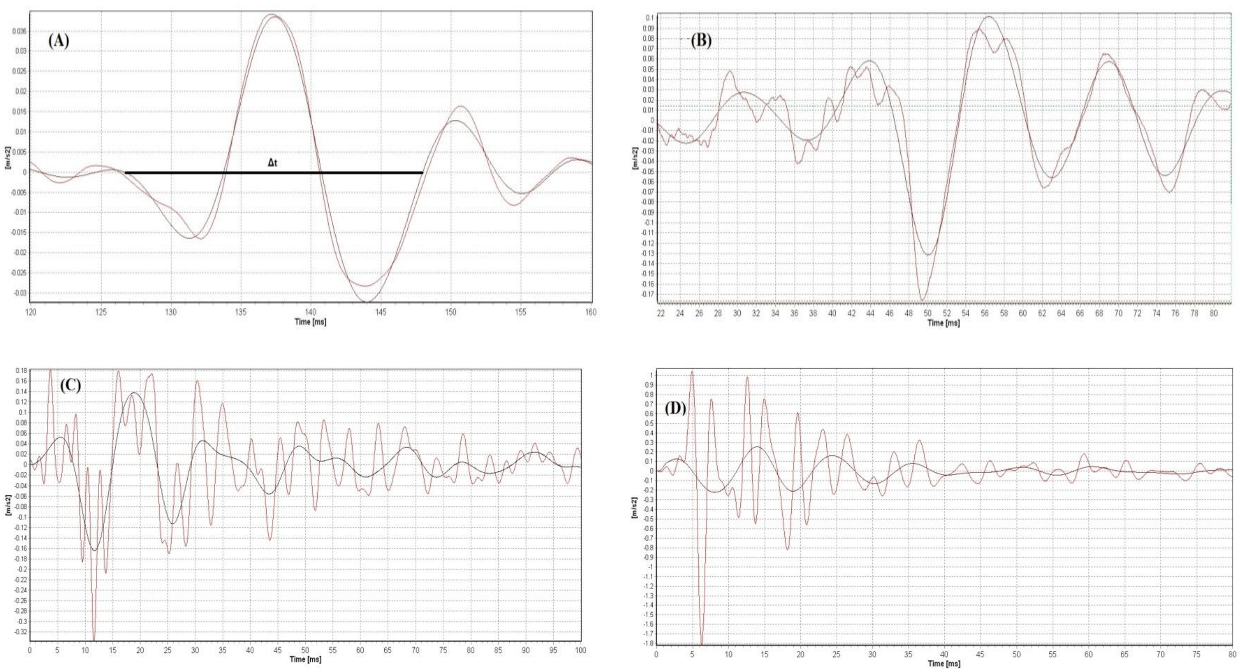

Figure 9. Examples of DST unfiltered (red traces) and corresponding filtered (black traces – low pass of 200 Hz applied) seismic time series.

To quantify this aspect the "Signal Noise Ratio" (SNR) parameter is used, which revolves around a comparison of the normalized peak response in the original seismic trace and that in the filtered trace:

The SNR parameter is determined as follows:

1. Identify the largest peak/trough of the filtered trace and derive an analysis time window by moving forward and backward in time (as shown by the solid black line in Figure 9(A)).
2. Normalize both the unfiltered and filtered responses within this time window.
3. Calculate the difference trace between the normalized and time windowed unfiltered and filtered traces. Figure 10 illustrates the difference time series for traces illustrated in Fig. 1 and implementing previously outlined Steps 1 and 2.
4. Calculate the standard deviation σ of the difference trace.
5. The SNR is then: for $\sigma \leq 0.03$ SNR = 1
   for $0.03 \leq \sigma \leq 0.7$ SNR = $1.045 - \sigma/0.67$
   for $\sigma \geq 0.7$ SNR = 0

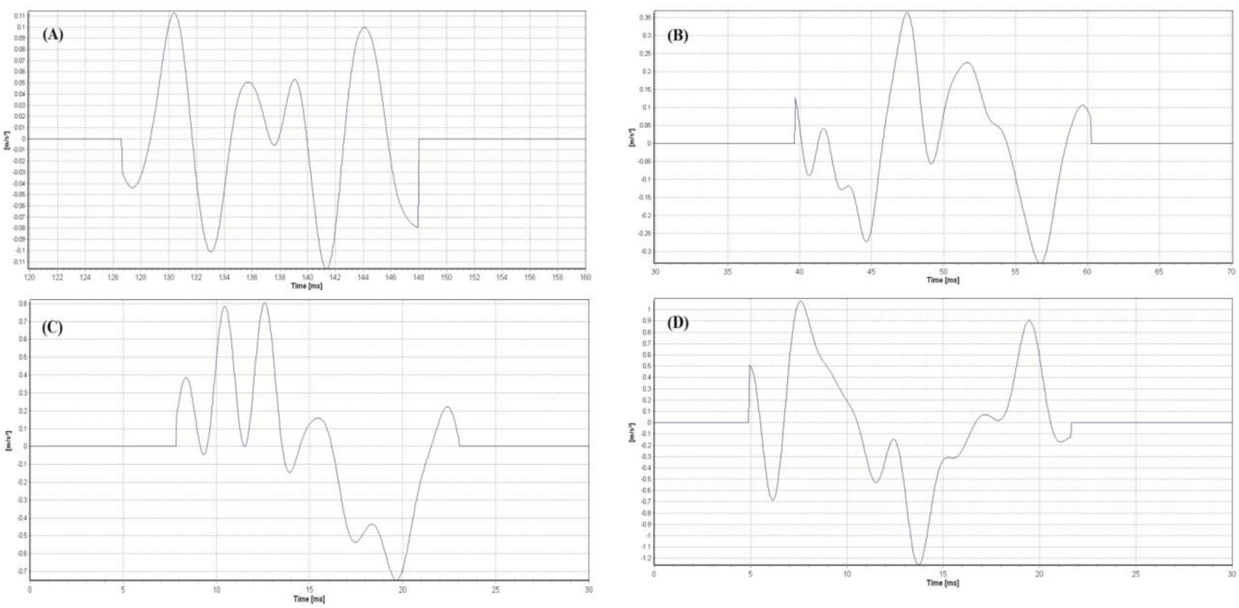

Figure 10. Calculated difference time series for traces illustrated in Fig. 9 and the SNR values (A) SNR = 0.95, (B) SNR = 0.79, (C) SNR = 0.52 and (D) SNR = 0.24.

Appendix 3 – "The use of seismic trace characterization to guide the analysis of DST results to obtain more accurate soil parameters" (Baziw, E. and Verbeek, G. (2018), Proceedings of the 43rd Annual Conference on Deep Foundations, 2018, Anaheim, CA, USA, (DFI), article #3137; publication #1045 (AM-2018))

The use of seismic trace characterization to guide the analysis of DST results to obtain more accurate soil parameters

Erick Baziw
Baziw Consulting Engineers Ltd., Vancouver, Canada
Gerald Verbeek
Baziw Consulting Engineers Ltd., Vancouver, Canada

ABSTRACT:
Downhole Seismic Testing (DST) is a very popular applied seismology site characterizing tool within geotechnical engineering. A challenging aspect of DST is to characterize the acquired seismic data sets to determine the analysis method that will result in the most accurate interval velocity values. BCE has invested considerable resources into developing Seismic Trace Characterization (STC), which uses various independent parameters of the acquired data at a particular depth. Initial work in this area resulted in the selection of the linearity estimate from the polarization analysis, the cross correlation coefficient of the full waveforms at the particular depth and the preceding depth and a uniquely developed parameter referred to as the signal shape parameter for this characterization. Subsequent analysis in STC identified two other parameters: the Signal-Noise-Ratio (SNR) and the Peak Symmetry Differential (PSD). The paper briefly describes these parameters and then outlines how they can guide the data analysis to derive more accurate results, especially near surface, which is especially important to assess the liquefaction potential in areas prone to earthquakes, such as California. The process will be illustrated with actual data from another area prone to earthquakes, namely New Zealand.

1. INTRODUCTION

The near surface characterization of low strain in-situ shear wave velocities (V_S) has proven critical for liquefaction assessment. Liquefaction is a phenomenon in which dynamic loading of saturated soil results in the material properties to change suddenly from a solid state to a liquefied state. V_S is an important parameter for evaluating liquefaction potential due to fact that it is influenced by many of the variables that influence liquefaction (e.g., void ratio, soil density, confining stress, stress history, and geologic age (Andrus et al., 1997)). Aki and Richards (2002) also outline that the amplitude of ground motion should depend on the density and shear wave velocity of near surface soils and rocks according to the theory of wave propagation. Since the change in density with the increase in depth is relative minor compared to that of the shear wave velocity, the latter is a very useful parameter to represent site conditions (Stewart et al., 1997). Bray (2014) and his colleagues carried out an extensive geotechnical analysis of the catastrophic liquefaction that occurred in Christchurch, New Zealand in 2010 and 2011 and found that near surface rather than deep liquefaction resulted in extensive foundation damage.

Downhole Seismic Testing (DST) has proven to be a very powerful technique for measuring in-situ near surface V_S values (ASTM, 2017). The main goal in DST is to obtain arrival times as the source wave travels through the soil profile of interest, and from these arrival times the velocities are then calculated by taking into account proper source wave raypaths (Baziw, 2002; Baziw and Verbeek, 2012 and 2016). Near surface DST seismic data set can be particularly challenging to process compared to relatively deeper acquired traces as they are more effected by near surface measurement noise, “rod noise”, near-field source waves, and reflections. Especially for those traces it is critical to have the ability to assess the quality of the DST seismic trace and to get guidance how to best analyze these traces.

BCE has invested considerable resources (Baziw and Verbeek, 2016a, 2016b, and 2017) into the characterization of acquired DST data sets and the guidance for data analysis that can be derived from this characterization. This paper summarizes that work and also describes proposed signal processing and post data analysis techniques for data sets with poor trace metrics.

2. THE STC PARAMETERS

The analysis of numerous seismic data sets, many of which were recorded with triaxial seismic sensors, has resulted in a better understanding of how a seismic trace can be characterized. Typically, investigators have utilized the Cross-Correlation Coefficient (CCC), which gives an indication of the similarity between traces used in obtaining relative arrival times (Baziw, 1993), but this parameter has been proven to be an unreliable indicator due to the fact that measurement noise (random and systematic) can also be correlated and result in high CCC values. In order to overcome these limitations other parameters were added and over the years the number of parameters considered by the authors has increased to five.

STC Trace Metric 1: Linearity (LIN) Estimates from the Polarization Analysis

The linearity or rectilinearity values can be obtained from hodograms, i.e. by plotting the responses recorded on different axes against one another and then fitting least squares best fit lines. Since hodograms with linearity values nearing 1.0 identify seismic recordings that have highly correlated responses and strong directionality, the quality of the data set with a high linearity value (such as shown in Figure 1) can be considered good. Hodograms with lower linearity values on the other hand indicate a lower quality trace (whether due to poor source generation, near-field waves, ambient noise that is not easily filtered out, source wave reflections, or differential probe coupling)

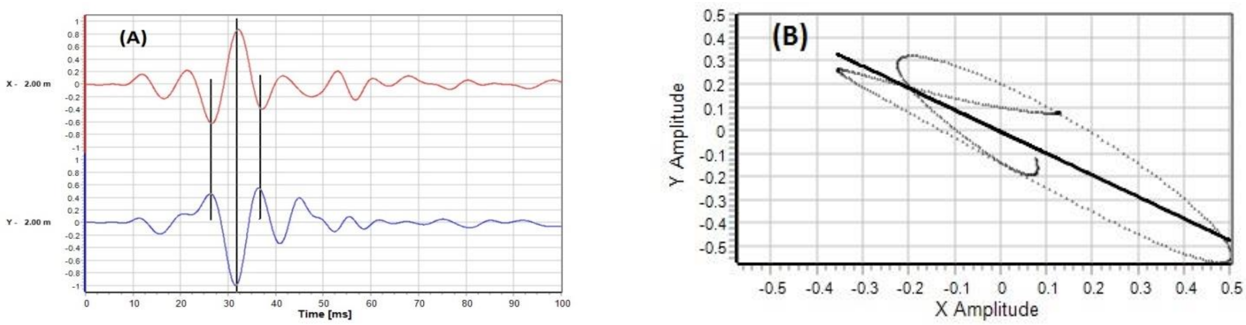

Figure 1: (A) DST X and Y axis seismic responses illustrating alignment of peaks and troughs. (B) Corresponding hodogram (light grey dots) and linear least squares best fit (dark black line) with a calculated linearity of 0.89

STC Trace Metric 2: Cross-Correlation Coefficient (CCC)

The cross-correlation between two time or distance offset seismograms is given as

$$\varphi_{xy}(\tau) = \sum_k X_k \, Y_{k+\tau} \tag{1}$$

Normalizing the cross-correlation of the zero mean seismic signals by their standard deviations gives the cross-correlation coefficient:

$$\rho_{xy}(\tau) = \sum_k X_k \, Y_{k+\tau} \Big/ \sqrt{\sum_k X_k^2} \, \sqrt{\sum_k Y_K^2} \tag{2}$$

The CCC between the two DST seismic traces gives an indication of the similarity between the two waves being correlated. CCC values approaching 1.0 indicate that the two waveforms are highly correlated. CCC values approaching 0 indicate very poor correlation.

STC Trace Metric 3: Signal Shape Parameter (SSP)

The SSP trace metric quantifies the deviation of the shape of the frequency spectrum from an ideal bell shape. Based upon frequency spectrum analysis of large sets of DST data it was determined that the shapes of high quality DST data sets had frequency spectrums closely resembling Gaussian bell-shape pdf curves (Baziw and Verbeek, 2016a), which can be described as follows:

$$p(f|\mu, \sigma^2) = \frac{1}{\sigma\sqrt{2\pi}} e^{-\frac{(f-\mu)^2}{2\sigma^2}} \tag{2}$$

where μ denotes the mean or expectation of the distribution and σ denotes the standard deviation with variance σ^2. Based on this observation a STC parameter was developed which quantified the deviation of the shape of the frequency spectrum of the seismic trace under analysis from a bell-shaped pdf curve.

*STC Trace Metric **4**: Peak Symmetry Differential (PSD)*

The PSD trace metric facilitates the identification of traces whose peak source wave responses have been significantly skewed due to measurement noise or source wave reflection interference. Figure 2 illustrates this phenomenon. In Fig. 2(A) we have an ideal source wave recording where no interference is present. In this case the time difference between the two zero crossings bounding the peak response (A1) are identical ($\Delta t1 = \Delta t2$). In Fig. 2(B) we have a source wave recording with interference, resulting in skewing or time shifting of the peak source wave response. The “peak symmetry” error assessment is also carried out on the adjacent peaks and/or troughs if the amplitude exceeds 70 % of that for the peak response. Obviously traces with a lower PSD value are of a lesser quality and require more attention during analysis.

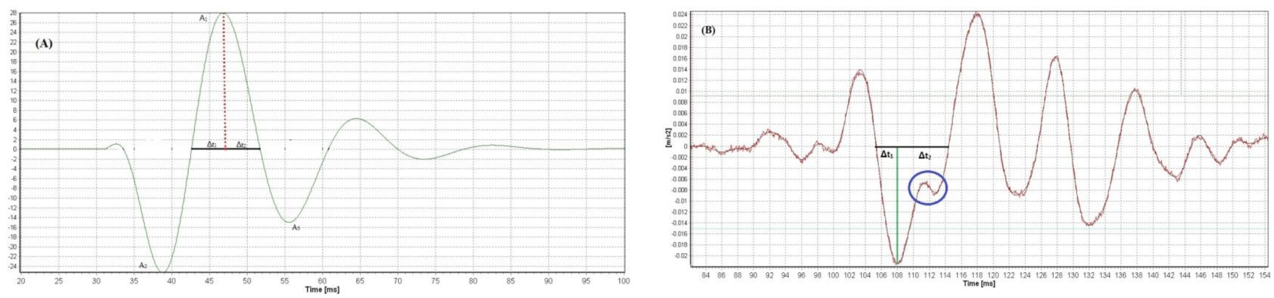

Figure 2. Source wave peak distortions due to measurement noise or source wave reflection interference. (A) Ideal source wave recording where no interference is present. (B) Source wave with interference resulting in skewing or time shifting of the peak source wave response. The black line is the unfiltered trace while the red line is the filtered trace where a low pass filter of 200 Hz was applied.

STC Trace Metric 5: Signal to Noise Ratio (SNR)

The SNR trace metric uses as input the as-recorded seismic trace and compares it with the filtered trace to quantify what portion of the spectral content of the recorded seismogram resides within the desired source frequency spectrum. While this parameter provides mainly insight in the quality of the data acquisition (such as gain settings, noise levels and testing environment) and does not really provide guidance for data analysis, it is nevertheless an important parameter. When during testing to establish SH interval velocities testing is performed from two sides, the SNR metric is very beneficial in selecting the outcome when there is a large spread between the two results.

It should be noted that it is possible for source wave distortions (such as near-field effects, reflections, refractions, and “dirty sources”) to have spectral content which resides within the source wave frequency spectrum. Consequently the parameter value may imply a better quality trace than it really is.

3.0 RECOMMENDED DATA ANALYSIS and SIGNAL PROCESSING BASED on STC

All STC trace metrics vary from 0 to 1 where it is desired that they approach the optimal 1.0 value. Low LIN values are typically handled separately from SSP, CCC and PSD values. This is due to the fact that the LIN values directs the investigator on whether the full waveforms should be utilized for analysis or a preferential axis response, while the SSP, CCC and PSD trace metrics give indications of the quality of the seismic traces under analysis. Different seismic signal processing techniques are then applied based upon the SSP, CCC and PSD values.

3.1 Post Analysis and Signal Processing: Linearity Values

LIN estimates are derived from triaxial or biaxial seismic sensor configurations. For data analyses to obtain horizontally polarized shear wave (V_{SH}) velocity values the X- and Y-axis responses are of interest. LIN values for these responses approaching 1.0 are highly desirable and indicate that there is a preferred directionality of the source wave responses, and therefore the X- and Y-axis responses can be rotated on to the full wave form axis, which increases the signal-to-noise ratio. Generally, LIN values 0.8 or better indicate that the full waveforms can be utilized without any cause of concern, while lower values require corrective action as illustrated in the four test cases below.

3.1.1 Test Case LIN 1 – overall linearity values ≥ 0.8 with a few outliers due to poorly correlated source wave responses.

DST Data sets with these LIN values are typically of very good quality and the full wave forms can be used for data analysis. Generally, there are either dominant responses on the X axis and/or Y axis or highly correlated responses on the X and Y axis, but a few lower LIN values may need to be addressed. Figure 3 illustrates filtered (200Hz low pass) Vertical Seismic Profile (VSP). The filtered VSP illustrates X- and Y-axis responses with the dominant source wave responses on the Y axis. The corresponding LIN values are given in Table 1 and for most depths they exceed 0.8, in which case the full wave forms are utilized. However, lower LIN values occur at depths 1m, 2m and 9m.

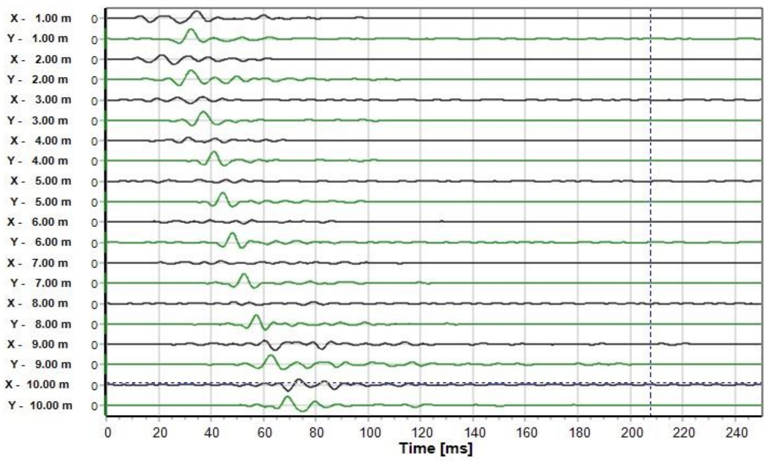

Figure 3. Filtered (200 Hz low pass) VSP [LIN 1]

Table 1. Linearity Values for [LIN 1]

Depth [m]	Linearity [0-1]
1	0.52
2	0.55
3	0.83
4	0.80
5	0.86
6	0.85
7	0.82
8	0.86
9	0.58
10	0.82

To overcome this the first step is to identify which axis shows the dominant response. If this is consistent with the full wave forms then the response on this axis can be used in the analysis. For example, the filtered VSP in Figure 3 clearly showed that the dominant responses reside on the Y axis. The filtered traces recorded at 1m are shown in Figure 4 and it is clear that the responses are not correlated (resulting in the low linearity value of 0.52 as shown in Table 1). It is also clear that there is a high quality Y-axis response recorded at this depth, which is in line with the dominant responses at the other depths. Therefore at 1 m the Y-axis response is utilized rather than the full wave form. This is also the case for the traces recorded at 2m and 9m which had associated low linearity values of 0.55 and 0.58, respectively.

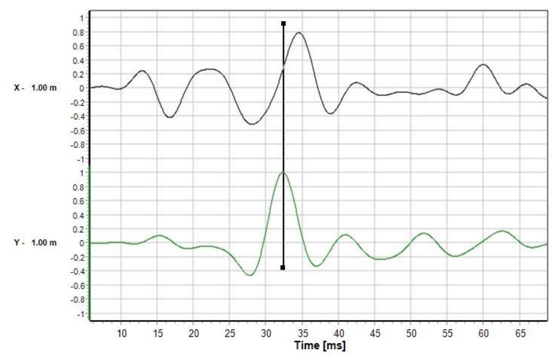

Figure 4. Filtered recorded traces at 1 m [LIN 1]

3.1.2 Test Case LIN 2 – overall linearity values ≥ 0.8 with a few outliers due to low SNR

Data sets with these LIN values are typically of very good quality and the full wave forms can be used for post analysis. Generally, there are either dominant responses on the X axis and/or Y axis or highly correlated responses on the X and Y axis, but a few lower LIN values may need to be addressed. Figure 5 illustrates filtered (200Hz low pass) Vertical Seismic Profile (VSP) for test case LIN2. The filtered VSP in Figure 5 illustrates X and Y axis responses where there is no single axis that contains the dominant response at all depths. The corresponding and widely varying LIN values are given in Table 2.

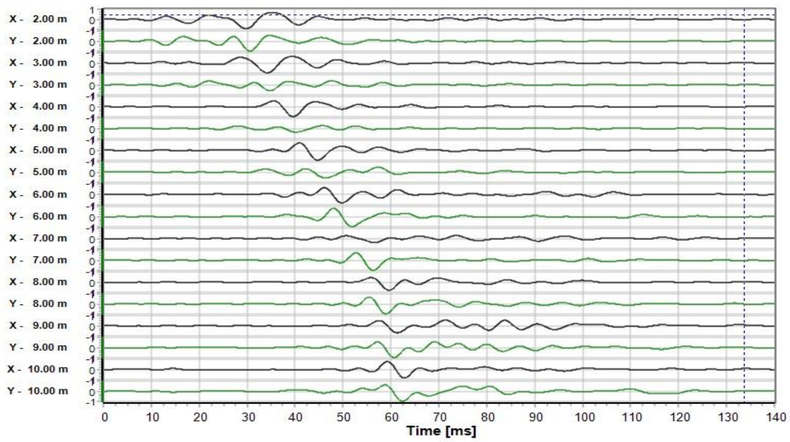

Figure 5. Filtered (200 Hz low pass) VSP [LIN 2]

Table 2. Linearity Values for [LIN2]

Depth [m]	Linearity [0-1]
2	0.58
3	0.70
4	0.84
5	0.62
6	0.30
7	0.80
8	0.81
9	0.48
10	0.81

Figure 6 illustrates the X- and Y-axis responses recorded at 10m, which demonstrates that the high linearity is due to correlated X and Y axis responses and not due to dominant responses on either the X or Y axis. This in turn means that the X and Y axis responses can be utilized in post analysis where poor linearity values occur due to noise responses and not poorly correlated source wave responses. Figure 7 illustrates the filtered X- and Y-axis responses at 2 m, where again the peaks and troughs of the source wave responses align, but the interference on the X axis (highlighted by the red circle) introduces such distortion on the X axis so that the LIN value is significantly reduced. For this case we can utilize the higher quality Y-axis response along with the full wave forms for other depths.

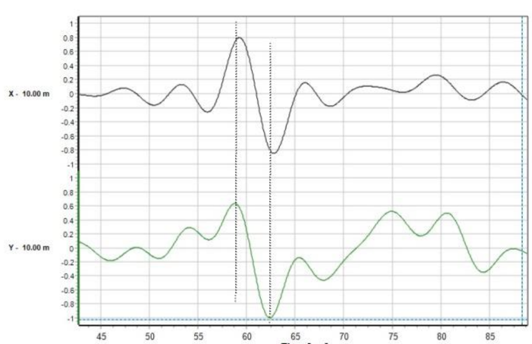

Figure 6. Recorded traces at 10 m [LIN 2]

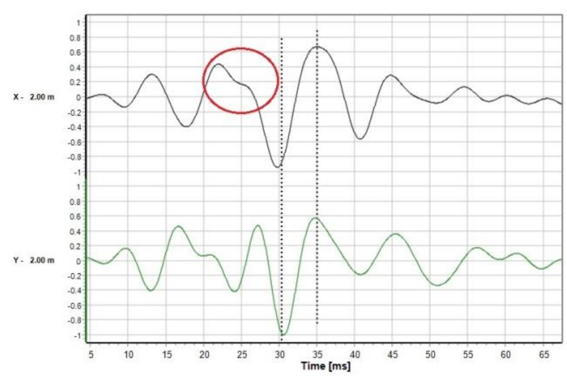

Figure 7. Recorded traces at 2 m [LIN 2]

3.1.3 Test Case LIN 3 – Overall low linearity values with poorly correlated X and Y axis responses, but with a dominant response at all depths on the same axis

For data sets with low LIN values we cannot utilize both X and Y axis responses in post analysis. The investigator must then select either the X or Y axis responses for data analysis and subsequently determine individual axis trace metrics values. Figure 8 illustrates filtered (200Hz low pass) Vertical Seismic Profile (VSP) for test case LIN3, where the Y-axis responses are clearly dominant and of higher quality. The corresponding LIN values are given in Table 3, suggesting very poorly correlated X- and Y-axis responses. In cases like this the investigator proceeds with the analysis using the higher quality responses, which in this case are obviously the Y axis responses.

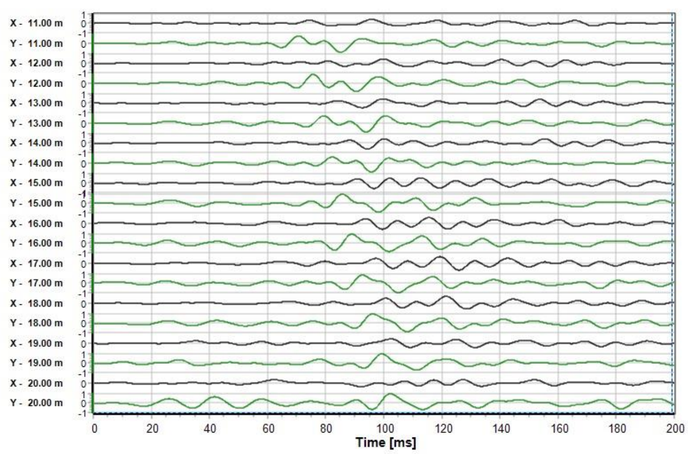

Figure 8. Filtered (200 Hz low pass) VSP [LIN 3]

Table 3. Linearity Values for [LIN3]

Depth [m]	Linearity [0-1]
11	0.76
12	0.80
13	0.72
14	0.69
15	0.65
16	0.61
17	0.57
18	0.67
19	0.75
20	0.67

3.1.4 Test Case LIN 4 – Overall low linearity values with poorly correlated X and Y axis responses and no dominant response on the same axis for all depths.

As mentioned before, for data sets with low LIN values the post-analysis cannot utilize X and Y axis responses randomly: the investigator must select either the X or the Y axis responses. But sometimes this is impossible and the X-axis responses have to be used for certain depth intervals and the Y-axis responses for others. In that case it is important that there is overlap when transitioning from X axis to Y axis responses and vice versa. For example, assume the investigator is going to use X axis responses for depths 1m to 6m and Y axis responses from 6m to 15m. In this case interval arrival times are obtained for traces between 1m and 6m utilizing the X-axis responses and a reference time for one of the depths between 1m to 6m. Next the Y axis responses for traces between 6m to 15m are utilized to obtain interval arrival times with the X axis arrival time for 6m as the reference time. The arrival time are then feed into an algorithm which takes into account raypath refraction when estimating interval velocities (Baziw, 2002; Baziw and Verbeek, 2012 and 2014).

3.2 Post Analysis and Signal Processing: CCC, SSP, and PSD Values

While the LIN value helps with the selection of the traces to be analyzed, the SSP, CCC and PSD trace metrics give indications of the quality of the seismic traces under analysis based upon the form and shape of the time series and corresponding spectral content. Several different combinations (high vs low) of SSP, PSD and CCC values can exist due to the fact that they address different characteristics of the acquired seismic trace. Based on the values of these parameters the most appropriate processing technique (batch signal decay, seismic feature decay and aggressive frequency filtering) is then selected as illustrated in the various test cases below, which assume threshold values for SSP, PSD and CCC of 0.6, 0.8 and 0.3, respectively.

3.2.1 Test Case SSP PSD CCC 1 – Good CCC and PSD values, but poor SSP values

Data sets with good CCC and PSD values but poor SSP values occur whenever there is source wave "ringing" as illustrated in the filtered (200 Hz low pass filter) VSP in Figure 9. Table 4 outlines the corresponding SSP, CCC, and PSD trace metric.

Table 4. SSP, CCC and PSD Values for [SSP PSD CCC 1]

Depth [m]	SSP [0-1]	CCC [0-1]	PSD [0-1]
20	0.547	0.9216	0.96
21	0.525	0.8266	0.48
22	0.379	0.8024	0.87
23	0.483	0.9151	0.65
24	0.556	0.9533	0.71
25	0.491	0.9671	0.79
26	0.51	0.9587	0.73
27	0.391	0.9379	0.96
28	0.428	0.9144	0.84
29	0.544	0.8841	0.61
30	0.363	0.8569	0.94

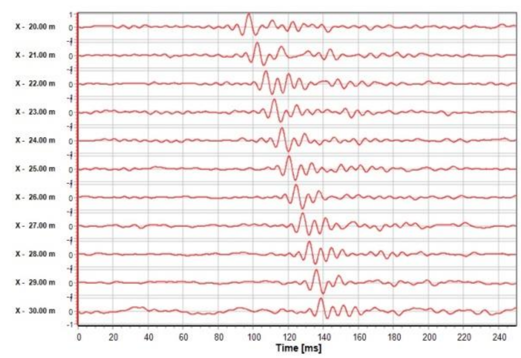

Figure 9. Filtered VSP [SSP PSD CCC 1]

Clearly only the SSP values are cause of concern and this is readily addressed through batch signal decay (BSD), which applies a time window around the peak responses moving forward and backward in time by two crossovers. The implementation of BSD on this data set is shown in Figure 10.

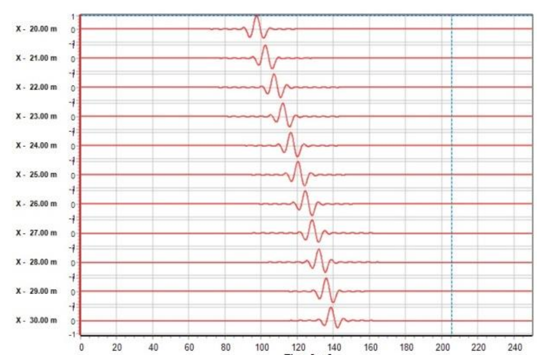

Figure 10. Filtered VSP after batch signal decay [SSP PSD CCC 1]

3.2.2 Test Case SSP PSD CCC 2 – Good CCC values, but poor PSD and SSP values

Data sets with very low PSD values generally are affected by extensive source peak skewing. This is illustrated in the filtered (200Hz low pass) VSP in Figure 11, while the trace metrics values of SSP, CCC and PSD are given in Table 5 with low PSD values between 10m and 13 m and also between 17 m and 20 m. The black circles outline in Fig. 11 outline the extensive peak skewing. To address the low PSD values a consistent portion of the seismic source wave signature where there is minimal to no skewing is isolated throughout the profile (so-called Signal Feature Decay (SFD)). The seismic traces recorded between 12 m and 14 m shown in Fig. 12 clearly show that there is minimal first trough distortion, and therefore SDF is applied on this data set to isolate the first troughs. The results are illustrated in Figure 13.

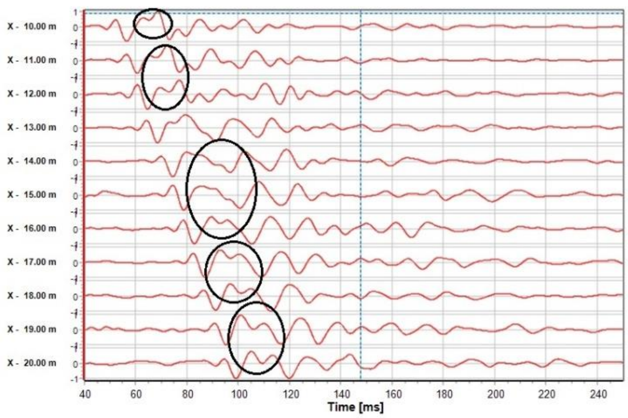

Figure 11. Filtered VSP with peak skewing areas highlighted [SSP PSD CCC 2]

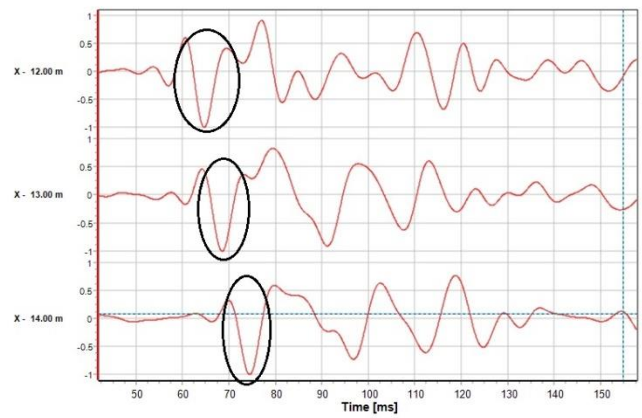

Figure 12. DST seismic traces between 12 m and 14 m [SSP PSD CCC 2] illustrating first trough responses.

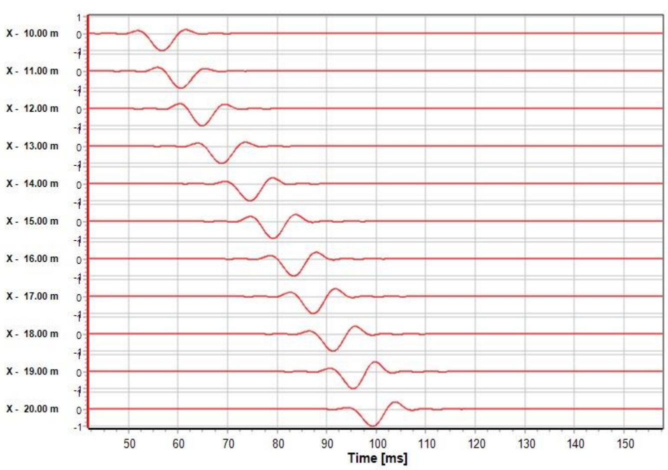

Figure 13. Filtered VSP after signal feature decay [SSP PSD CCC 2]

Table 5. SSP, CCC and PSD Values for [SSP PSD CCC 2]

Depth [m]	SSP [0-1]	CCC [0-1]	PSD [0-1]
10	0.49	0.9603	0.01
11	0.45	0.9239	0.01
12	0.39	0.9323	0.01
13	0.55	0.9144	0.01
14	0.47	0.8582	0.39
15	0.58	0.9283	0.96
16	0.53	0.9553	0.84
17	0.52	0.952	0.01
18	0.59	0.9884	0.01
19	0.56	0.9464	0.01
20	0.54	0.9814	0.01

3.2.3 Test Case SSP PSD CCC 3 – Good SSP and PSD values, but poor CCC values

If only the CCC values are low, SFD is again the suggested remedial action. In Fig. 14 a filtered (200Hz low pass) VSP is shown with the corresponding SSP, CCC and PSD trace metrics outlined in Table 6, which shows low CCC values between 3 m and 5 m with very good PSD values and SSP values very close to the desired 0.6 threshold except at a depth of 5 m. The dashed line in Fig. 14 clearly identifies the first trough responses in the entire VSP and Figure 15 then shows the VSP after isolating the first trough responses by SDF.

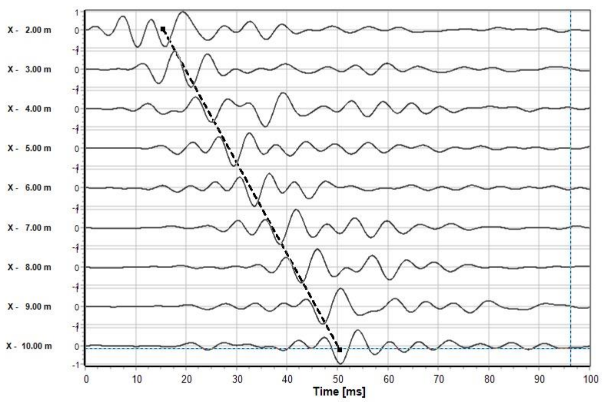

Figure 14. Filtered VSP with the first trough trend line [SSP PSD CCC 3].

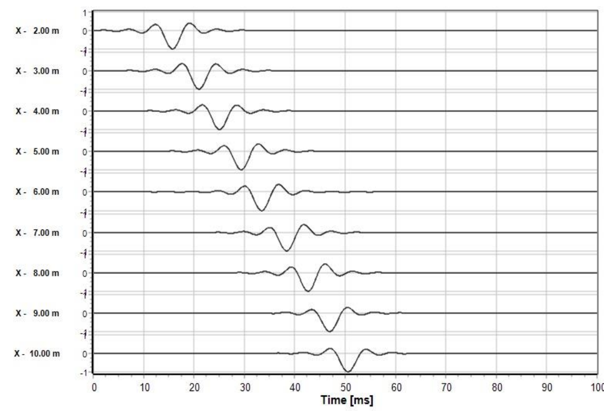

Figure 15. Filtered VSP after SDF applied [SSP PSD CCC 3]

Table 6. SSP, CCC and PSD Values for [SSP PSD CCC 3]

Depth [m]	SSP [0-1]	CCC [0-1]	PSD [0-1]
2	0.60	N/A	0.54
3	0.64	0.6497	0.69
4	0.59	0.5229	0.73
5	0.48	0.6394	0.75
6	0.46	0.8639	0.78
8	0.50	0.6862	0.85
9	0.59	0.8853	0.87
10	0.59	0.8558	0.83

Table 7. SSP, CCC and PSD Values for SSP PSD CCC 4

Depth [m]	SSP [0-1]	CCC [0-1]	PSD [0-1]
1	0.563	N/A	0.67
2	0.462	0.7526	0.07
3	0.45	0.6931	0.01
4	0.517	0.7264	0.37
5	0.75	0.833	0.99
6	0.6	0.9513	0.09

3.2.4 Test Case SSP PSD CCC 4 – Poor SSP, PSD and CCC values

In certain cases the entire VSP shows evidence of interference, resulting in poor SSP, PSD and CCC values. To address this type of data set an aggressive 120Hz low pass filter is applied so that the source wave interference is "smoothed". The "smoothed" responses then have SFD applied. This is illustrated on the filtered (200Hz low pass) VSP shown in Fig. 16, where there is evidence of significant source wave distortions throughout the source wave responses. Table 7 outlines the corresponding SSP, CCC and

PSD trace metrics, while Figure 17 shows the data set after applying an aggressive 120Hz low pass filter and SDF on the “smoothed” second peak responses.

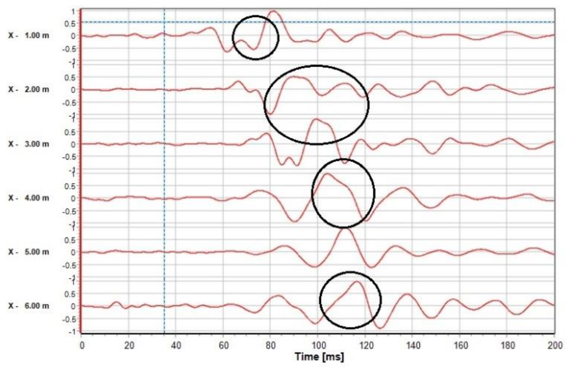

Figure 16. Filtered VSP with the evidence of interference at all depths [SSP PSD CCC 4]

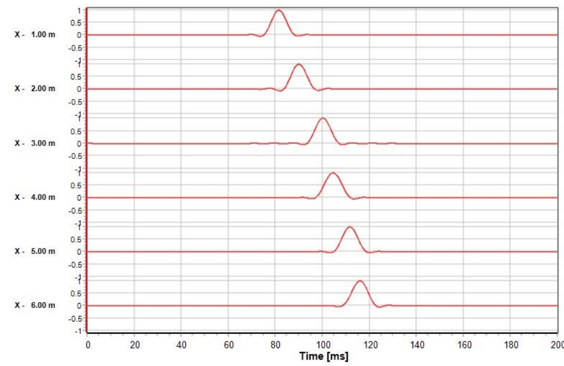

Figure 17. Aggressively filtered VSP after SDF [SSP PSD CCC 4]

3.3 Post Analysis and Signal Processing: SNR Values

When based on the LIN values the traces to be analyzed are selected, and based on the PSD, SSP and CCC values the most appropriate processing technique is determined, the SNR value can provide inside when there is a substantial difference between the outcome for the signals from the right side and the left side.

In Table 8 below the calculated interval velocities are shown for the right side and the left side, which reflect a larger spread (defined as ½ x (LS Velocity – RS)/Avg. Velocity) than desired (the objective is to have the spread within 10 %). Given the SNR values it can be concluded that the results for the right side are most likely more reliable, given the higher quality seismic traces at that side.

Table 8. RS and LS SNR and Interval Velocity Values

Depth [m]	SNR RS [0-1]	SNR LS [0-1]	RS Velocity [m/s]	RS Velocity [m/s]	Percent Difference (%)
2.000	0.95	0.74	N/A	N/A	
2.500	0.89	0.57	290	230	11.5
3.000	0.87	0.64	265	200	14

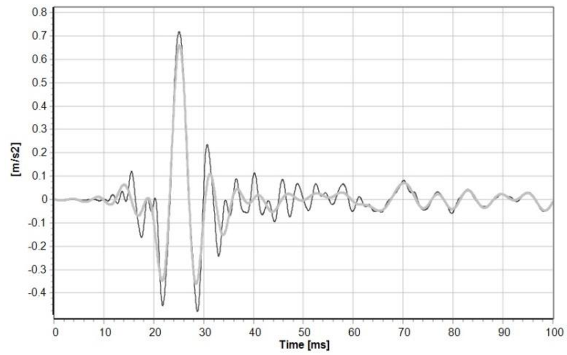

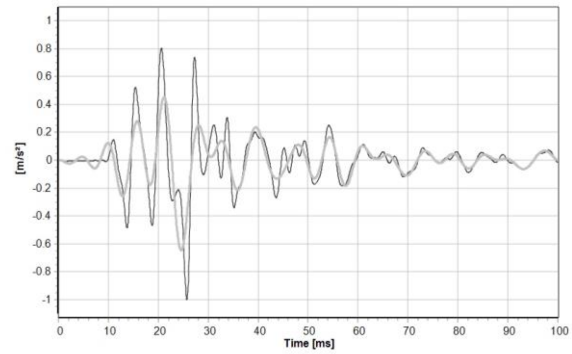

Figure 18. Unfiltered (black trace) superimposed upon filtered trace (light grey) for RS recorded at 2.5m.

Figure 19. Unfiltered (black trace) superimposed upon filtered trace (light grey) for LS recorded at 2.5m.

CONCLUSIONS

Downhole seismic testing (DST) is a very popular applied seismology site characterizing tool within geotechnical engineering. One of the fundamental goals of DST is to quantify the shear wave interval velocities (V_S) as this is an important parameter for evaluating the liquefaction potential due to fact that it is influenced by many of the variables that influence liquefaction. This paper has outlined BCE's newly Seismic Trace Characterization (STC), which is based on various independent seismic trace metrics of the acquired DST data at a particular depth. There are currently five independent trace metrics which are linearity, cross correlation coefficient, signal shape parameter, peak symmetry differential and signal-to-noise ratio. This paper also outlined how these 5 parameters can guide the data analysis to derive more accurate results.

REFERENCES

Aki, K. and Richards, P.G. 2002. Quantitative Seismology, 2nd edition, Sausalito, California: University Science Books.

Andrus, R.D., & Stokoe, K.H. (1997). "Liquefaction resistance based on shear wave velocity". National Center for Earthquake Engineering Research (NCEER) Workshop. Salt Lake, Utah, pp. 89-128.

ASTM (American Standards and Testing Methods). (2017). "D7400: Standard Test Methods for Downhole Seismic Testing." ASTM Vol. 4.09 Soil and Rock (II): D5877-latest.

Baziw, E. (2002), "Derivation of Seismic Cone Interval Velocities Utilizing Forward Modeling and the Downhill Simplex Method", Can. Geotech. J., 39(5), pp.1181-1192.

Baziw, E., and Verbeek, G. (2012). "Deriving Interval Velocities from Downhole Seismic Data", Geotechnical and Geophysical Site Characterization 4 – Mayne (eds), CRC Press, 1019–1024.

Baziw, E. and Verbeek, G. (2014). "Identifying Critical Layers using SCPT and Seismic Source Moveout." In the Proceedings of the 3rd International Symposium on Cone Penetration Testing, CPT'14, May 12-14, 2014 - Las Vegas, Nevada, 357-364.

Baziw, E., and Verbeek, G. (2016a), "Frequency spectrum "bell-curve" fitting as a component of SCPT interval velocity accuracy assessment", 5th International Conference on Geotechnical Site Characterization (ISC-5), Queensland – Australia, 5-9 Sept. Australian Geomechanics Society, 1431-1436.

Baziw, E. and Verbeek, G., (2016b)," Interval Velocity Classification Technique in Downhole Seismic Testing", http://www.bcengineers.com/images/BCE_IVC_2016.pdf.

Baziw, E. and Verbeek, G. (2017), "Quality Assessment of Seismic Data Sets and the Impact on Interval Velocity Estimates in DST", In Proceedings of the DFI 42nd Annual Conference on Deep Foundations, New Orleans - USA, October 24-27, 2017. Article #2821; publication #1037 (AM-2017).

Bray, J.D., Zupan, J.D., Cubrinovski, M. and Taylor, M., (2014), "CPT-based liquefaction assessments in Christchurch, New Zealand". Las Vegas, NV, USA: 3rd International Symposium on Cone Penetration Testing (CPT '14), 12-14 May 2014. 1-21. http://www.cpt14.com/cpt14-papers. (Conference Contributions - Papers in published proceedings).

National Research Council, Commission on Engineering and Technical Systems (1985), Committee on Earthquake Engineering Liquefaction of soils during Earthquakes: Washington, D.C., National Academy Press.

Seed, H.B. (1979) "Soil liquefaction and cyclic mobility evaluation for level ground during earthquake", J. Geotech. Engr. Div., ASCE, 105, GT2, 201-225.

Seed, H.B., & Idriss, I.M. (1982) Ground motions and soil liquefaction during earthquakes: Earthquake Engineering Institute Monograph Series.

Appendix 4 – "Analytically modelling DST arrival time databases with high order polynomials for optimal high resolution imaging" to be presented and published in the DFI 47th Annual Conference on Deep Foundations conference proceedings. October 4–7, 2022 – National Harbor, Maryland

Note: The above paper will be included in this training manual once it has been presented and published in the 2022 DFI conference proceedings. Technical Note 33 is included at this time for reference.

Fitting higher order polynomials to DST arrival time data sets for high resolution imaging

Introduction

BCE has developed a new DST analysis technique which "best fits" a high order polynomial to arrival time data sets. In this current mathematical design a Kalman filter formulation is utilized to estimate the coefficients of polynomials which "best fit" DST arrival time data sets. The best fit polynomial arrivals are then feed into BCE's FMDSM technique. This technique has the following highly desirable features:

1. Ability to utilize all arrival time estimates irrespective of measurement errors.
2. Ability to process small depth interval (≤ 0.5m) arrival time data sets.
3. Polynomial "best fit" function allows for user specification of desired depth intervals for data interpolation.
4. Facilitates sophisticated data fusion for significantly more accurate DST interval velocity estimation.
5. *RMS*, *MAPE*, R^2, and R^{2C} accuracy parameters facilitate selecting the appropriate polynomial order and quantify the accuracy of the "best fit" polynomial.

Implementation of this technique on both DST onshore and offshore arrival times has resulted in very impressive results. It is the intention of BCE to expand this analytical technique to tomographic modelling and absorption estimation.

On Shore DST Example:

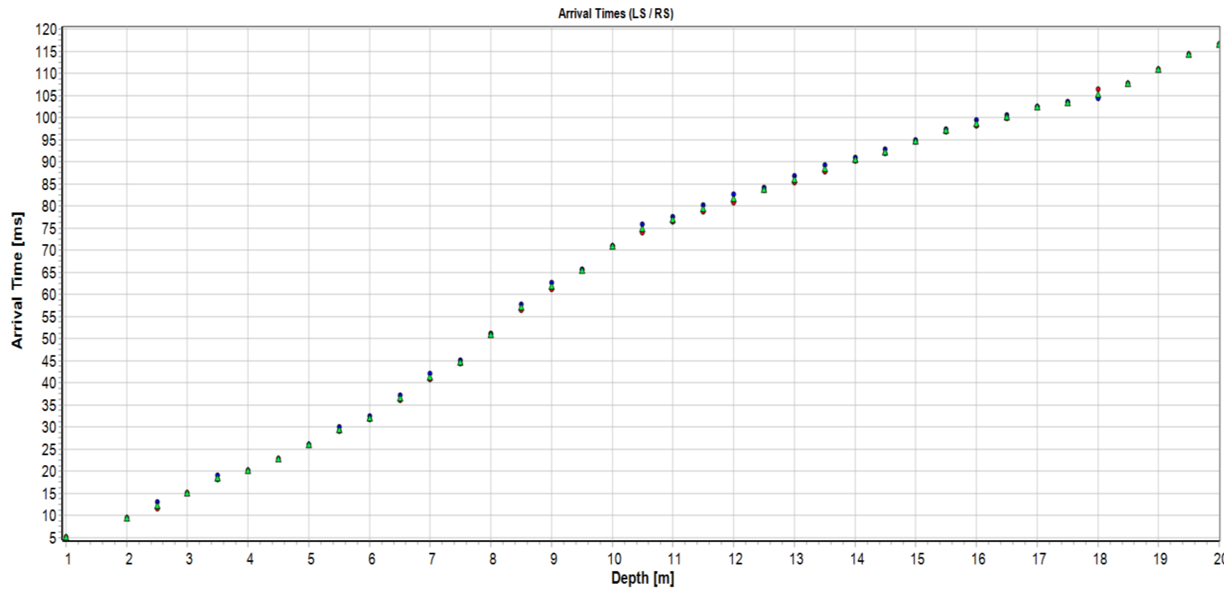

Figure 1. Left Side (LS), Right Side (RS), and averaged arrival times.

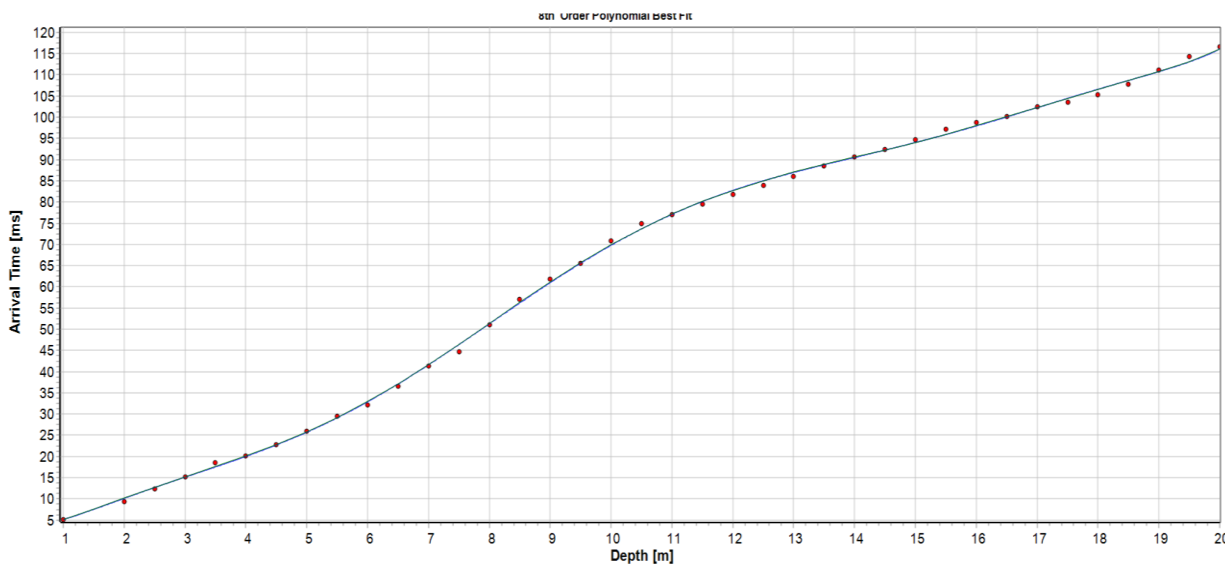

Figure 2. 8th order polynomial best fit estimate to averaged results of Fig. 1.

BEST FIT 8th ORDER S WAVE – 0.5m DEPTH INCREMENT		
Depth [m]	**Arrival Time [ms]**	**Interval FMDSM Velocity [m/s]**
1	5.1198	336
1.5	7.589288	181
2	10.18546	177.5
2.5	12.72785	183.1
3	15.17359	191.7
3.5	17.58675	196
4	20.08186	191.7
4.5	22.78291	179.1
5	25.79552	162
5.5	29.19001	144.7
6	32.9933	129.7
6.5	37.18784	118
7	41.71574	109.6
7.5	46.48668	104.2
8	51.38802	101.5
8.5	56.29613	101.5
9	61.08768	104
9.5	65.65014	109.3
10	69.89065	117.5
10.5	73.74286	129.3
11	77.17118	145.2
11.5	80.1724	165.6
12	82.77439	190.6
12.5	85.03231	219.2
13	87.02226	248.2
13.5	88.83311	272.5
14	90.55693	286.2
14.5	92.27886	286.8
15	94.06745	276.5
15.5	95.96638	260.9
16	97.98908	245.3
16.5	100.1174	233.4
17	102.3065	227.2
17.5	104.4965	227.3
18	106.635	232.9
18.5	108.7099	240
19	110.797	238.5
19.5	113.1239	213.7
20	116.1525	164

Best Fit Polynomial FMDSM results 0.5m Depth Increments

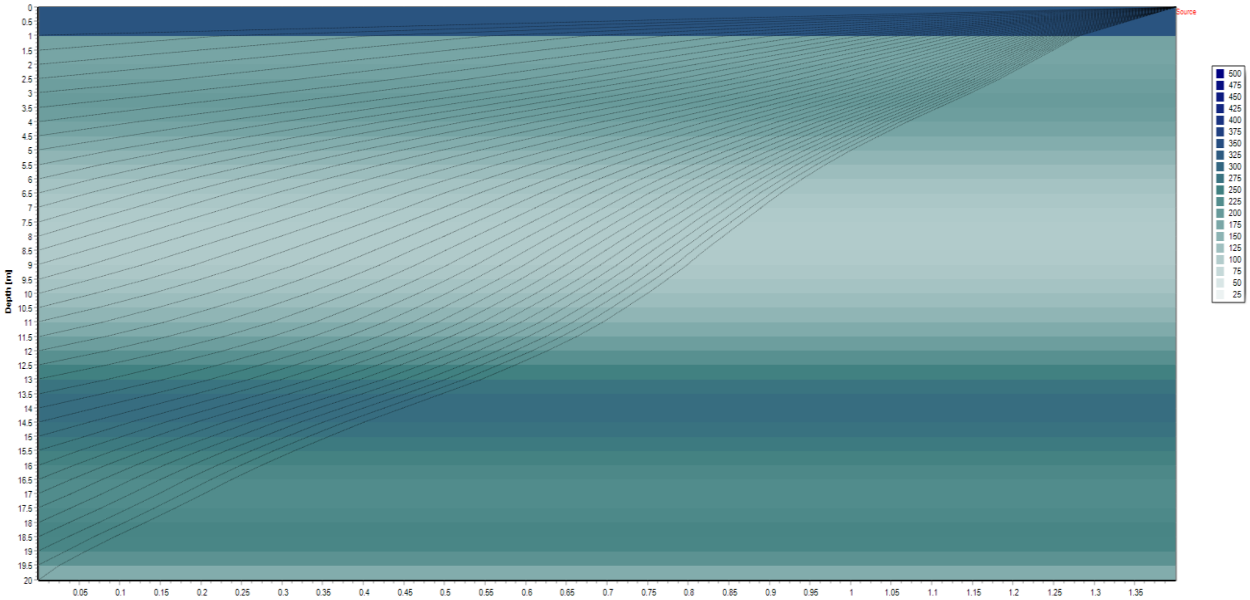

Figure 3. "Best fit" polynomial FMDSM profile.

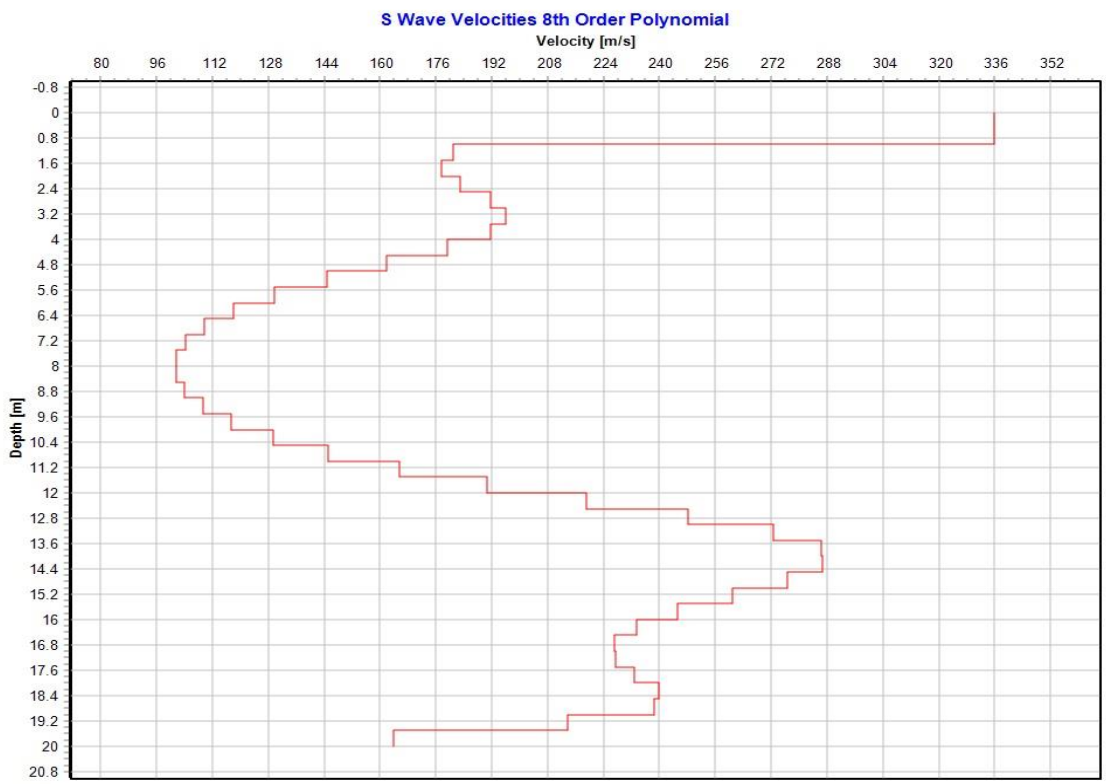

Figure 4. "Best fit" polynomial interval velocity plot.

Off Shore DST Example 1:

Four sets of SH source waves acquired (left side top and bottom sensors (LS TS and LS BS, respectively) and right side top and bottom sensors (RS TS and RS BS, respectively).

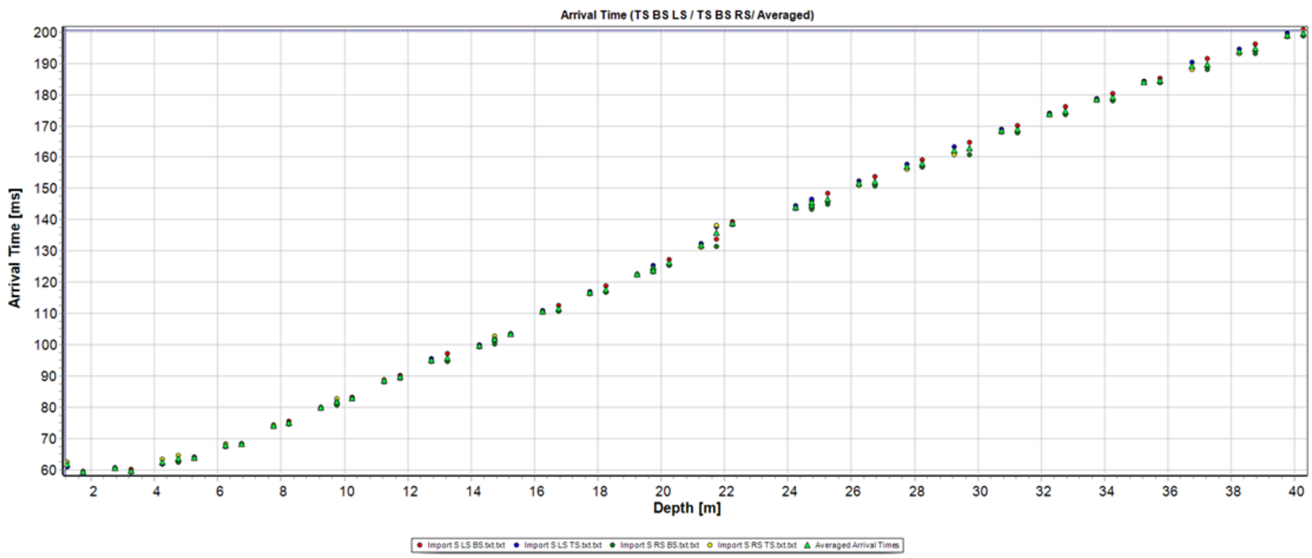

Figure 5. Left Side (LS TS and LS BS), Right Side (RS TS and BS), and averaged arrival times.

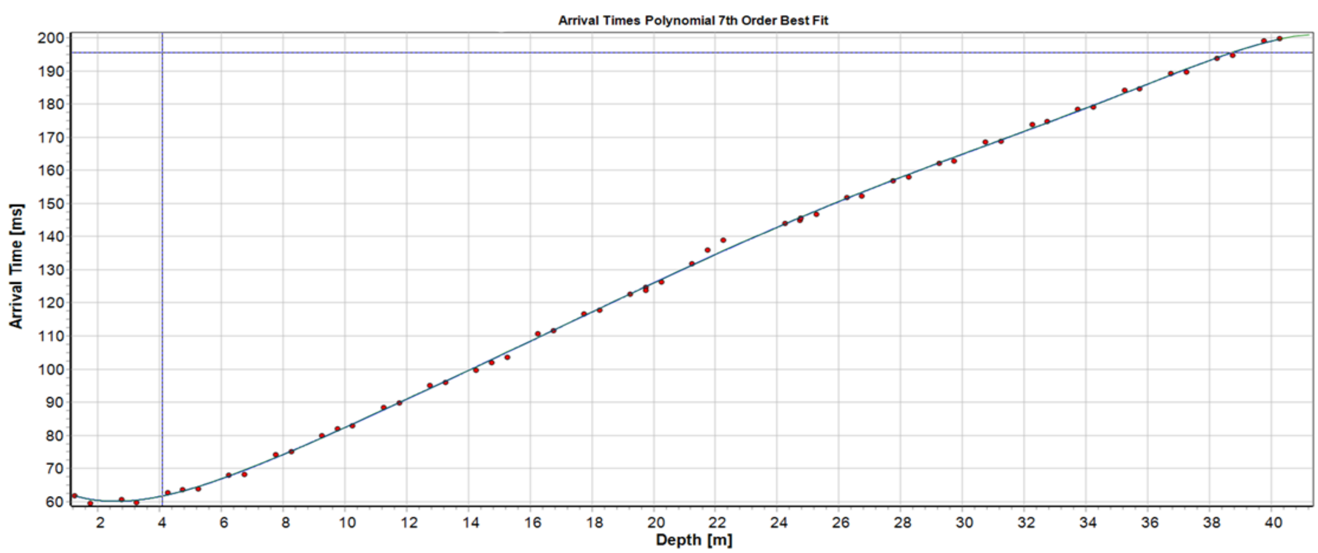

Figure 6. 7th order polynomial best fit estimate to averaged results of Fig. 5.

BEST FIT 7th ORDER S WAVE – 0.5m DEPTH INCREMENT		
Depth [m]	**Arrival Time [ms]**	**Interval FMDSM Velocity [m/s]**
1.24	61.7406	89.7
1.74	60.65947	99.6
2.24	60.13957	108
2.74	60.07694	116.5
3.24	60.40377	125
3.74	61.06047	133.1
4.24	61.99495	140.6
4.74	63.16193	147.3
5.24	64.52227	153.3
5.74	66.04235	158.7
6.24	67.69348	163.4
6.74	69.45141	167.8
7.24	71.29577	171.7
7.74	73.20963	175.4
8.24	75.17906	178.8
8.74	77.19274	181.9
9.24	79.24159	184.8
9.74	81.31842	187.6
10.24	83.41764	190.1
10.74	85.53499	192.4
11.24	87.66726	194.6
11.74	89.81209	196.6
12.24	91.96777	198.4
12.74	94.13304	200
13.24	96.30699	201.4
13.74	98.48888	202.7
14.24	100.6781	203.8
14.74	102.8738	204.9
15.24	105.0754	205.8
15.74	107.282	206.7
16.24	109.4924	207.6
16.74	111.7054	208.4
17.24	113.9195	209.3
17.74	116.1329	210.3
18.24	118.3437	211.4
18.74	120.5497	212.6
19.24	122.7488	214
19.74	124.9384	215.5
20.24	127.1161	217.2
20.74	129.2793	219.2
21.24	131.4256	221.4
21.74	133.5525	223.8
22.24	135.6577	226.5
22.74	137.739	229.4
23.24	139.7947	232.6
23.74	141.823	236
24.24	143.8227	239.7
24.74	145.7931	243.5
25.24	147.7336	247.4
25.74	149.6442	251.5
26.24	151.5255	255.7

26.74	153.3785	259.8
27.24	155.2047	263.8
27.74	157.0061	267.7
28.24	158.7853	271.2
28.74	160.5451	274.5
29.24	162.289	277.2
29.74	164.0207	279.5
30.24	165.744	281.1
30.74	167.4632	282.1
31.24	169.1824	282.4
31.74	170.9057	282.1
32.24	172.6368	281.1
32.74	174.3791	279.7
33.24	176.1353	277.8
33.74	177.9073	275.6
34.24	179.6956	273.4
34.74	181.4996	271.3
35.24	183.3165	269.6
35.74	185.1418	268.6
36.24	186.9684	268.6
36.74	188.786	270.1
37.24	190.5813	273.6
37.74	192.337	279.8
38.24	194.0314	289.9
38.74	195.638	305.5
39.24	197.1248	329.7
39.74	198.4534	368
40.24	199.5789	432.3
40.74	200.4486	553.5
41.24	201.0016	843.4

Figure 7. "Best fit" polynomial FMDSM profile.

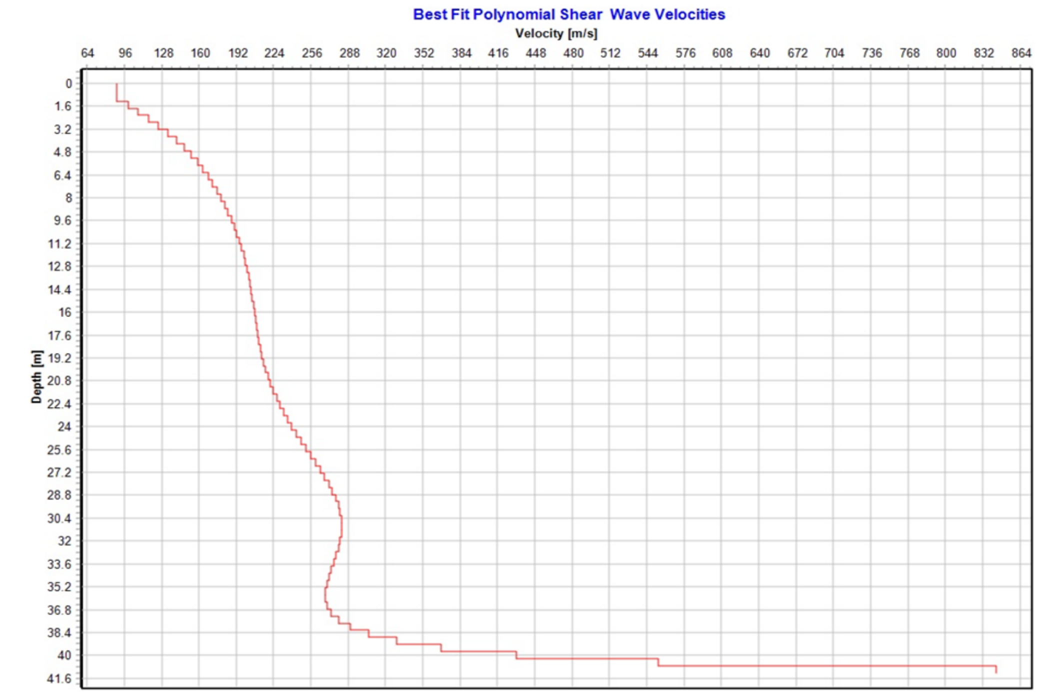

Figure 8. "Best fit" polynomial interval velocity plot.

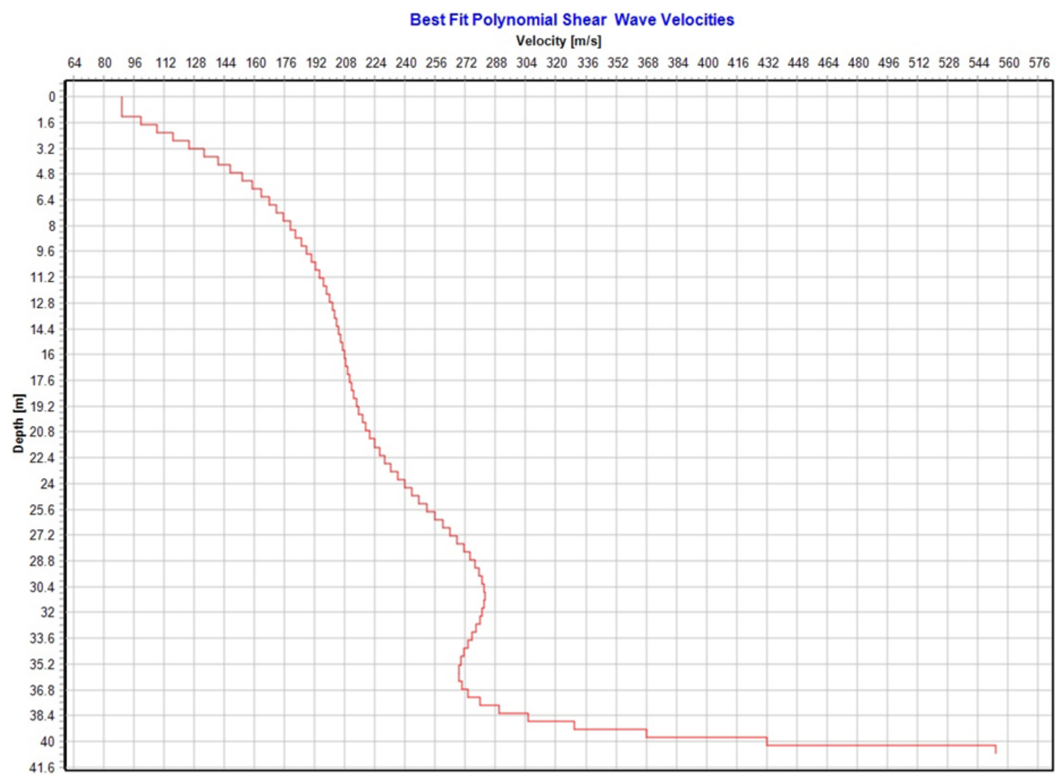

Figure 9. "Best fit" polynomial interval velocity plot (41.24m dropped) .

Off Shore DST Example 2:

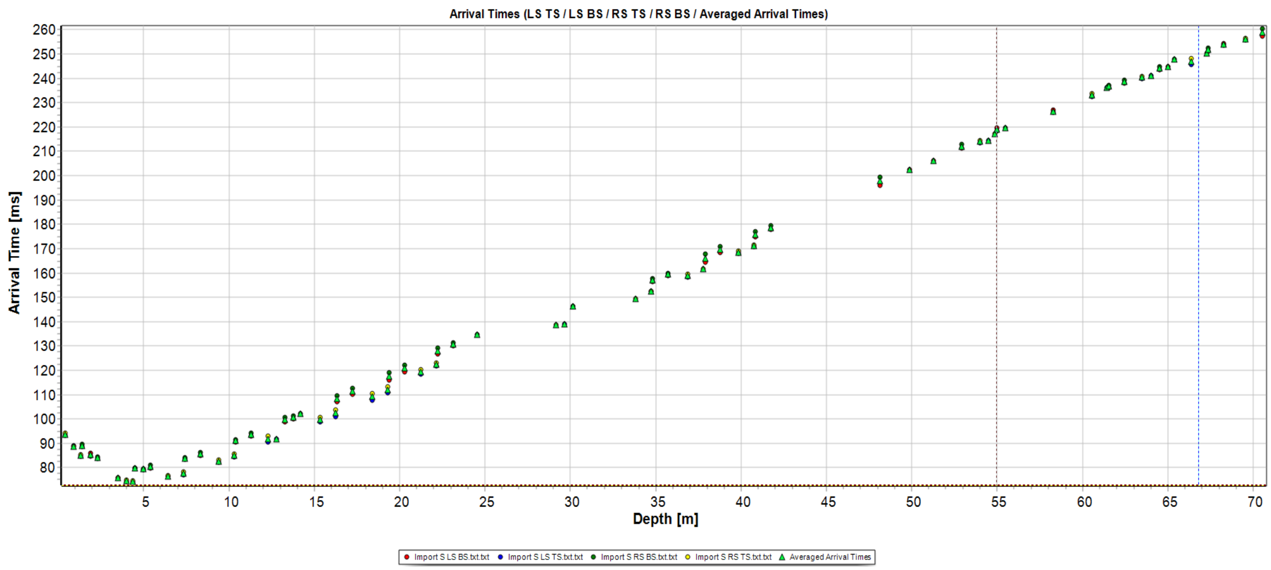

Figure 10. Left Side (LS TS and LS BS), Right Side (RS TS and BS), and averaged arrival times.

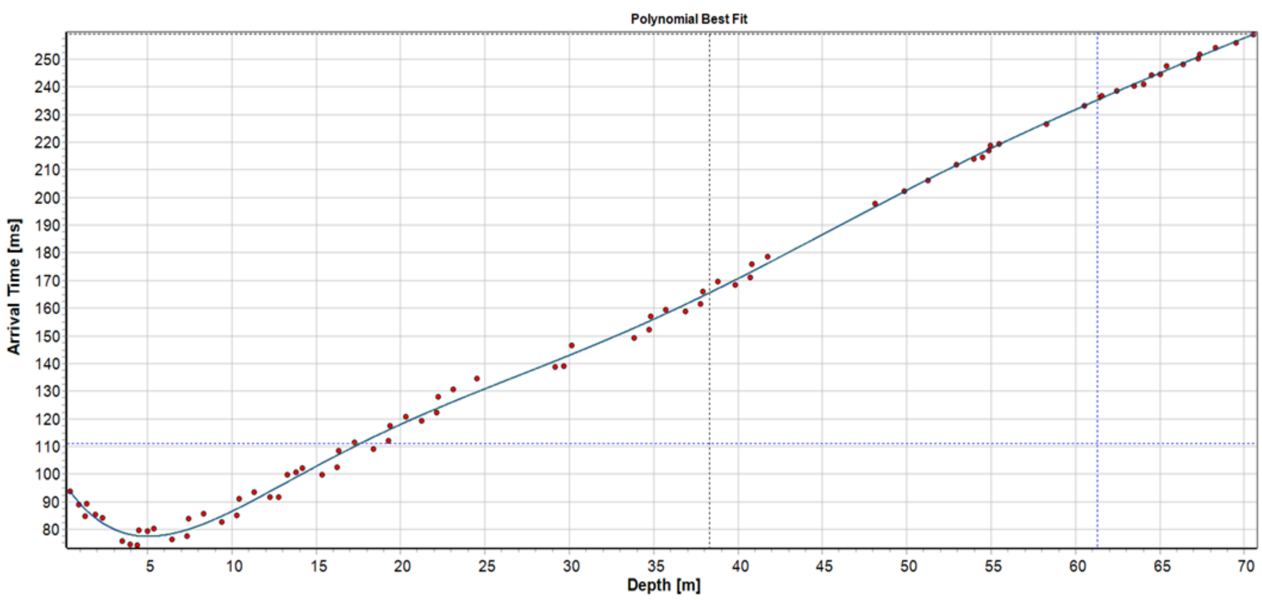

Figure 11. 7th order polynomial best fit estimate to averaged results of Fig. 5.

BEST FIT 7th ORDER S WAVE – 1m DEPTH INCREMENT		
Depth [m]	**Arrival Time [ms]**	**Interval FMDSM Velocity [m/s]**
0.41	93.77395	50.6
1.41	85.90899	58.8
2.41	81.12878	74.6
3.41	78.58437	99.3
4.41	77.68655	133.3
5.41	77.98234	174.5
6.41	79.13037	215.5
7.41	80.87925	245.9
8.41	83.04863	260.3
9.41	85.51293	263.7
10.41	88.18739	263
11.41	91.01646	262.3
12.41	93.96423	263.3
13.41	97.00677	266.5
14.41	100.1263	272
15.41	103.3067	279.5
16.41	106.5308	288.9
17.41	109.7786	299.9
18.41	113.0267	312
19.41	116.2487	325.1
20.41	119.4159	338.6
21.41	122.4994	352
22.41	125.4718	364.8
23.41	128.3095	376.4
24.41	130.9951	386.3
25.41	133.5193	394
26.41	135.8833	399.2
27.41	138.0999	401.8
28.41	140.1946	401.8
29.41	142.2055	399.4
30.41	144.1824	395
31.41	146.1853	388.8
32.41	148.2804	381.6
33.41	150.5362	373.5
34.41	153.0165	365
35.41	155.7724	356.5
36.41	158.8327	348.3
37.41	162.191	340.5
38.41	165.7918	333.3
39.41	169.5129	327
40.41	173.1466	321.4
41.41	176.3765	316.8
42.41	178.3231	313
43.41	181.5233	310.2
44.41	184.7442	308.4
45.41	187.9763	307.4
46.41	191.2096	307.4
47.41	194.4348	308.3
48.41	197.6429	310
49.41	200.8257	312.5
50.41	203.9757	315.8

51.41	207.0869	319.8
52.41	210.1542	324.4
53.41	213.1741	329.5
54.41	216.1443	335.1
55.41	219.0641	340.9
56.41	221.9343	346.8
57.41	224.7567	352.7
58.41	227.5347	358.3
59.41	230.2725	363.6
60.41	232.9751	368.3
61.41	235.6476	372.5
62.41	238.2954	376
63.41	240.9231	378.9
64.41	243.5342	381.4
65.41	246.1301	383.7
66.41	248.7099	386.1
67.41	251.2687	389.3
68.41	253.7971	394
69.41	256.2802	401.3
70.41	258.6958	412.5

FMDSM results 1m Depth Increments

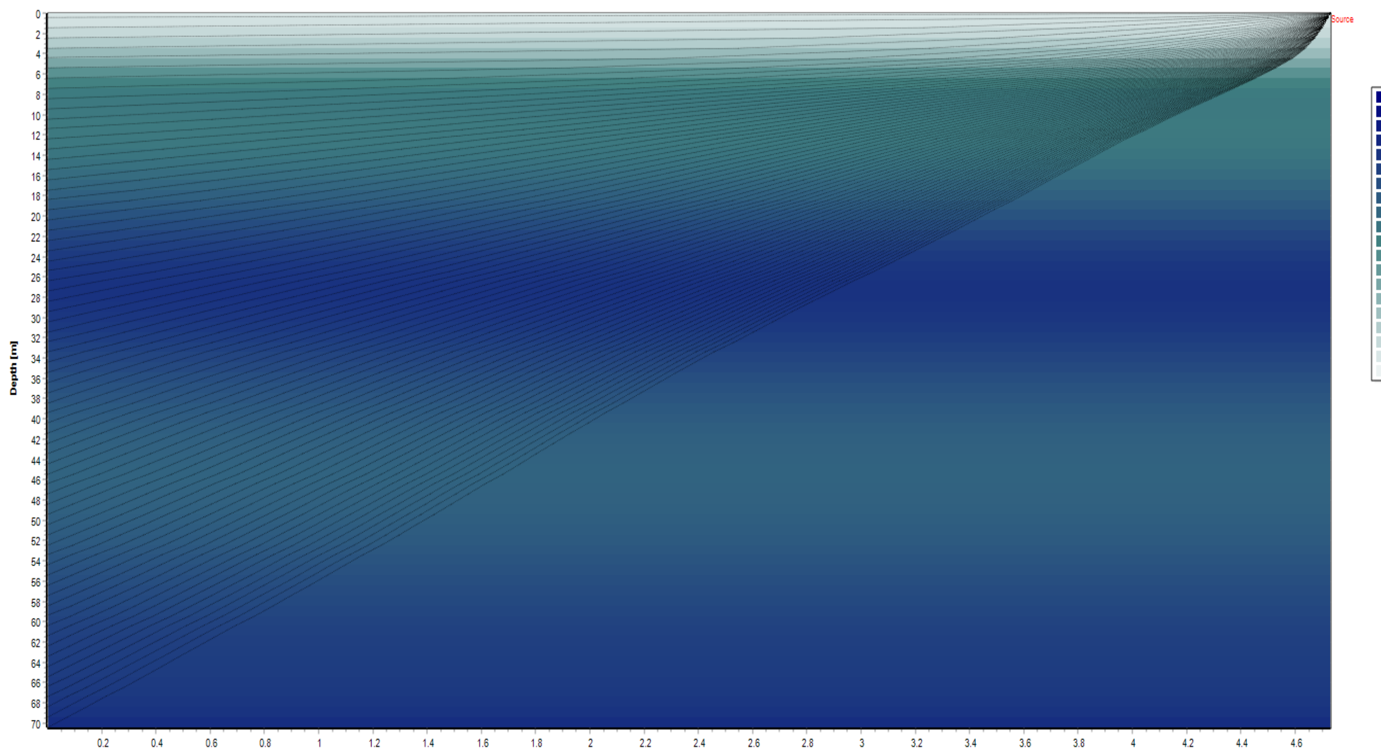

Figure 12. "Best fit" polynomial FMDSM profile.

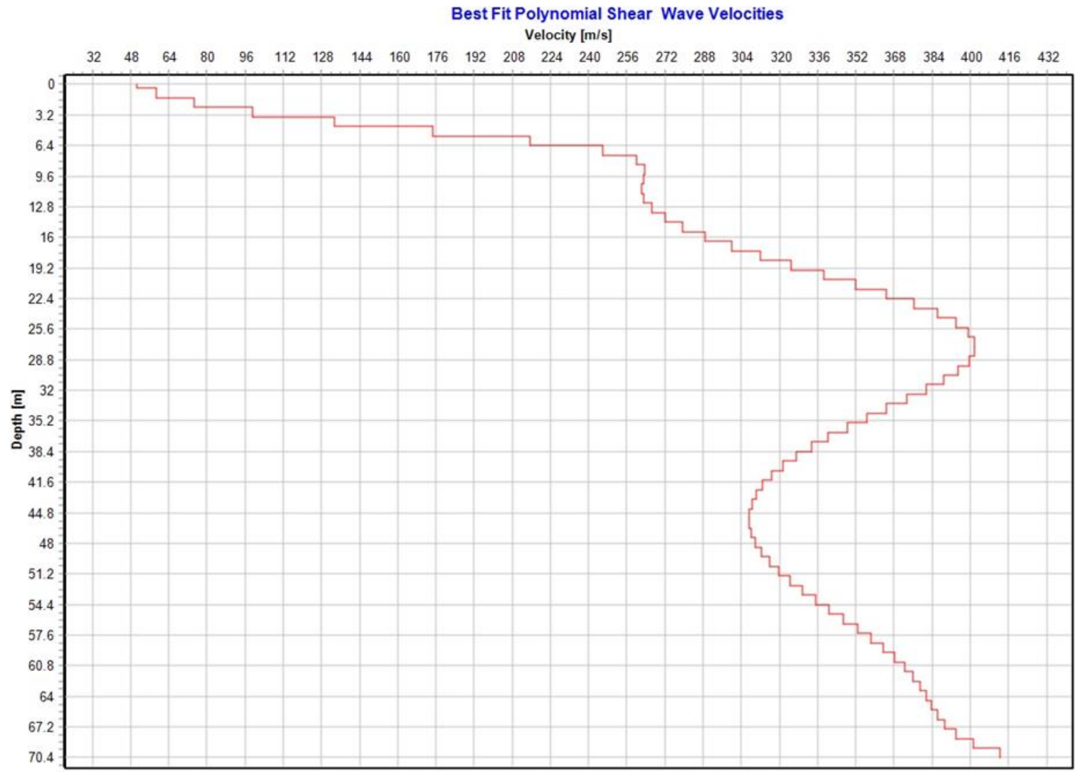

Figure 13. "Best fit" polynomial interval velocity plot.

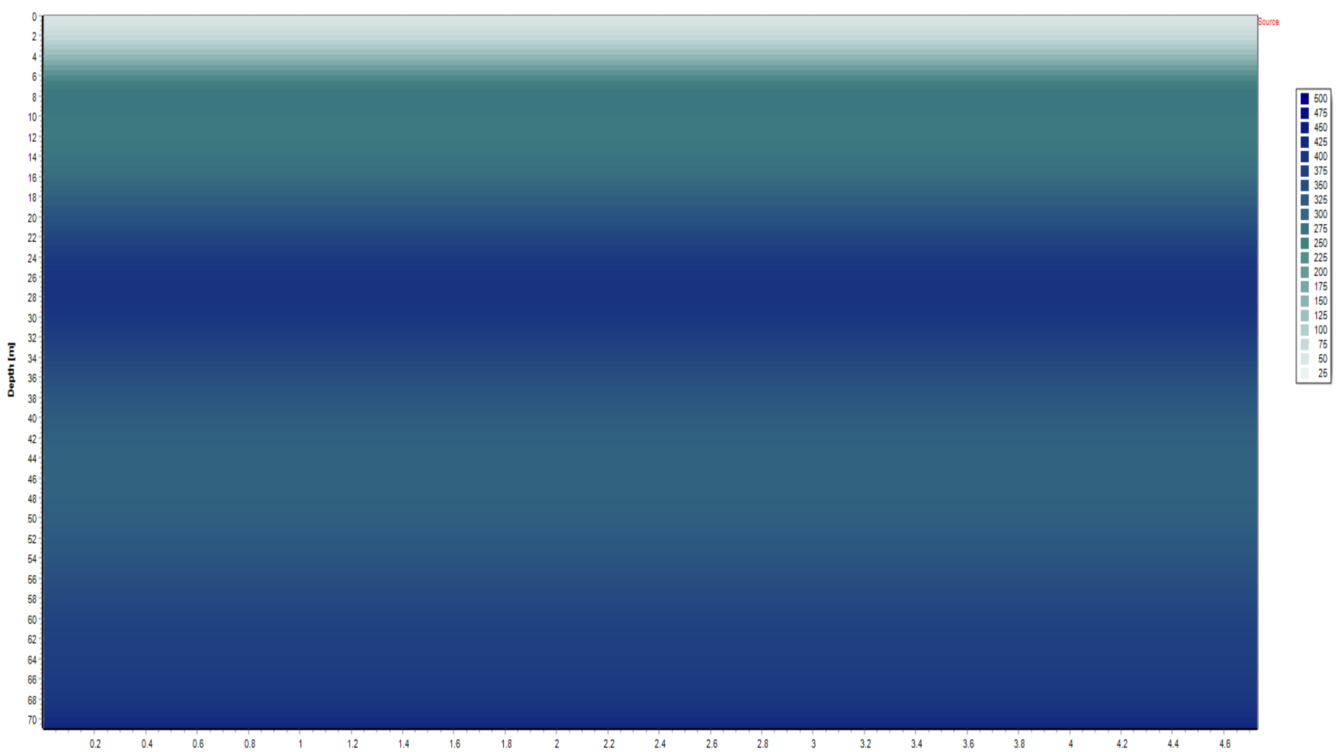

Figure 14. "Best fit" polynomial FMDSM profile (0.5m depth increment).

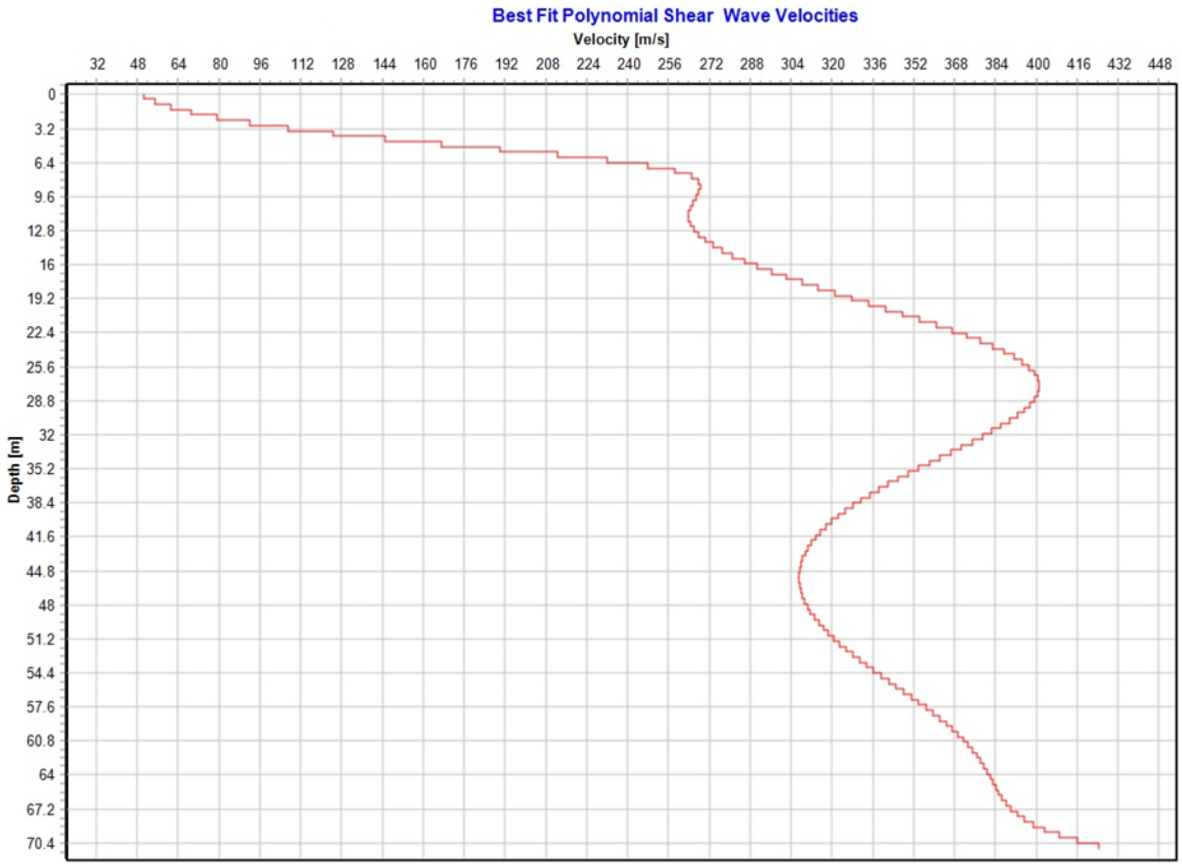

Figure 15. "Best fit" polynomial interval velocity plot (0.5m depth increment).

Off Shore DST Example 3:

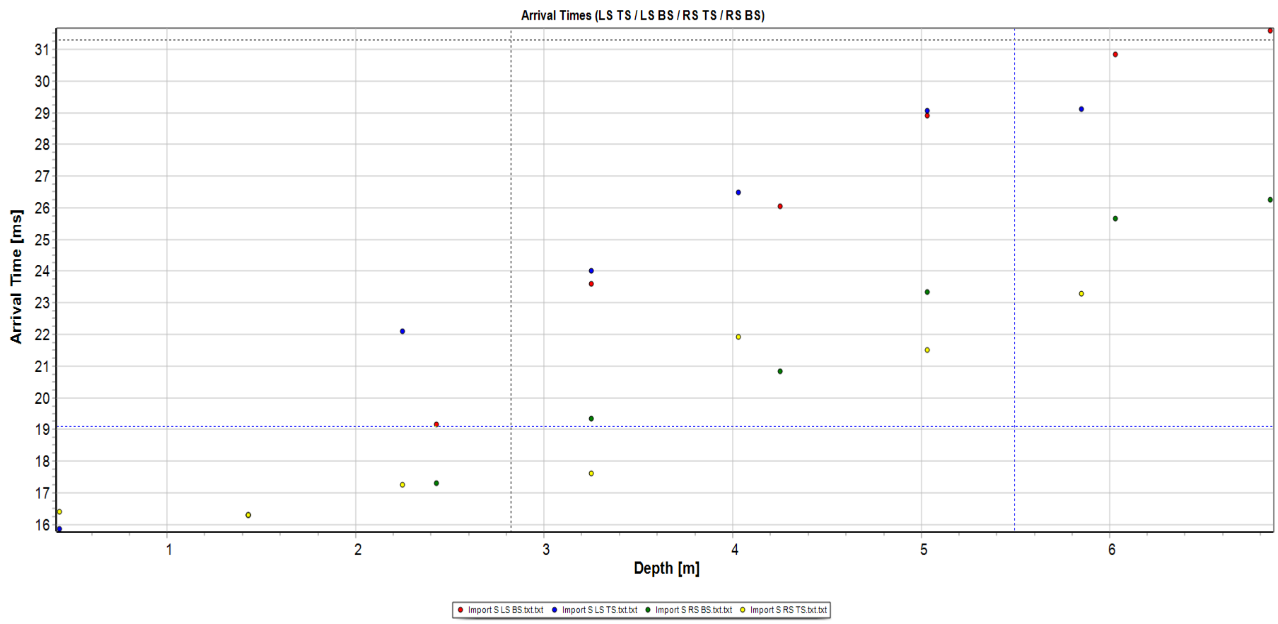

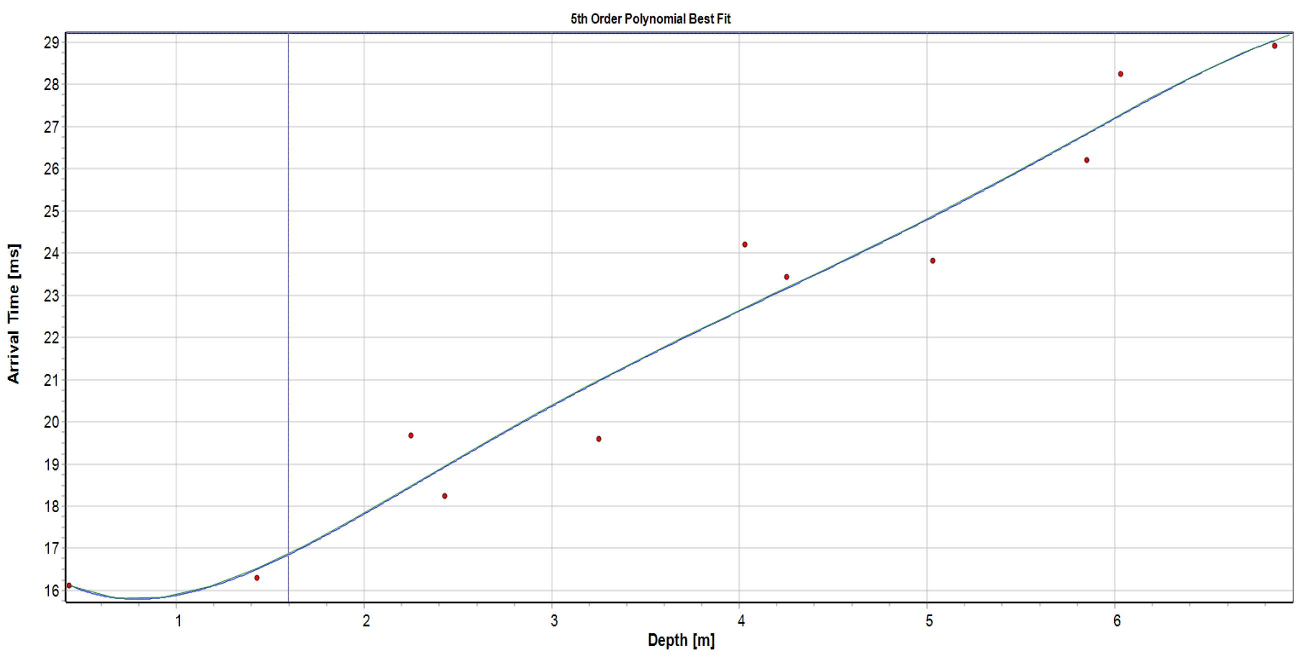

BEST FIT 5th ORDER S WAVE – 0.25m DEPTH INCREMENT		
Depth [m]	**Arrival Time [ms]**	**Interval FMDSM Velocity [m/s]**
0.43	16.12815	208.2
0.68	15.81966	221.4
0.93	15.84154	227.4
1.18	16.0963	226.1
1.43	16.51827	220.2
1.68	17.05338	215.5
1.93	17.65814	213.5
2.18	18.29866	214.5
2.43	18.94968	218.4
2.68	19.59355	224.8
2.93	20.21926	233.2
3.18	20.82146	243.5
3.43	21.39945	255.1
3.68	21.95619	267.5
3.93	22.49736	279.9
4.18	23.0303	291.6
4.43	23.56308	301.5
4.68	24.10347	309.1
4.93	24.65798	314
5.18	25.23087	316.4
5.43	25.82314	317.3
5.68	26.43157	318.1
5.93	27.04769	321.1
6.18	27.65685	328.8
6.43	28.23719	345.2
6.68	28.75865	377
6.93	29.18201	438.9

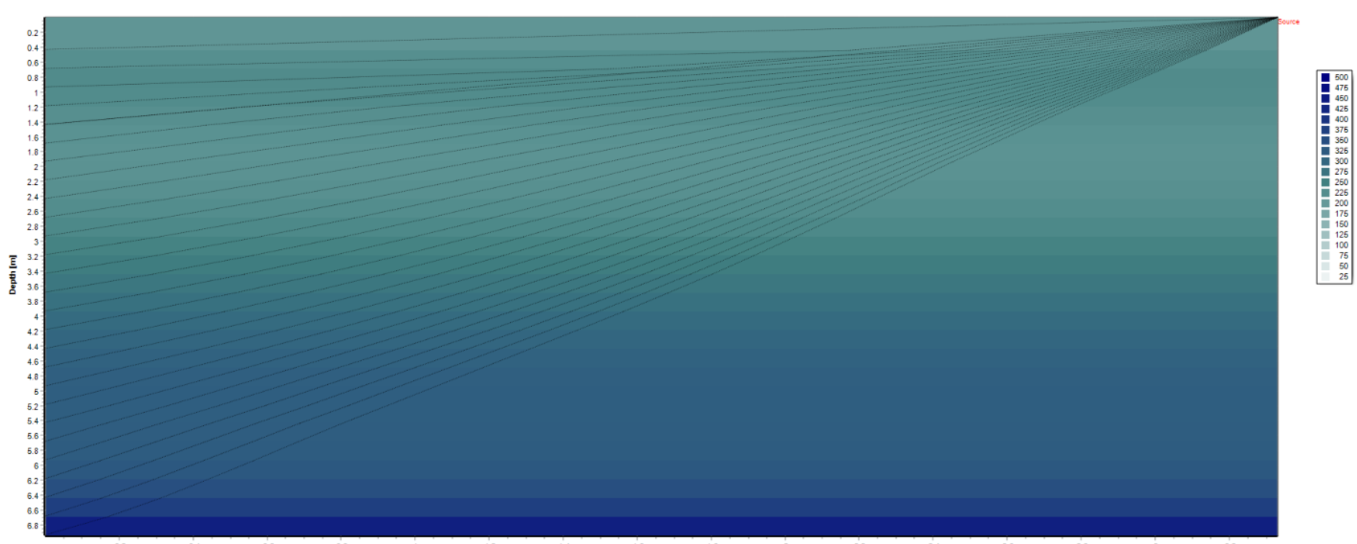

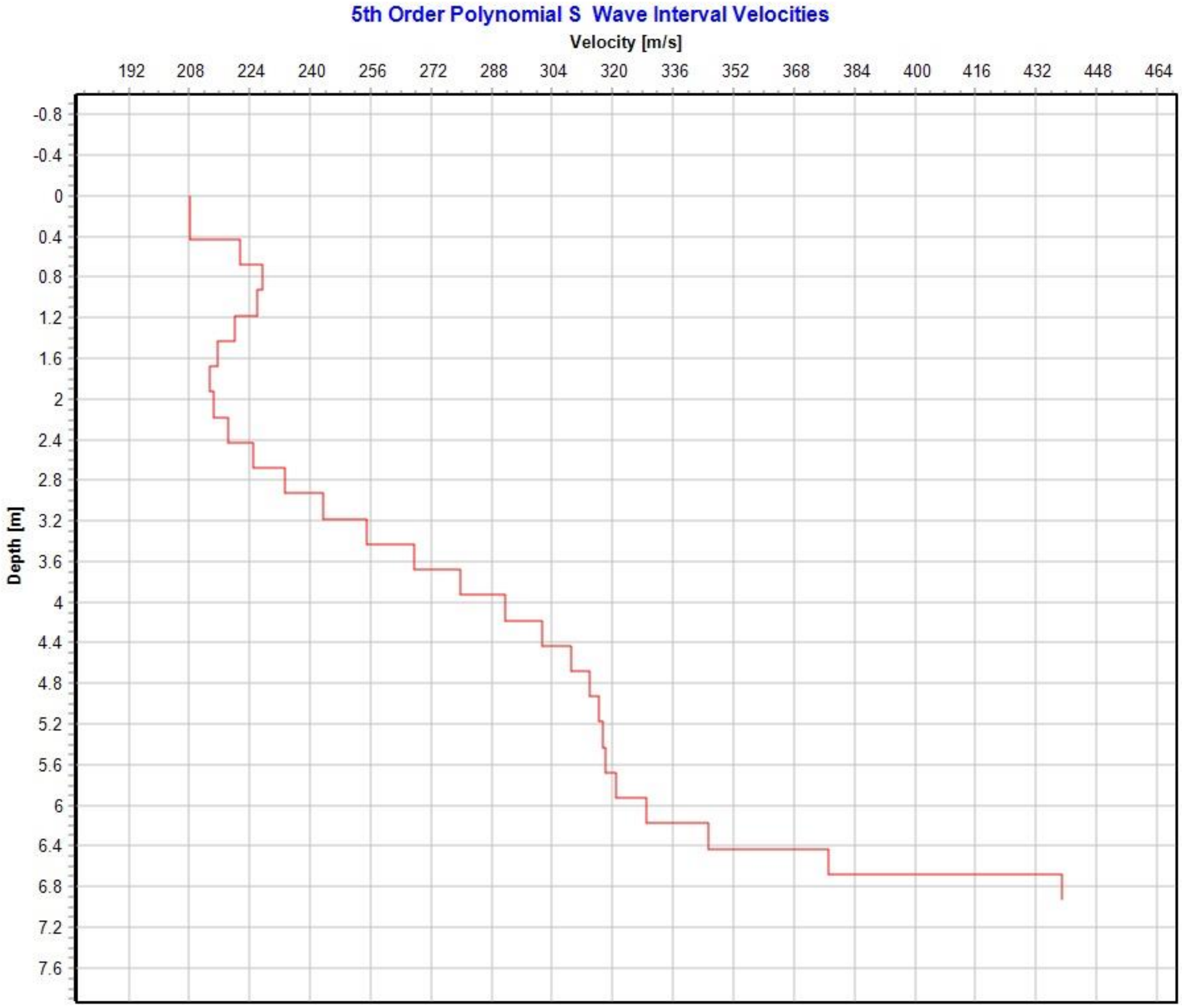
5th Order Polynomial S Wave Interval Velocities
Velocity [m/s]
192
208
224
240
256
272
288
304
320
336
352
368
384
400
416
432
448
464
Depth [m]
-0.8
-0.4
0
0.4
0.8
1.2
1.6
2
2.4
2.8
3.2
3.6
4
4.4
4.8
5.2
5.6
6
6.4
6.8
7.2
7.6